Report No. BMI-1317
UC-25 Metallurgy and Ceramics
(TID-4500, 14th Ed.)

Contract No. W-7405-eng-92

OXIDATION AND CONTAMINATION REACTIONS OF NIOBIUM AND NIOBIUM ALLOYS

by

William D. Klopp
Daniel J. Maykuth
Chester T. Sims
Robert I. Jaffee

February 3, 1959

BATTELLE MEMORIAL INSTITUTE
505 King Avenue
Columbus 1, Ohio

DISCLAIMER

TABLE OF CONTENTS

OXIDATION AND CONTAMINATION REACTIONS OF NIOBIUM AND NIOBIUM ALLOYS

William D. Klopp, Daniel J. Maykuth,
Chester T. Sims, and Robert I. Jaffee

Niobium was found to react linearly with air (600 to 1200 C) and with oxygen (400 to 1400 C). At 1400 C, a very rapid reaction with oxygen was observed. Contamination hardening during oxidation was attributed to diffusion of oxygen into the metal from the predominantly Nb_2O_5 scale.

Alloying effects could be correlated with relative ionic size and valence of the alloy addition and with properties of the alloy-element oxides. Additions with smaller ionic size or higher valence improved oxidation behavior up to 15 a/o alloying. These additions included chromium, molybdenum, tungsten, and vanadium. Size effects predominated over valence effects. At alloying levels greater than 15 a/o, elements having solid stable oxides, such as titanium and zirconium, improved the oxidation behavior. Elements with volatile oxides, such as molybdenum, rhenium, and vanadium, decreased the oxidation resistance when added in amounts greater than 15 a/o.

The most effective binary additions for improving oxidation resistance were chromium, molybdenum, titanium, and vanadium. A molybdenum-chromium alloy oxidized about 20 per cent slower than the best binary alloy. The degree of improvement for the best alloys over unalloyed niobium ranged from a hundredfold at 600 C to sixfold at 1200 C.

The most effective additions were concluded to be those which form solid stable oxides of their own or which are capable of forming complex oxides such as spinels.

INTRODUCTION

In comparison with other refractory metals, niobium appears relatively attractive as a base for high-temperature alloys, considering its low cross section, good high-temperature strength, and possibilities for improvement in oxidation resistance. While its oxidation resistance leaves much to be desired, the oxides formed are solid up to 1400 or 1500 C, offering the possibility of improved oxidation resistance through alloying. Niobium also has a medium density and is easily fabricable. The room-temperature strength of niobium is not exceptional, about 50,000 psi in the annealed condition, but it decreases more slowly with increasing temperature than is true of lower-melting-point metals. Alloying can also be expected to improve the strength of niobium.

Thus, niobium appears as one of the most attractive of the refractory metals as a high-temperature alloy base.

The present investigation was undertaken to investigate the possibilities for improving the oxidation resistance of niobium by alloying. The investigation included both a study of the oxidation behavior of the unalloyed metal at 400 to 1400 C and a study of binary and ternary alloys at 600 to 1200 C.

BACKGROUND INFORMATION

The oxides of niobium have been studied by Brauer, Zachariasen, and Pranatis and Seigle. Brauer[1] reported three stable niobium oxides, NbO, NbO_2, and Nb_2O_5. The monoxide forms a cubic structure, with a = 4.203 A. NbO_2 has a rutile-type structure, with a = 4.84 A, c = 2.99 A, and c/a = 0.618. This oxide can be formed as a black powder by reduction of Nb_2O_5 with hydrogen or niobium metal powder. The pentoxide is normally white to yellow-white and exists in three modifications, designated by Brauer as low (T), middle (M), and high temperature (H). The T form is stable to 900 C, the M form between 1000 and 1100 C, and the H form above 1100 C.

Zachariasen[2] found the crystal structure of Nb_2O_5 (unknown form) to be isomorphous with Ta_2O_5, which is pseudohexagonal orthorhombic.

The variation of electrical conductivity of Nb_2O_5 was studied by Pranatis and Seigle[3] as a function of temperature (650 to 1050 C) and oxygen pressure (8×10^{-3} to 760 mm of mercury). The conductivity increases with temperature according to

$$\chi\,(1\text{ atm}) = 6.5 \times 10^4\, e^{-46,000/RT}\ \text{ohm}^{-1}\ \text{cm}^{-1},$$

while the pressure dependency is expressed by

$$\chi_p = \chi\,(1\text{ atm})\ P_{O_2}{}^{-1/4}\ \text{ohm}^{-1}\ \text{cm}^{-1}.$$

The observation that conductivity increases with decreasing oxygen pressure indicates the presence of interstitial metal ions or oxygen ion holes in the Nb_2O_5 lattice.

The reactions of niobium with oxygen, nitrogen, and air have been investigated previously by Gulbransen and Andrew[4,5] and Inouye[6]. Gulbransen and Andrew determined that the reaction with 1/10 atm of oxygen followed the parabolic rate law at 200 to 375 C. At 375 to 500 C, the reaction was initially parabolic followed by a transition to linear behavior, while the reactions above 500 C were entirely linear.

Inouye found that the niobium-air reaction was also linear at 600 to 1200 C, the rates being less than those for niobium-oxygen at the same temperatures. At 400 C, the reaction was initially parabolic, changing to linear after approximately 21 hr.

The niobium-nitrogen reaction is parabolic at 500 to 800 C, the reaction being appreciably slower than the niobium-oxygen reaction.

EXPERIMENTAL PROCEDURE

Materials

Commercial-purity niobium sheet and rod were obtained from Fansteel Metallurgical Corporation and Murex, Limited, for use in this investigation. A typical analysis of this material is given in Table 1. High-purity iodide-type chromium,

(1) References at end of text.

TABLE 1. TYPICAL ANALYSIS OF COMMERCIAL-PURITY NIOBIUM

Element	Amount, w/o
Oxygen	0.05
Nitrogen	0.01
Hydrogen	0.0001
Carbon	0.005
Aluminum	0.002
Calcium	0.002
Copper	0.003
Iron	0.003
Magnesium	<0.001
Manganese	0.001
Molybdenum	0.01
Nickel	0.006
Silicon	0.01
Titanium	0.002
Zirconium	0.01-0.6

titanium, and zirconium and high-purity ingots of molybdenum and vanadium were employed as alloy additions. The aluminum, beryllium, boron, cobalt, iron, manganese, nickel, silicon, tantalum, and tungsten additions were of commercial purity.

Sample Preparation

Cylindrical samples machined from arc-cast unalloyed niobium were employed in the niobium-oxygen and -nitrogen tests. The cylinders measured 0.3 in. in diameter and 0.5 in. in length. They were polished to a 600-grit finish and degreased before testing.

The intermittent-weighing air tests were conducted on small brick-shaped samples cut from 20-g arc-cast ingots of niobium and niobium alloys. These samples measured 0.1 by 0.2 by 0.4 in. and were finished by polishing through 600 grit and degreasing.

Continuous-weighing air tests were performed on sheet samples of niobium and niobium alloys. The sheets were prepared from arc-cast 50-g ingots by cold or hot (1000 or 1200 C) rolling to a thickness of 0.050 in. The strips were annealed at 1500 C in a vacuum of 10^{-4} mm of mercury after rolling. The oxidation samples measured 0.75 by 1 in. and were metallographically polished before testing.

Equipment and Procedure

The niobium-oxygen tests at 500 to 1400 C and the niobium-nitrogen test were conducted at 1 atm of pressure in a modified Sieverts-type apparatus. Details of the test procedure have been described previously.[7] Pure oxygen was obtained by partial decomposition of $KMnO_4$, while Matheson prepurified nitrogen was employed for the nitrogen test.

The niobium-oxygen reaction at 400 C was followed gravimetrically using a microbalance.

The intermittent-weighing tests were conducted in undried air for periods up to 20 hr. The samples were placed in shallow prefired crucibles and exposed at 600, 800, 1000, and 1200 C. The reaction rates were calculated from weight-gain data after 1, 5, 10, 15, and 20 hr of exposure.

The continuous-weighing tests were conducted by suspending the sample from one beam of an analytical balance on a quartz rod into a resistance-heated vertical tube furnace. The weight gain as the sample oxidized was followed by taking weight readings at approximately 5-min intervals for periods up to 6 hr. Dried air was passed through the furnace at approximately 7 ipm during testing. Tests were also conducted in humid air by bubbling the dried air through solutions known to maintain constant humidities.

EXPERIMENTAL RESULTS

Reactions of Unalloyed Niobium

Niobium-Oxygen Reaction

The reaction of niobium with 1 atm of oxygen at 400 to 1200 C followed the linear relationship with rates as given in Table 2. Although scatter was evident in the early portions of several runs, no tendency toward initial parabolic oxidation was detected in these tests. At 1400 C, niobium reacted very rapidly with oxygen, resulting in overheating and fusion of the sample. No reaction data were obtained at this temperature.

Correlation of the reaction rates with temperature by an Arrhenius-type plot is shown in Figure 1. Two inflections are noted in this plot, one at 580 C and the other at 1100 C. The activation energies for the range below 580 C and the 580 to 1100 C range are 41,000 cal per g mole and 5,400 cal per g mole, respectively. No activation energy is calculated for the range above 1100 C. The inflections in this plot indicate changes in the rate-controlling reaction. These may result from a change from metal-ion diffusion to oxygen-ion diffusion in the adherent portion of the scale, or a change in the structure or composition of the adherent scale.

The effect of pressure on this reaction was investigated at 800 C. Decreasing the oxygen pressure decreased the rate of reaction and promoted parabolic behavior. Curves for reactions at 0.1, 0.5, and 1.0 atm of oxygen pressure are shown in Figure 2. The reaction at 0.5 atm became linear after 40 min, while the 0.1-atm reaction curve was approximately parabolic for at least 90 min, the duration of the test. The reaction rates are given in Table 2.

Examination of the scales revealed that, at all temperatures from 400 to 1200 C, two scale layers were formed. These consisted of an outer, porous, white to yellow-white scale and an inner, thin, dark, adherent scale. The outer scale was loose and formed in thin layers at the lower temperatures (600 C), but was slightly more dense and tended to form as slabs at higher temperatures (1000 C to 1200 C). This was interpreted as a result of sintering of the oxide particles.

The oxides formed in oxygen and air at temperatures from 500 through 1000 C were identified by X-ray diffraction techniques as consisting primarily of Nb_2O_5 in both the outer and the inner scales. These data are given in Table 3. The temperature regions in which each of the three Nb_2O_5 modifications was formed are in agreement with the data of Brauer.[1] A small amount of NbO was present in the inner scale of the sample reacted with 0.1 atm of oxygen at 800 C. No NbO_2 was present in either scale. Back-reflection patterns on the oxidized samples showed that the inner scale was preferentially oriented while the outer scale was not. This was taken as evidence that the inner scale is adherent to the metal. Metallographically, the scales appeared to consist of a single phase, generally being porous in the outer portion and becoming denser near the metal-oxide interface.

TABLE 2. RATE CONSTANTS FOR NIOBIUM-OXYGEN REACTION

Temperature, C	Oxygen Pressure, atm	Parabolic Reaction Rate, $g^2/(cm^4)(sec)$	Linear Reaction Rate, $g/(cm^2)(sec)$	Oxygen-Diffusion Rate in Niobium, cm^2 per sec
400	1.0	--	8.2×10^{-9}	--
500	1.0	--	5.6×10^{-7}	1.0×10^{-9}
550	1.0	--	2.3×10^{-6}	--
600	1.0	--	6.5×10^{-6}	3.7×10^{-9}
800	1.0	--	1.2×10^{-5}	3.7×10^{-8}
	0.5	--	6.5×10^{-6}	3.8×10^{-8}
	0.1	2.8×10^{-7}	--	3.7×10^{-8}
1000	1.0	--	1.8×10^{-5}	1.25×10^{-7}
1100	1.0	--	2.0×10^{-5}	6.3×10^{-7}
1150	1.0	--	7.9×10^{-5}	7.9×10^{-7}
1200	1.0	--	7.3×10^{-5}	6.4×10^{-7}
1400	1.0	(Very rapid reaction)		--

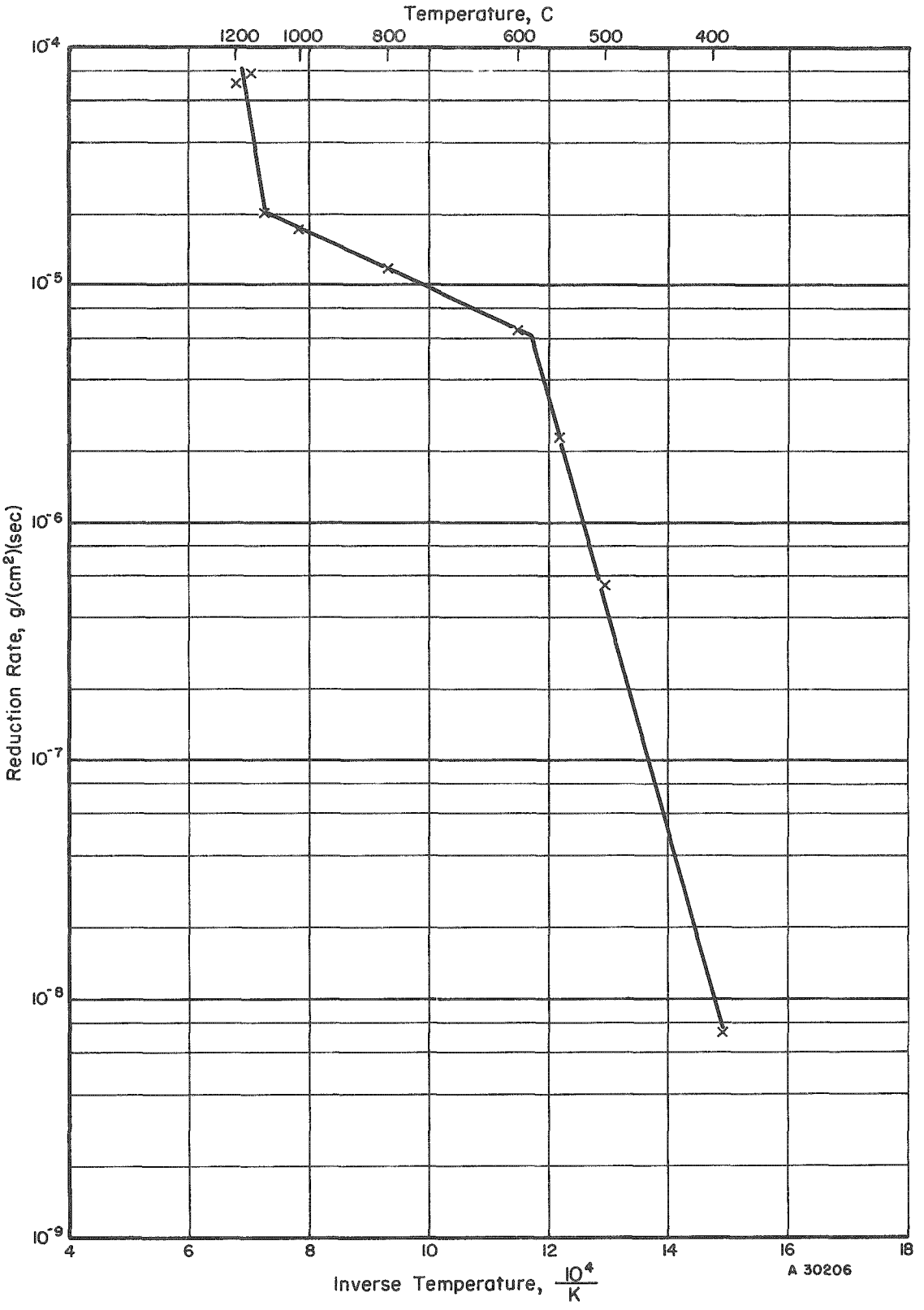

FIGURE 1. TEMPERATURE DEPENDENCY OF NIOBIUM-OXYGEN REACTION

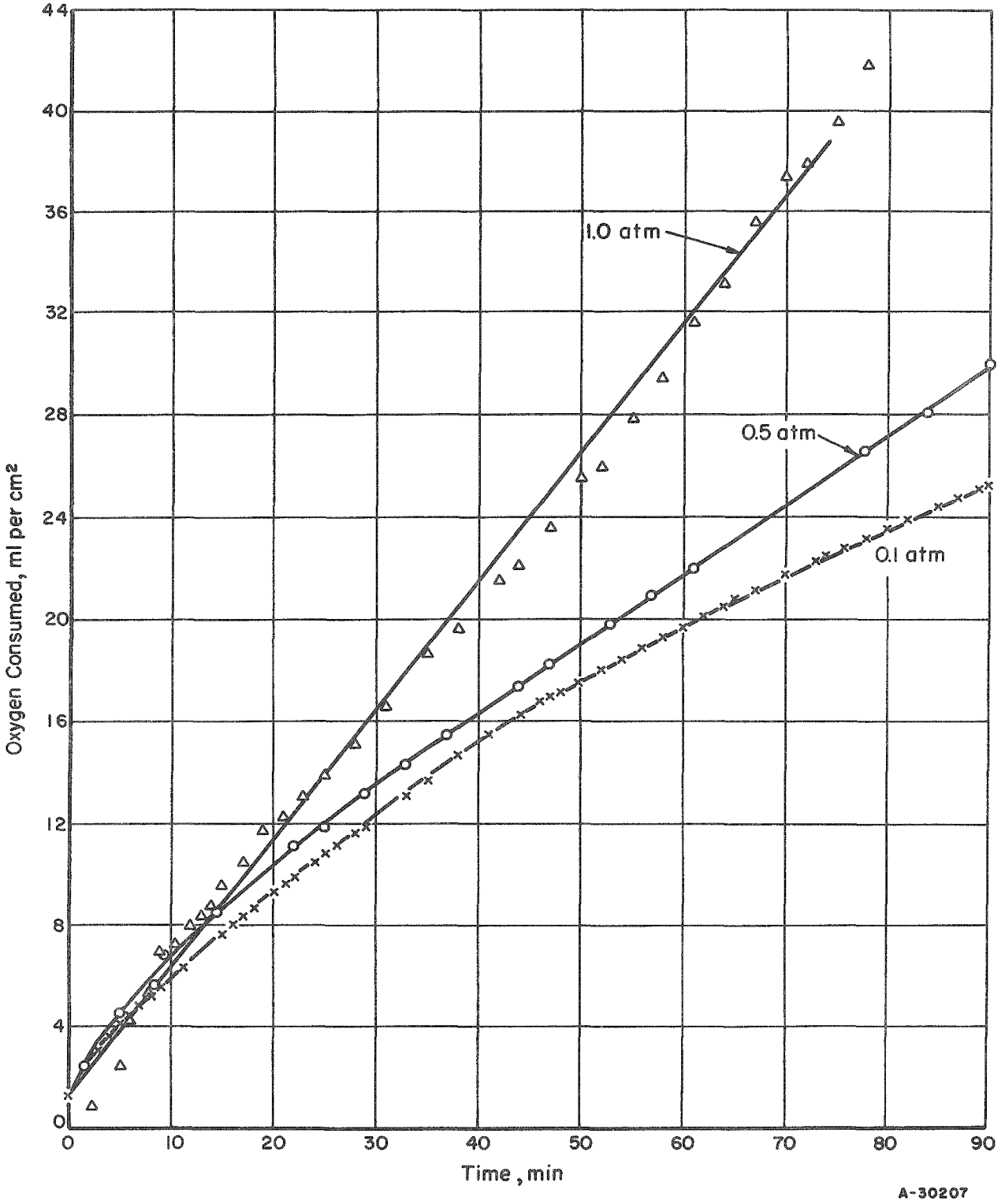

FIGURE 2. EFFECT OF PRESSURE ON NIOBIUM-OXYGEN REACTION AT 800 C

TABLE 3. OXIDES FORMED ON NIOBIUM IN OXYGEN AND AIR

Oxidation Conditions		Oxide Phases Present	
Temperature, C	Atmosphere	Outer Scale	Inner Scale
500	1.0 atm oxygen	T-Nb_2O_5	--
600	1.0 atm of oxygen	T-Nb_2O_5	--
800	0.1 atm of oxygen	T-Nb_2O_5	Oriented T-Nb_2O_5 plus small amount of NbO
1000	1.0 atm of oxygen	M-Nb_2O_5	--
600	Dry air	T-Nb_2O_5	Oriented T-Nb_2O_5
800	Dry air	T-Nb_2O_5 plus small amount of M-Nb_2O_5	Oriented T-Nb_2O_5
1000	Dry air	M-Nb_2O_5 plus H-Nb_2O_5	M-Nb_2O_5 plus H-Nb_2O_5 and trace of NbO

Niobium-Nitrogen Reaction

A machined niobium cylinder was heated in nitrogen for 50 min at 800 C, followed by 18 min at 1000 C. No reaction (i.e., no changes in the equilibrium nitrogen pressure of 1 atm) could be detected at either temperature, although a faint tarnish film was present at the conclusion of the test. Previous work by Gulbransen and Andrew[4] indicated that this reaction follows the parabolic law and is quite slow. Calculations based on their data indicate that the total amount of nitrogen reacted under the above condition was about 0.3 ml. This small volume change is near the detection limit of the modified Sieverts apparatus used.

Niobium-Air Reaction

The niobium-air reaction was studied in the range 600 to 1200 C by the intermittent-weighing method using arc-cast slabs and wrought rod samples and by the continuous-weighing method using wrought sheet samples. The effects of humidity and cold working were also evaluated.

The niobium-air reaction was found to be essentially linear over the entire range studied, although deviations from linearity were observed at higher temperatures, as determined from the continuous-weighing tests. Data from the intermittent and continuous tests are given in Tables 4 and 5, respectively.

The effects of moisture were evaluated in several continuous-weighing tests at 600, 800, and 1000 C. At 600 C, increasing the humidity from 0 to 100 per cent (relative 20 C humidity) increased the linear reaction rates by a factor of about 5. At 800 C, the scatter observed in results from dry-air tests precludes any deductions from the moist-air tests, while at 1000 C, no effects of moisture were observed. This work indicates that moisture increases the oxidation rate at low temperature but has no effect at higher temperatures. The greater reaction rates observed at 600 C in undried air compared with the rates in dry air are probably the result of moisture in the undried air.

The effects of cold work were investigated by both the intermittent- and continuous-weighing methods at 600 to 1000 C, but no significant difference in behavior, compared with annealed samples, could be detected.

The reaction rates obtained in both the intermittent and continuous tests are plotted against temperature in Figure 3. It is seen that the slope of rates determined by intermittent testing is less than the slope of dry-air rates determined by continuous weighing. This reflects the higher rates in undried air at lower temperatures. The activation energies associated with the two plots were determined by least-squares calculations as 9,900 ± 2,000 cal per g mole for the undried-air reaction and 15,800 ± 4,600 cal per g mole for the dry-air reaction.

The scales formed in air were similar to those formed in oxygen; thus, these also consisted of an inner, dark, adherent layer, and a porous, white outer layer. Typical scales formed on sheet niobium samples at 600, 800, 1000, and 1200 C are illustrated in Figures 4 and 5. Metallographic examination failed to show any significant difference between the adherent and nonadherent portions of the scale in any of these samples.

TABLE 4. RATE CONSTANTS FOR REACTION OF NIOBIUM WITH UNDRIED AIR

Test Series	Condition and Shape[a]	Oxidation Conditions: Temperature, C	Oxidation Conditions: Time, hr	Oxidation Rate, 10^{-6} g/(cm^2)(sec)	Depth of Contamination[b], cm	Oxygen-Diffusion Rate, cm^2 per sec
Nb-1	Cast slab	600	1	1.39	0.006	2.35×10^{-9}
		800	1	9.05	0.032	6.44×10^{-8}
		1000	1	7.08	0.067	1.30×10^{-7}
Nb-2	Cast slab	600	5	1.50	0.013	2.87×10^{-9}
		800	5	8.55	0.049	4.06×10^{-8}
		1000	5	7.17	>0.12	1.74×10^{-7}
Nb-3	Cast slab	600	10	2.22	0.013	1.70×10^{-9}
		800	10	10.0	(c)	--
		1000	10	3.56	>0.1	--
Nb-4	Cast slab[d]	600	2	1.64	--	--
		800	2	5.33	--	--
		1000	2	10.7	--	--
		1200	2	16.0	--	--
Nb-5	Cast rod	600	5	1.22	0.012	2.95×10^{-9}
		800	5	9.85	0.049	3.50×10^{-8}
		1000	5	9.11	0.115	1.63×10^{-7}
Nb-6	Annealed rod[e]	600	5	2.31	--	--
		700	5	3.86	--	--
		800	5	8.66	--	--
		900	5	6.17	--	--
		1000	5	8.45	--	--
Nb-7	Cold-worked rod	600	5	2.20	--	--
		700	5	2.69	--	--
		800	5	11.1	--	--
		900	5	6.66	--	--
		1000	5	9.42	--	--

(a) Slab dimensions, 0.1 by 0.2 by 0.45 in.; rod dimensions, 0.3 in. in diameter by 0.45 in. long. All specimens labeled "cast" were machined from arc-melted buttons.

(b) The depth of contamination was taken as the point on the hardness-versus-depth curve which was 50 KHN above the hardness of the uncontaminated metal.

(c) Sample was completely oxidized.

(d) One side was painted with Cr_2O_3 for marker experiment.

(e) Annealed 1/2 hr at 2150 C in vacuum.

TABLE 5. RATE CONSTANTS FOR REACTION OF NIOBIUM WITH DRY AND WET AIR

Sample	Thickness of Original Metal, 10^{-3} in.	Special Treatment Before Oxidation	Humidity at 20 C, per cent	Total Length of Run, min	Time to Become Linear, min	Linear Reaction Rate, 10^{-6} g/(cm^2)(sec)	Weight Gain in 1 Hr, 10^{-3} g per cm^2
				600 C			
1	20		0	120	20	0.495	2.31
6	20		0	120	20	0.472	2.33
7	20		0	120	17	0.472	2.32
8	20		0	120	40	0.445	2.72
31	95	Annealed	0	360	40	0.489	2.8
32	95	Cold Worked	0	360	20	0.475[a]	2.8
10	20		35	120	8	1.67	6.5
13	20		76	120	14	1.58	6.0
16	20		100	120	5	2.36	8.6
				800 C			
2	19		0	120	--	--[b]	29.9
5	21		0	120	--	--[b]	28.7
9	19		0	120	--	--[b]	34.2
25	17	Annealed	0	120	6	7.78	37.0
26	17	Annealed	0	120	55	5.06	31.0
24	35	Annealed	0	325	--	--[b]	35.0
28	95	Cold Worked	0	360	110	4.22	24.5
29	95		0	360	45	3.36[c]	18.2
11	20		35	120	50	3.20	10.5
14	20		76	120	2	4.45	17.3
23	35	Annealed	100	360	200	2.86	28.8
				1000 C			
3	20		0	120	--	--[b]	45.4
4	20		0	120	--	--[b]	43.8
68	28	Annealed	0	360	60	2.92	21.6
27	95	Annealed	0	120	40	8.56	40.4
30	95	Cold Worked	0	360	2	8.34[d]	31.0
12	20		35	120	--	--[b]	43.5
15	20		76	120	--	--[b]	40.8
				1200 C			
77	54	Annealed	0	60	1	26	107.8

(a) Rate increased after 150 min to 0.75 x 10^{-6} g/(cm^2)(sec).
(b) Rates were nonlinear.
(c) Rate increased after 170 min to 4.72 x 10^{-6} g/(cm^2)(sec).
(d) Rate decreased after 180 min to 6.14 x 10^{-6} g/(cm^2)(sec).

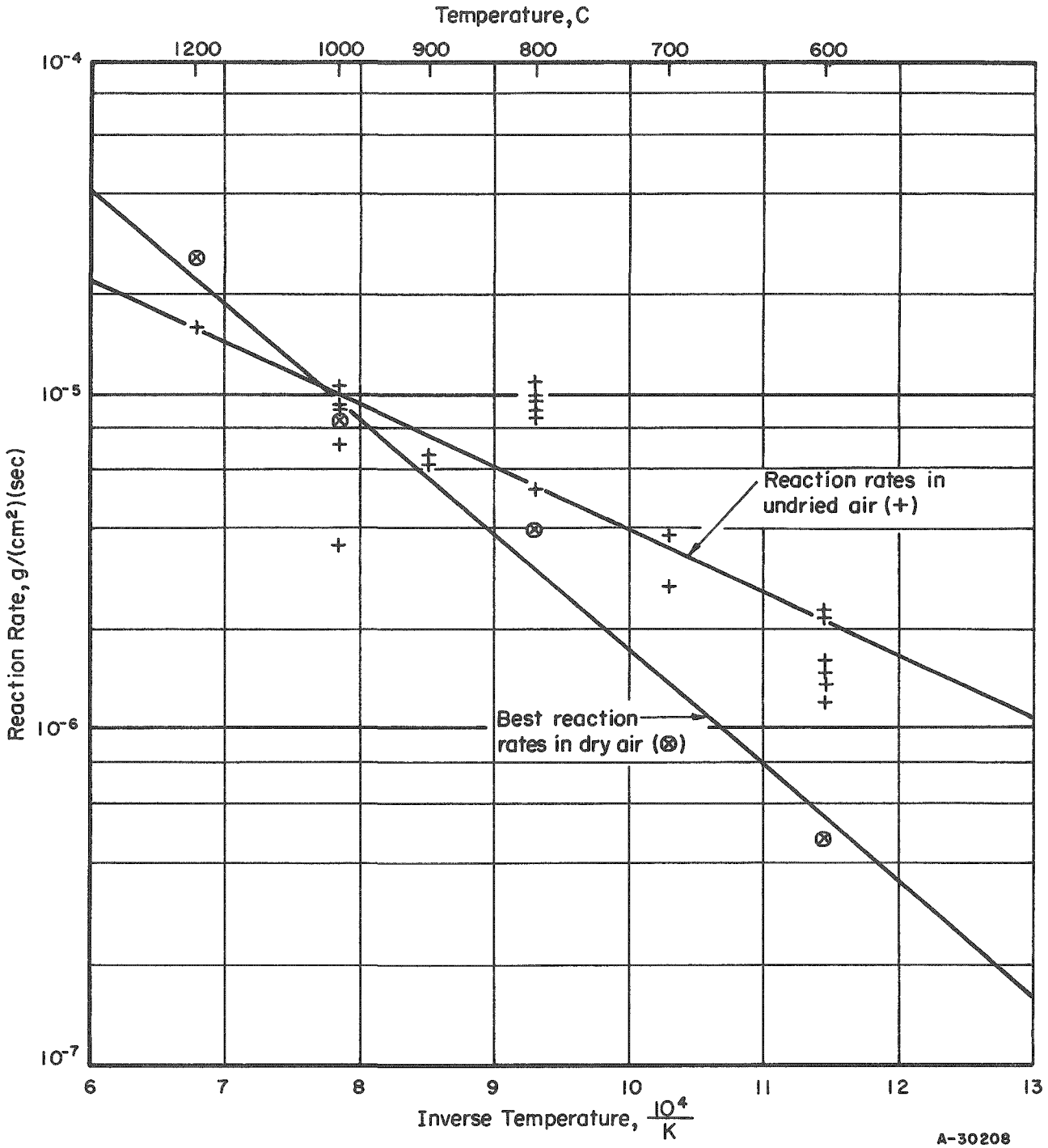

FIGURE 3. TEMPERATURE DEPENDENCY OF NIOBIUM-AIR REACTION

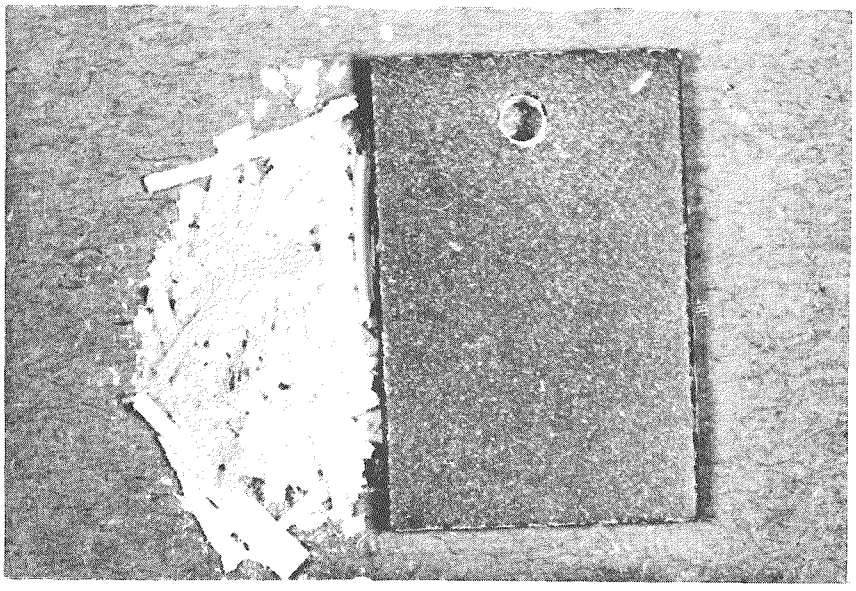

a. 600 C, 6 Hr (Sample 31)

b. 800 C, 6 Hr (Sample 29)

FIGURE 4. PHOTOGRAPHS OF PURE NIOBIUM AFTER REACTION WITH DRY AIR AT 600 AND 800 C

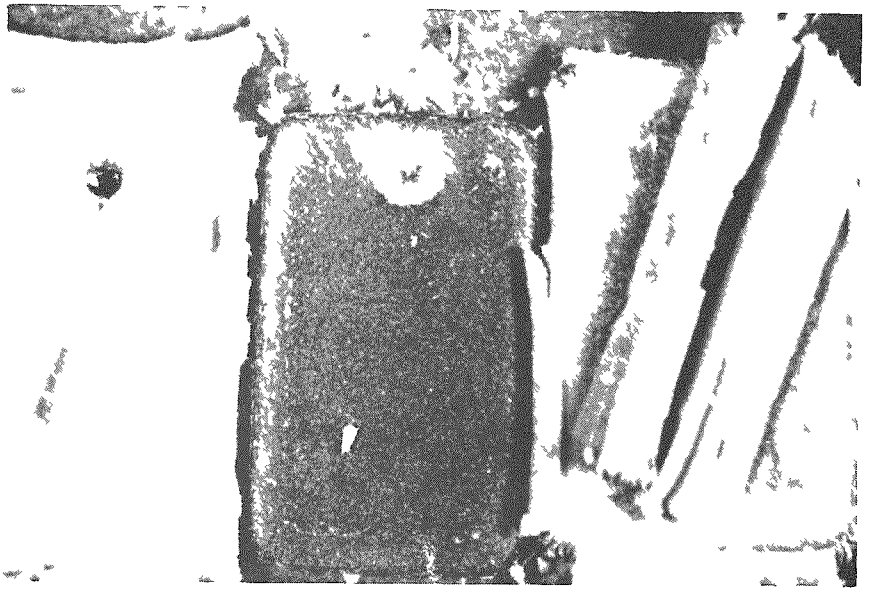

a. 1000 C, 6 Hr (Sample 30)

b. 1200 C, 1 Hr (Sample 77)

FIGURE 5. PHOTOGRAPHS OF PURE NIOBIUM AFTER REACTION WITH DRY AIR AT 1000 AND 1200 C

The oxides were identified by X-ray diffraction techniques as primarily Nb_2O_5, as indicated in Table 3. The adherent portions were preferentially oriented, and two lines corresponding to NbO were observed in the scale formed at 1000 C.

A marker experiment was performed on one series of samples in an attempt to identify the diffusing ion in the adherent portion of the oxide film. A thin layer of fine Cr_2O_3 powder (80 per cent smaller than 1 μ, 20 per cent between 1 and 2 μ) was applied to one face of several niobium slabs in a methanol slurry. After drying and oxidizing these samples at 600 to 1200 C, the scales were examined visually. The Cr_2O_3 layer was found on the surface of the porous scale, indicating that oxygen ions diffuse faster through the scale than metal ions, and that the oxidation reaction occurs at or near the metal-oxide interface.

Contamination Studies

The contamination of niobium resulting from oxygen and nitrogen diffusion is of importance, since small amounts of these elements significantly harden and embrittle niobium.[8,9] The degree of contamination resulting from oxygen, nitrogen, and air exposure was determined from Knoop hardness traverses on cross sections of the reacted samples. The hardness traverses shown in Figure 6 are typical of the data obtained.

Diffusion rates were calculated using an appropriate solution to Fick's second law which is given as

$$\frac{c - c_o}{c_m - c_o} = 1 - \phi\left(\frac{x}{2\sqrt{Dt}}\right), \qquad (1)$$

where

c = concentration of diffusing element at distance x from the surface

c_o = original concentration of the diffusing element

c_m = surface concentration of the diffusing element

ϕ = probability function

x = distance from surface, cm

D = diffusion coefficient, cm^2 per sec

t = diffusion time, sec.

Assuming a linear relationship between gas concentration and hardness, Equation (1) can be rewritten as

$$D = \frac{x^2}{4\left(\phi^{-1}\left[\frac{H_m - H}{H_m - H_o}\right]\right)^2} t, \qquad (2)$$

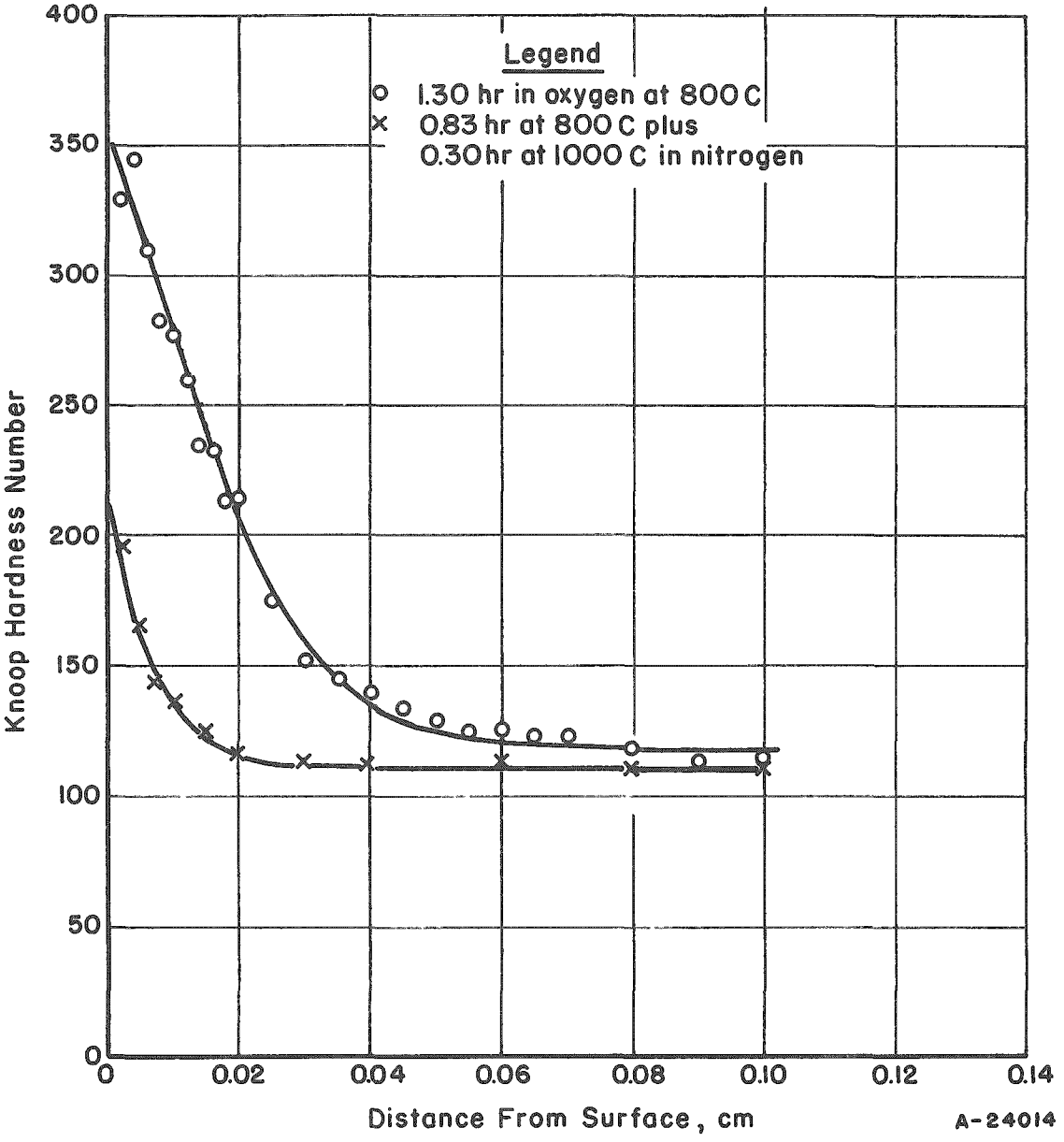

FIGURE 6. CONTAMINATION HARDENING OF NIOBIUM BY OXYGEN AND NITROGEN AT 800 C

where the term $\phi^{-1}\left[\frac{H_m - H}{H_m - H_o}\right]$ is the inverse probability function of the hardness ratio.

The diffusivities calculated from the oxygen-reacted and air-reacted samples are given in Tables 2 and 4 and are plotted against temperature in Figure 7. No calculations were made on the nitrogen-reacted sample since it was exposed at two different temperatures. It is apparent, however, from Figure 6, that nitrogen diffuses slower than oxygen, since the depth of hardening was less in a "nitrogenated" sample than in an "oxygenated" sample even though exposure conditions for the former were more severe. Also, comparison of the diffusivities calculated from the oxygen-reacted and air-reacted samples shows that they are substantially identical. This indicates that oxygen is the primary contaminant in the air-reacted samples, as expected, since only oxide scales were formed. A second important observation is that the amounts of contamination in the samples reacted with 1.0 and 0.1 atm of oxygen at 800 C were similar, indicating that the oxygen source was an adherent film and oxygen did not have direct access to the metal.

The diffusivities of oxygen in niobium are related to temperature by the relationship

$$D = 4.07 \times 10^{-3} e^{-\frac{24,900}{RT}},$$

where D is the diffusion rate in cm^2 per sec at absolute temperature, T, deg K. The diffusion rates agree with the data of Ang[10], who obtained a value of 27,600 cal per g mole for the activation energy.

Reaction of Niobium Alloys With Air

The reactions of niobium alloys with air were studied in an initial screening survey by the intermittent-weighing method and, subsequently, in more detail by the continuous-weighing method. The oxidation rates from the intermittent tests were calculated from the specific weight gains, assuming the reaction-rate curves to be linear. Data from the continuous tests gave information as to the exact nature of the reaction, i.e., whether parabolic or linear.

Niobium Binary Alloys

Intermittent Weight-Gain Tests. Binary niobium alloys evaluated in the screening study contained nominal additions of up to 35 a/o chromium, titanium, and zirconium, up to 25 a/o molybdenum, tantalum, tungsten, and vanadium, and 5 a/o beryllium, boron, cobalt, iron, manganese, nickel, and silicon. Several of these additions were difficult to retain in the 20-g ingots because of relatively high vapor pressures, notably aluminum, beryllium, chromium, and manganese. The compositions of most alloys were corrected, therefore, on the basis of analyses and/or weight losses during melting.

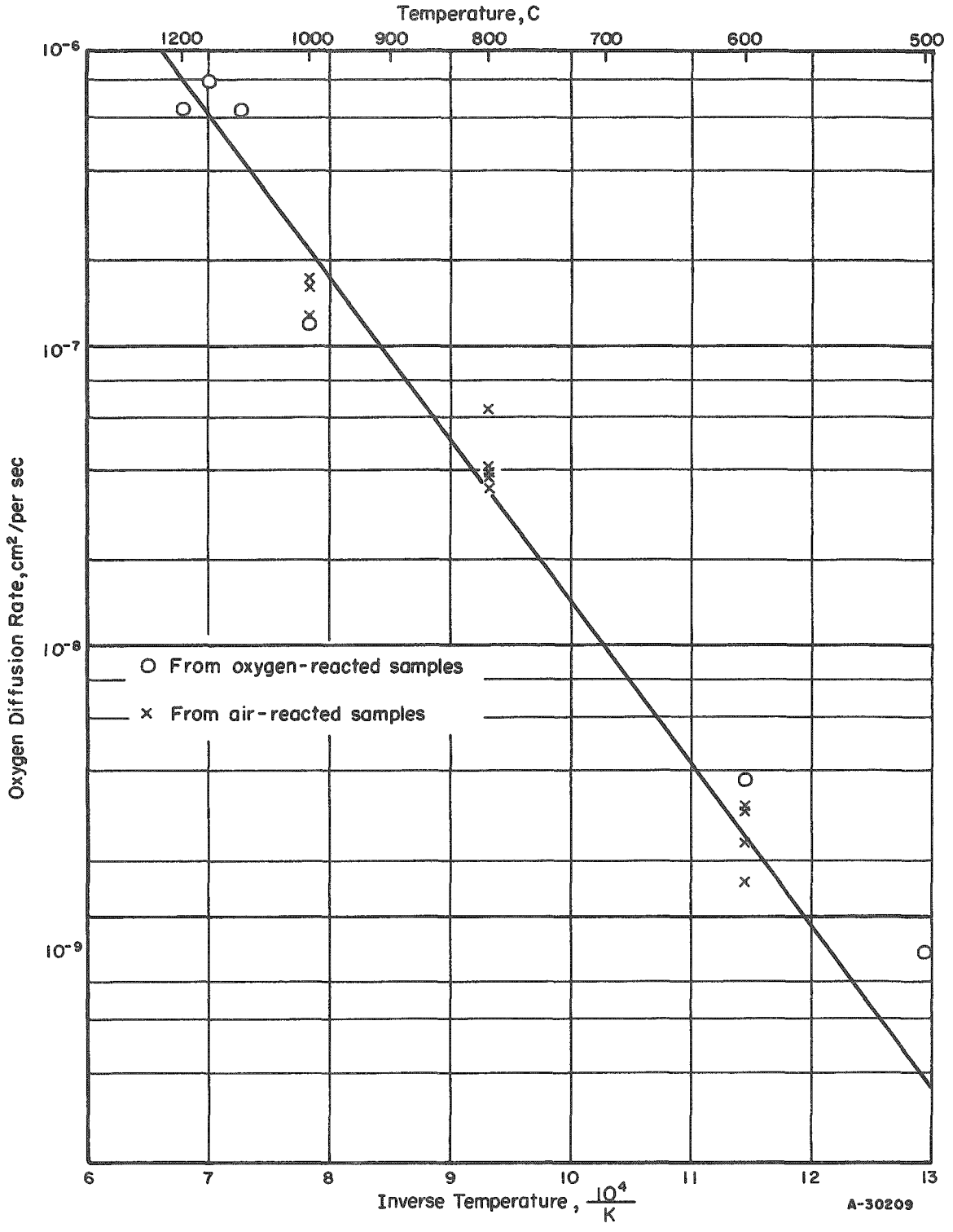

FIGURE 7. TEMPERATURE DEPENDENCY OF OXYGEN DIFFUSION RATE IN NIOBIUM

Exposure conditions and weight-gain rates from the intermittent-weighing oxidation tests are given in Table 6. The weight-gain rates for most of the alloys are plotted against composition in Figures 8, 9, and 10. The rates are expressed as linear rates because it was not possible from the nature of the tests to determine the type of reaction.

The most effective additions for reducing the weight gains are chromium, molybdenum, titanium, and vanadium. Titanium additions are most effective at the 25 a/o level, reducing the weight gain at 1000 C by a factor of about 20. Molybdenum, vanadium, and chromium produced minima in the 1000 C weight gains at lower levels than titanium, about 5, 10, and 15 a/o, respectively. At higher alloying levels, these additions resulted in higher oxidation rates than were obtained in pure niobium.

Zirconium additions beyond 5 a/o were increasingly effective at 600 C, while at 800 and 1000 C a sharp rise in oxidation rate was observed at the 1 and 10 a/o level. At these temperatures, increasing the zirconium content above 25 a/o promoted reduced rates.

Tungsten and tantalum additions at the 1 a/o level caused increased weight gains, but at higher levels, the rates were reduced to levels comparable to that of pure niobium. Neither addition was significantly effective in improving the oxidation behavior up to 1000 C.

The remaining eight additions (aluminum, beryllium, boron, cobalt, iron, manganese, nickel, and silicon) were investigated only up to the 5 a/o level, as these elements form intermetallic compounds with niobium at higher levels. At these levels none of the additions improved the oxidation resistance at 600 to 1000 C. Silicon additions increased the weight gains at 800 and 1000 C.

Continuous Weight-Gain Tests. Selected binary alloy systems were further evaluated by continuous-weighing oxidation tests in dry air at 1000 and 1200 C for periods up to 6 hr. The alloy systems and ranges evaluated in this manner were 4.5 to 24 a/o chromium, 1 to 5 a/o iron, 2.5 to 10 a/o molybdenum, 5 a/o rhenium, 10 to 35 a/o titanium, 1 to 10 a/o tungsten, 5 to 25 a/o vanadium, and 10 to 45 a/o zirconium.

The hardnesses and fabrication characteristics of these systems were noted as the alloys were processed. These data, given in Appendix A, generally showed that titanium binary alloys are cold fabricable to at least 35 a/o, while alloys with molybdenum, tungsten, and vanadium can be hot fabricated to the 10, 10, and 25 a/o alloying levels, respectively. Iron and rhenium binaries can be hot fabricated to the 5 a/o alloying level. One chromium alloy, containing 24 a/o chromium, was hot rolled to strip, but other alloys containing 3.5 to 12.5 a/o chromium could not be fabricated.

Results of the continuous-weighing tests generally confirmed the information obtained in the screening survey regarding the composition areas of maximum oxidation resistance and also showed that many of the attractive alloys oxidized parabolically and formed fully protective scales.

The oxidation behaviors of these binary alloys are summarized in Figures 11 and 12, where the weight gains at 1000 and 1200 C are plotted against composition. Table 7 gives reaction data for all of the binary alloys investigated by the continuous-weighing method. Reaction curves for these alloys are given in Appendix B.

TABLE 6. RATE CONSTANTS FOR REACTION OF NIOBIUM BINARY ALLOYS WITH UNDRIED AIR (INTERMITTENT-WEIGHING TESTS)

Alloy Addition (Balance Niobium), a/o		As-Cast Hardness,	Weight-Gain Rate, 10^{-6} g/(cm^2)(sec), at Indicated Temperature			Weight-Loss Rate[a], 10^{-6} g/(cm^2)(sec), at Indicated Temperature			Oxygen-Diffusion Rate, 10^{-4} cm^2 per sec, at Indicated Temperature		
Nominal	Adjusted	VHN	600 C	800 C	1000 C	600 C	800 C	1000 C	600 C	800 C	1000 C
100 Nb		115	1.58	9.37	6.73	5.12	20.2	8.90	0.0865	1.26	7.56
1 Ti	0.9 Ti	108	1.61	6.01	7.24	3.25	14.46	17.15	0.068	3.0	9.4
5 Ti	4.5 Ti	115	1.31	5.84	4.37	2.12	12.70	9.85	0.013	0.50	1.6
10 Ti	9.0 Ti	135	0.04	2.08	2.14	0.0	4.95	4.98	0.0062	0.29	0.71
15 Ti	14.0 Ti	151	0.02	0.67	1.57	--	--	--	--	--	--
20 Ti	18.5 Ti	150	0.03	0.58	1.47	--	--	--	--	--	--
25 Ti	23.0 Ti	156	0.01	0.17	0.53	0.0	0.25	1.39	0.0052	0.03	0.24
30 Ti	28.0 Ti	189	0.25	0.14	1.06	--	--	--	--	--	--
35 Ti	32.5 Ti	181	0.04	1.95	1.19	0.0	0.083	2.19	0.0058	0.024	0.49
1 Mo	0.9 Mo	126	0.47	3.33	3.67	1.64	1.47	5.39	0.085	1.9	4.7
2.5 Mo	2.0 Mo	132	0.04	0.51	1.47	--	--	--	--	--	--
5 Mo	4.5 Mo	166	0.07	0.58	1.28	--	--	--	0.14	2.0	(0.029)[b]
7.5 Mo	6.5 Mo	231	0.04	1.60	2.88	--	--	--	--	--	--
10 Mo	9.0 Mo	201	0.11	0.53	2.81	0.11	4.95	46.5	0.15	1.5	--
25 Mo	22.0 Mo	299	0.56	1.06	11.8	0.195	7.34	39.9	0.025	0.33	--
1 Cr	0.6 Cr	120	0.95	8.29	9.21	1.95	15.73	17.80	0.16	1.5	8.0
5 Cr	3.0 Cr	124	0.97	6.73	7.82	1.31	8.87	16.30	0.19	1.5	9.2
10 Cr	6.0 Cr	147	0.36	6.79	7.28	0.195	12.34	15.45	0.098	0.9	6.1
20 Cr	11.5 Cr	233	0.014	1.89	2.45	--	--	--	--	--	--
25 Cr	14.5 Cr	345	0.139	1.42	1.70	1.03	1.28	9.01	1.1	0.15	0.92
30 Cr	17.5 Cr	327	0.206	1.28	4.20	--	--	--	--	--	--
35 Cr	20.5 Cr	429	0.023	0.118	6.20	0.0	0.25	13.34	0.09	(0.56)	0.045
1 V	0.9 V	114	1.0	1.75	3.84	2.60	2.30	8.98	0.022	0.99	6.7
5 V	4.5 V	160	0.25	0.39	1.28	0.36	0.17	3.06	0.012	0.51	4.2
7.5 V	6.5 V	164	0.05	0.56	1.92	--	--	--	--	--	--
10 V	8.5 V	172	0.014	0.195	0.98	(c)	+	1.95	0.011	0.34	2.2
12.5 V	11.0 V	218	0.026	0.33	1.25	--	--	--	--	--	--
25 V	21.5 V	194	0.056	1.69	53.7	+	3.86	110.8	0.079	0.080	0.13
1 Zr	--	176	1.97	18.0	19.7	3.06	29.0	29.7	0.048	0.38	3.4
5 Zr	--	167	1.06	11.4	37.6	2.72	21.60	39.6	0.027	0.064	--
10 Zr	--	209	0.083	7.01	28.1	0.0	15.30	38.3	0.035	0.023	0.012
25 Zr	--	272	1.31	2.97	13.8	5.36	7.37	24.0	0.087	0.064	0.066
35 Zr	--	289	0.056	0.61	8.35	0.33	0.58	16.82	0.0	0.0	0.012
1 W	--	127	1.69	11.4	16.4	3.94	26.5	36.8	0.12	1.8	8.4
5 W	--	165	0.86	3.42	15.01	2.01	9.24	38.8	0.12	1.8	8.0
10 W	--	196	0.81	4.72	7.23	1.95	12.18	20.2	0.09	2.0	(0.71)
25 W	--	299	2.31	8.62	26.1	7.54	24.20	70.5	0.0	2.0	5.1
1 Ta	--	125	1.72	8.06	18.97	4.25	19.45	44.9	0.022	1.1	11.0
5 Ta	--	122	2.34	9.65	7.09	5.28	22.15	15.19	0.025	1.1	(9.4)
10 Ta	--	120	2.85	11.03	5.64	4.89	26.70	10.75	0.57	1.0	(1.3)
25 Ta	--	130	0.56	7.31	17.03	13.90	19.55	14.40	0.12	1.3	6.4

TABLE 6. (CONTINUED)

Alloy Addition (Balance Niobium), a/o		As-Cast Hardness,	Weight-Gain Rate, 10^{-6} g/(cm^2)(sec), at Indicated Temperature			Weight-Loss Rate, 10^{-6} g/(cm^2)(sec), at Indicated Temperature			Oxygen-Diffusion Rate, 10^{-4} cm^2 per sec, at Indicated Temperature		
Nominal	Adjusted	VHN	600 C	800 C	1000 C	600 C	800 C	1000 C	600 C	800 C	1000 C
0.2 Mn	--	140	2.17	11.12	6.06	4.34	25.5	14.19	0.20	1.3	(11)
1 Mn	--	139	1.20	10.55	6.14	2.47	24.65	14.52	0.13	1.7	(5.7)
5 Mn	0.7 Mn	140	1.25	10.92	6.64	2.67	25.20	16.05	0.10	1.6	(6.0)
0.2 Fe	<0.1 Fe	114	1.83	8.90	9.90	4.20	20.25	21.55	0.16	1.5	(13)
1 Fe	0.4 Fe	146	1.94	11.27	6.95	4.53	26.15	15.0	0.099	2.1	(7.3)
5 Fe	1.9 Fe	178	1.53	6.26	6.95	3.34	13.48	15.20	0.041	1.7	(3.0)
0.2 Co	--	136	1.45	11.34	12.18	3.02	26.15	15.12	0.12	2.0	(12)
1 Co	--	165	1.03	11.64	10.45	2.36	29.19	36.0	0.17	1.1	(9.2)
5 Co	--	249	1.14	10.90	10.70	2.50	28.50	19.50	0.16	(0.1)	(1.8)
0.2 Ni	<0.1 Ni	144	1.99	7.59	8.43	4.70	18.15	18.70	0.059	0.79	(6.5)
1 Ni	0.5 Ni	147	1.43	7.37	16.25	3.59	19.15	39.2	0.022	0.39	(0.35)
5 Ni	2.3 Ni	230	1.42	8.76	12.87	4.12	22.85	31.25	0.11	0.78	(2.0)
0.2 Al	--	132	2.08	10.91	5.51	4.51	25.0	13.82	0.15	2.8	(14)
1 Al	--	131	2.22	10.33	6.26	4.81	23.65	15.30	0.13	2.9	(1.2)
5 Al	<0.7 Al	114	1.97	12.29	5.39	4.39	27.75	13.20	0.10	0.79	(8.2)
0.2 Si	0.1 Si	156	1.92	14.45	5.95	4.31	26.05	14.98	0.04	0.61	0.41
1 Si	0.7 Si	186	1.69	14.80	12.92	3.59	26.80	26.93	0.034	3.2	20
5 Si	3.7 Si	330	2.86	18.63	28.8	6.48	41.2	64.2	0.56	3.8	18
0.2 Be	--	122	1.58	7.68	6.67	3.48	17.6	15.11	--	--	--
1 Be	--	113	1.92	8.65	5.98	4.17	20.05	13.55	--	--	--
5 Be	<0.1 Be	110	1.81	11.29	5.01	4.06	26.20	11.09	--	--	--
0.2 B	0.2 B	103	1.61	10.92	5.54	3.56	25.20	12.50	--	--	--
1 B	1.0 B	111	1.57	7.73	5.62	2.17	17.70	12.50	--	--	--
5 B	5.0 B	160	0.83	2.86	4.20	1.61	5.29	18.35	--	--	--

(a) Weight loss determined by mechanically removing scale.

(b) Diffusion rates in parentheses are estimated; oxygen diffused through the centers of the samples.

(c) Sample showed weight gain after removing scale.

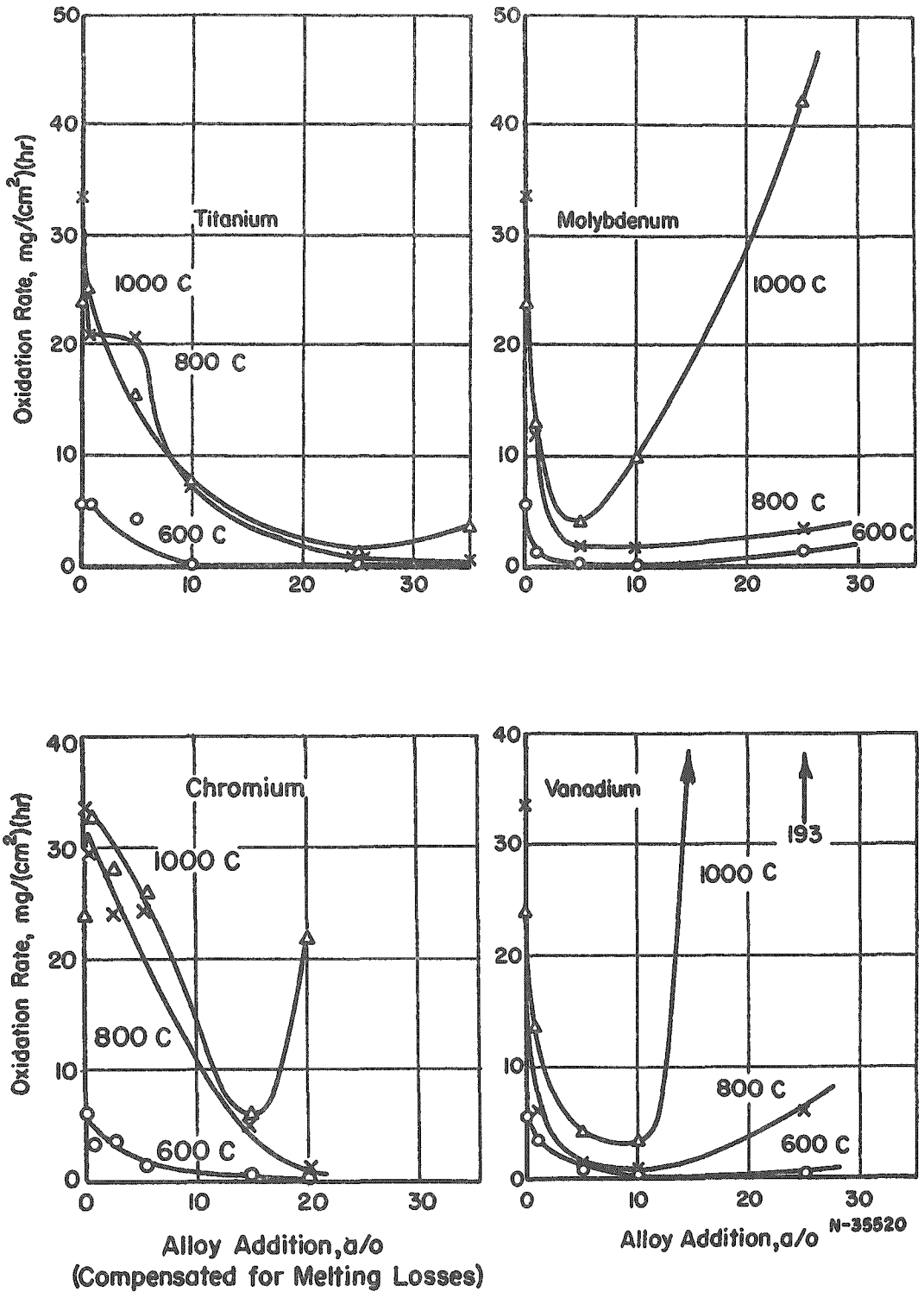

FIGURE 8. AIR OXIDATION RATES OF NIOBIUM ALLOYS CONTAINING TITANIUM, MOLYBDENUM, CHROMIUM, AND VANADIUM CALCULATED FROM WEIGHT-GAIN DATA

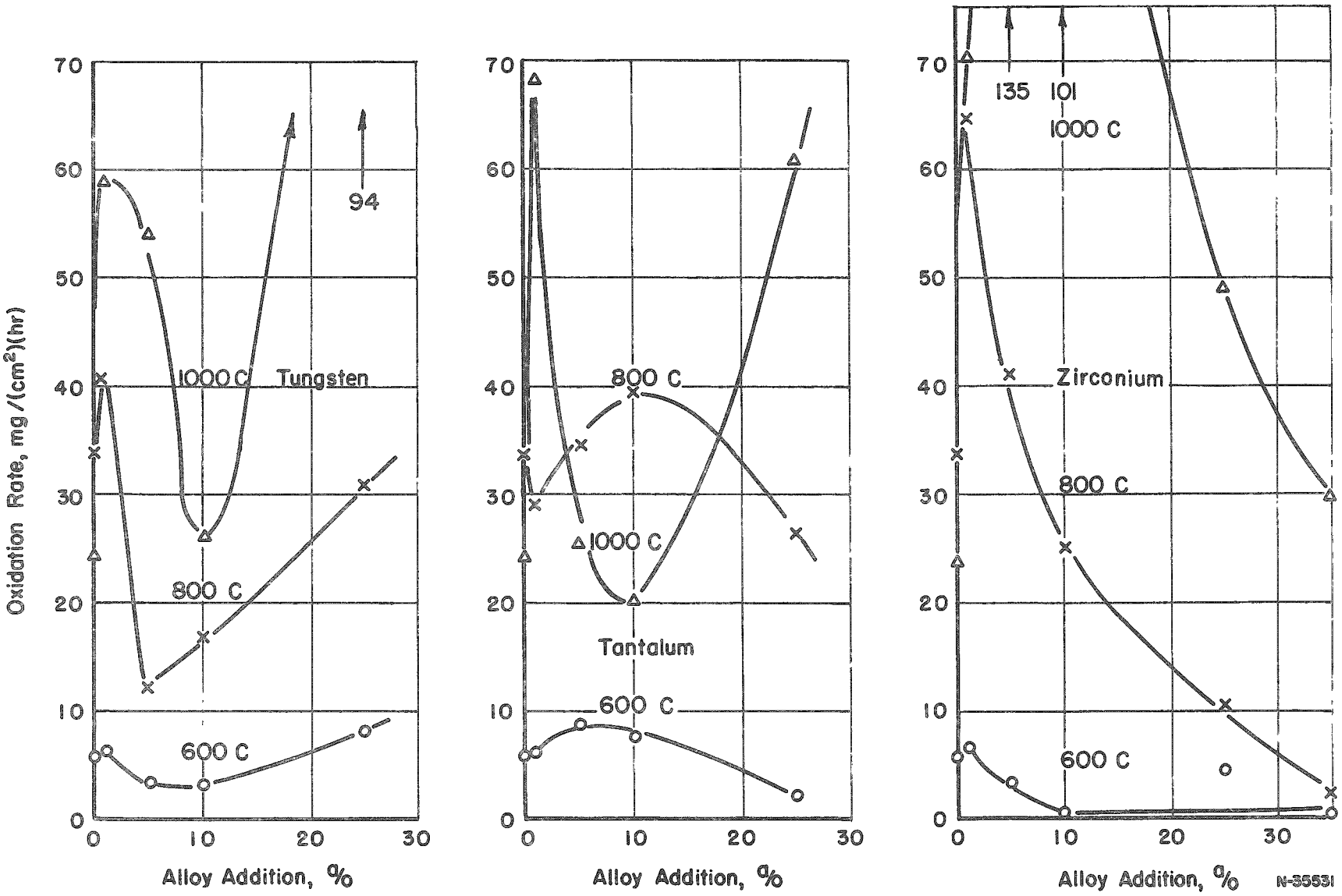

FIGURE 9. AIR-OXIDATION RATES OF NIOBIUM ALLOYS CONTAINING TUNGSTEN, TANTALUM, AND ZIRCONIUM, CALCULATED FROM INTERMITTENT WEIGHT-GAIN DATA

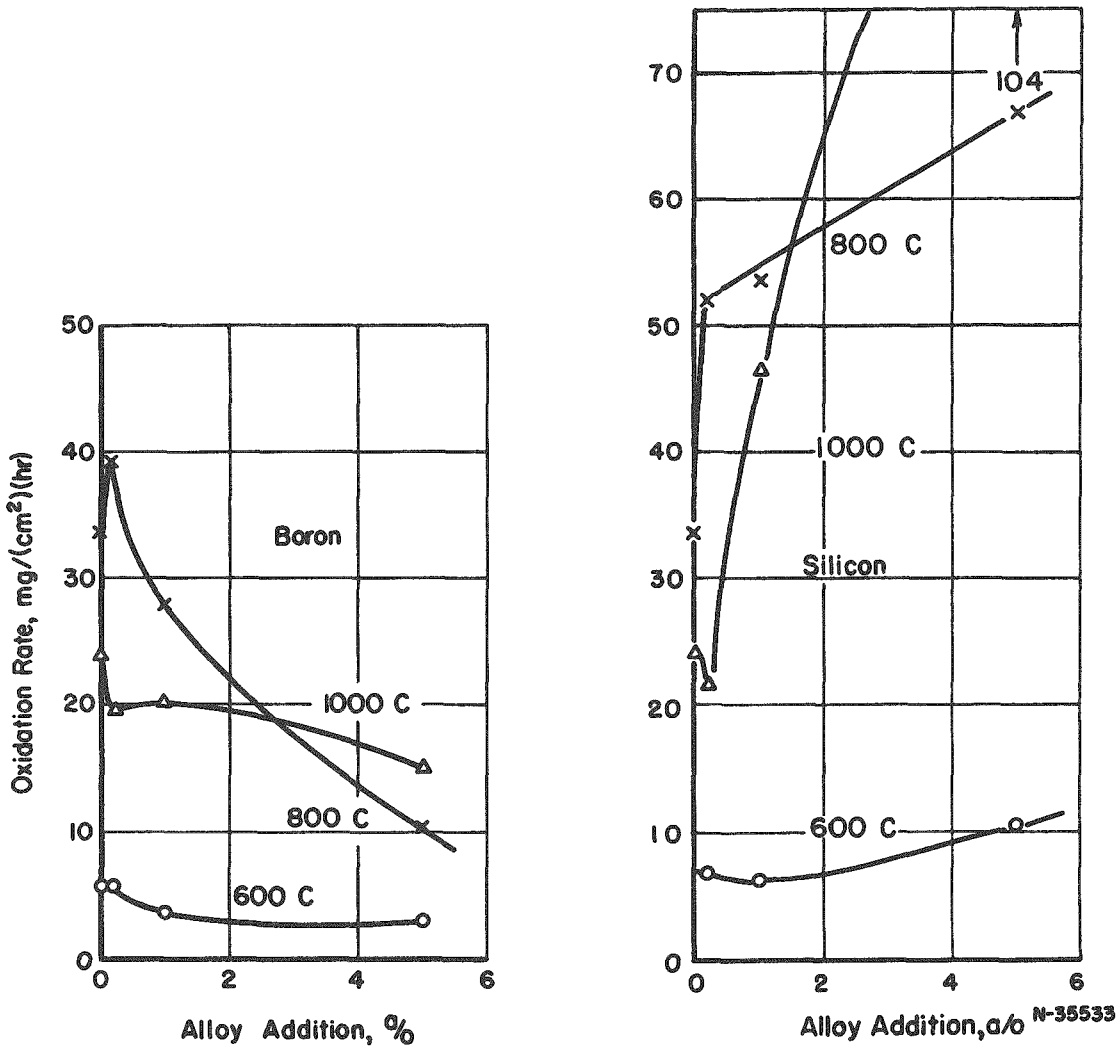

FIGURE 10. AIR-OXIDATION RATES OF NIOBIUM ALLOYS CONTAINING BORON AND SILICON, CALCULATED FROM INTERMITTENT WEIGHT-GAIN DATA

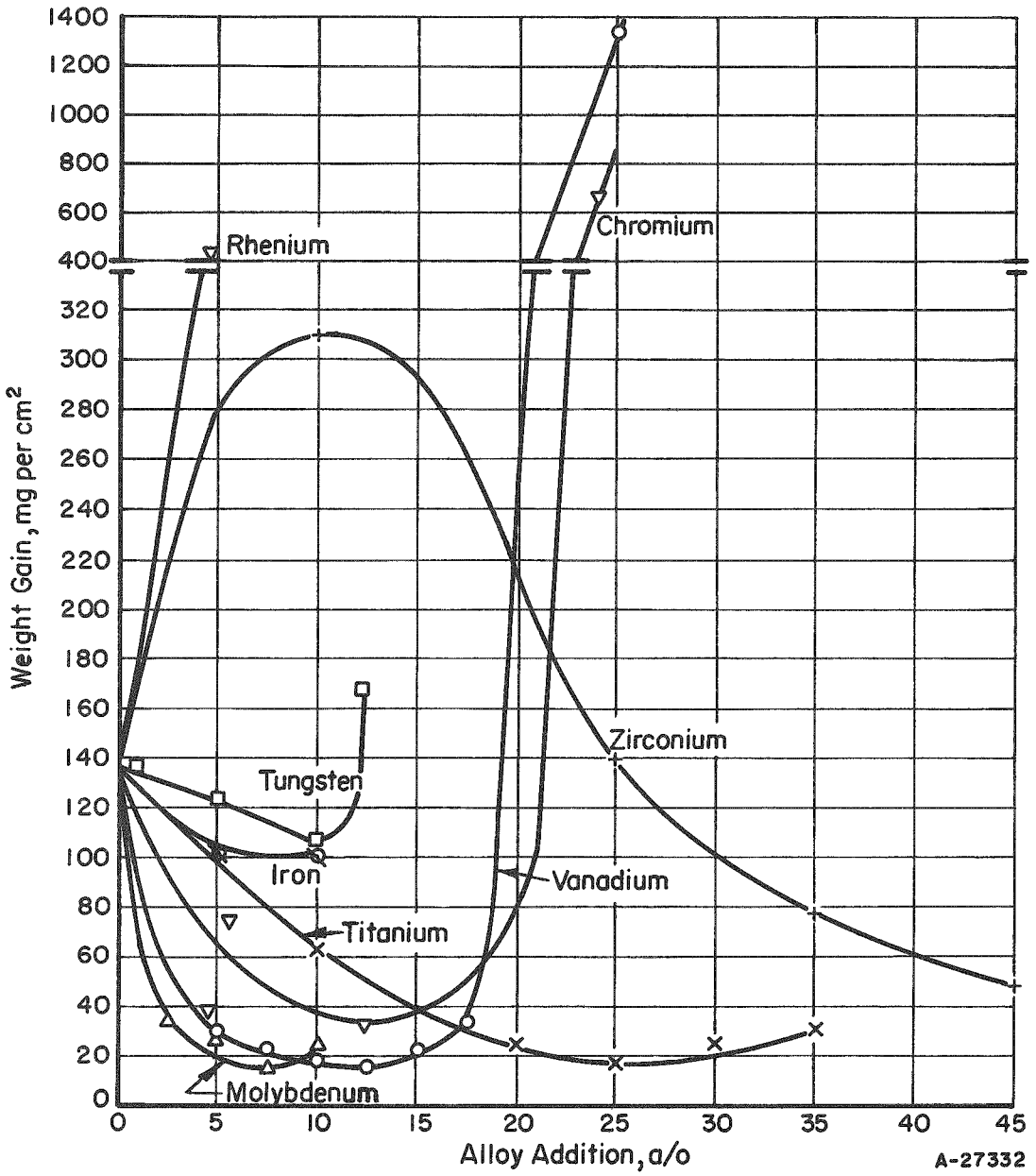

FIGURE 11. WEIGHT GAINS OF NIOBIUM ALLOYS EXPOSED 5 HR IN DRY AIR AT 1000 C (CONTINUOUS-WEIGHING TESTS)

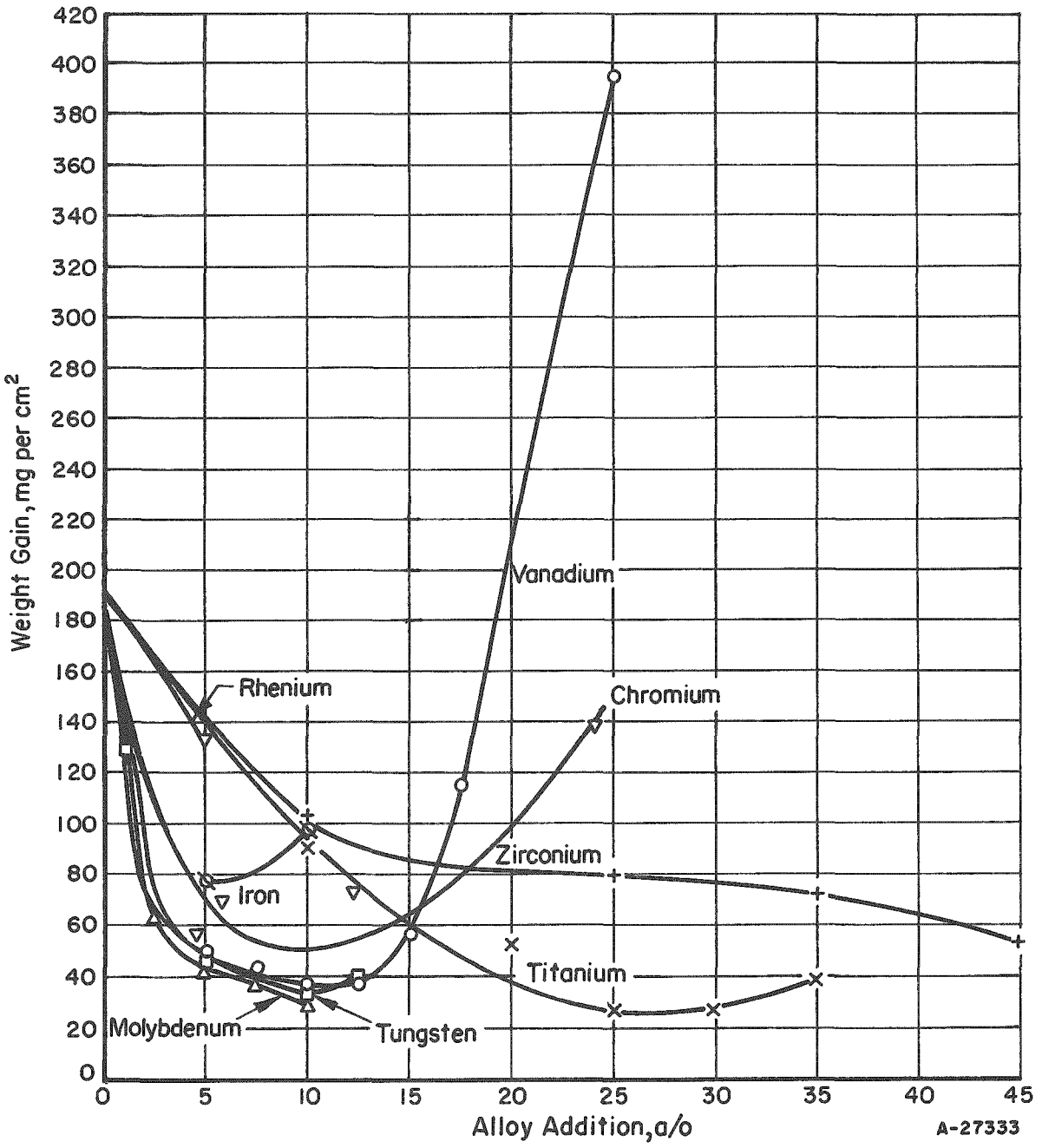

FIGURE 12. WEIGHT GAINS OF NIOBIUM ALLOYS EXPOSED 2 HR IN DRY AIR AT 1200 C (CONTINUOUS-WEIGHING TESTS)

TABLE 7. OXIDATION BEHAVIOR OF NIOBIUM BINARY ALLOYS IN DRY AIR (CONTINUOUS WEIGHING TESTS)

Alloy System	Nominal Addition (Balance Niobium), a/o	Oxidation Behavior at 1000 C				Oxidation Behavior at 1200 C			
		Parabolic Reaction Rate, 10^{-8} $g^2/(cm^4)(sec)$	Time for Transition to Linear, min	Linear Reaction Rate[a], 10^{-6} $g/(cm^2)(sec)$	Weight Gain After 5 Hr[b], 10^{-3} g per cm^2	Parabolic Reaction Rate[a], 10^{-8} $g^2/(cm^4)(sec)$	Time for Transition to Linear, min	Linear Reaction Rate[a], 10^{-6} $g/(cm^2)(sec)$	Weight Gain After 2 Hr[b], 10^{-3} g per cm^2
V	5	4.35	>360	--	27	15.9	35	4.97	44
	7.5	2.73	>360	--	22	9.30	30	4.30	43
	10	1.71	>360	--	17	4.95	50	4.22	36
	12.5	1.19	>360	--	15	7.22	55	6.83	37
	15	2.48	200	0.722	22	7.55	20	7.91	57
	17.5	2.20	80	3.11	33	(5.6)	35	19.1	115
	25	--	0	73.9	(1330)	--	0	(55)	(400)
Mo	2.5	6.20	240	1.01	33	26.0	15	10.0	63
	5	3.69	210	0.827	25	15.7	20	5.84	43
	7.5	1.14	>360	--	15	6.14	55	6.42	37
	10	2.13	100	0.911	23	6.72	35	2.5	29
W	1	--	0	(9.7)	136	--	0	(19.4)	(140)
	5	3.11	10	(8.3)	(150)	28.3	80	3.75	45
	10	3.03	5	(7.5)	106	17.8	180	1.75	35
	12.5	3.17	5	9.5	(170)	21.9	>360	--	39
Cr	4.5[c]	1.65	15	(1.9)	36	16.0	10	6.45	56
	6[c]	--	--	(3.6)	37	--	--	(8.3)	72
	12.5[c]	--	--	(1.3)	15	--	15	(9.2)	72
	24[c]	--	0	41.6	(750)	--	0	19.7	139
Ti	10	6.11	30	3.14	61	--	0	11.8	91
	20	1.41	40	1.06	24	16.7	20	6.50	53
	25	1.42	250	0.722	17	5.36	30	2.94	27
	30	1.19	190	1.61	25	6.00	25	2.78	27
	35	1.54	20	1.44	30	8.33	10	4.89	39
Zr	10	--	0	17.2	(310)	32.2	20	13.5	(97)
	25	41.6	35	7.08	135	62.5	30	8.66	80
	35	29.6	120	2.72	78	44.5	15	7.61	71
	45	12.6	>360	--	48	32.8	50	4.42	52
Fe	1	--	0	7.0	(130)	(3.2)	10	10	79
	5	--	0	7.3	(130)	(5.3)	15	13.2	48
Re	5	--	0	21.4	(390)	--	--	(19)	(130)

(a) Reaction rates in parentheses are estimated.
(b) Weight gains in parentheses are extrapolated.
(c) Corrected compositions.

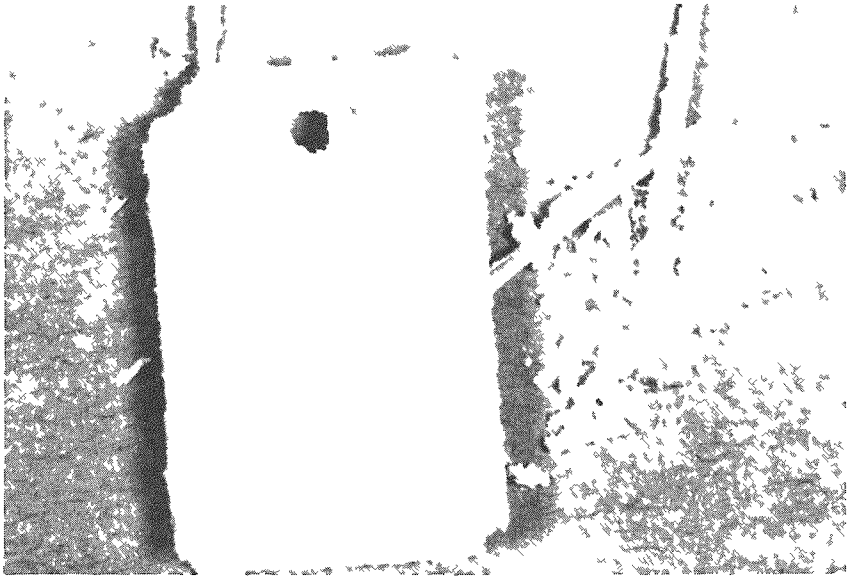

a. Niobium-10 a/o Titanium

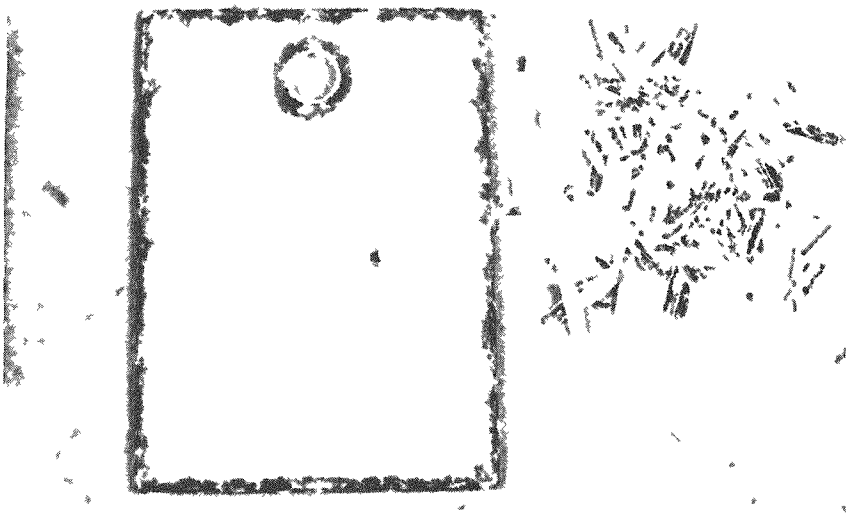

b. Niobium-25 a/o Titanium

FIGURE 13. PHOTOGRAPHS OF NIOBIUM-TITANIUM ALLOYS OXIDIZED 6 HR IN AIR AT 1000 C

Titanium additions up to 25 a/o are effective in improving the oxidation resistance at both 1000 and 1200 C. The reaction curves changed from completely linear for unalloyed niobium to almost completely parabolic at 25 a/o titanium, as seen in Appendix B. Photographs illustrating the character of scale formed are shown in Figure 13. The presence of the white porous layer formed on the 25 a/o titanium alloy is indicative of the transition from parabolic to linear behavior.

Zirconium additions up to 25 a/o effected no improvement at 1000 C and only slight improvement at 1200 C. Additions of 35 and 45 a/o were increasingly effective, promoting protective scales and parabolic behavior. The scale on niobium-45 a/o zirconium is illustrated in Figure 14.

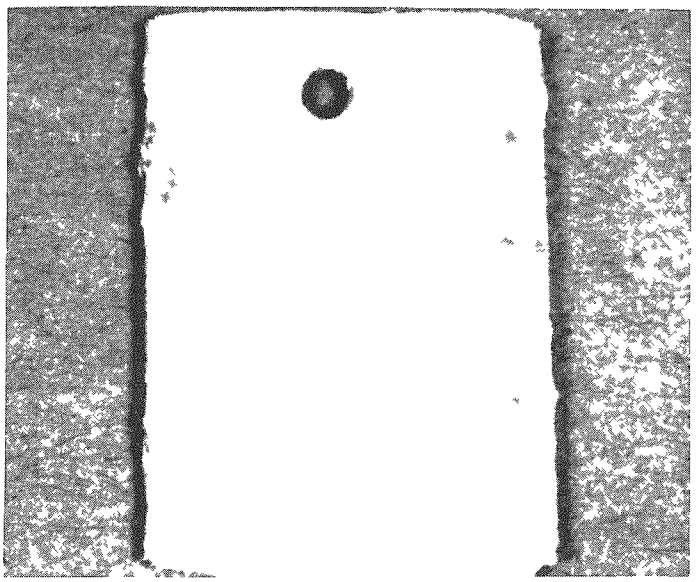

FIGURE 14. PHOTOGRAPH OF NIOBIUM-45 a/o ZIRCONIUM OXIDIZED 6 HR IN AIR AT 1000 C

Vanadium and molybdenum additions were similar in that both effectively improved the oxidation behavior at low alloying levels but decreased the oxidation resistance at higher levels. The most oxidation-resistant compositions in these systems are niobium-12.5 a/o vanadium and niobium-7.5 a/o molybdenum. Photographs of oxidized samples are shown in Figures 15 and 16.

Tungsten additions produced a minor beneficial effect on oxidation behavior at 1000 C but were quite effective in improving the oxidation behavior at 1200 C. The niobium-10 a/o tungsten alloy exhibited parabolic behavior longer at 1200 C than did any other binary alloy. Two oxidized samples of the 5 a/o tungsten alloy are shown in Figure 17.

Four chromium alloys were tested, two of which were exposed as cast owing to the fabrication difficulties encountered in this system. Alloys containing up to 12.5 a/o chromium showed improved oxidation resistance, but a 24 a/o chromium alloy oxidized more rapidly than unalloyed niobium.

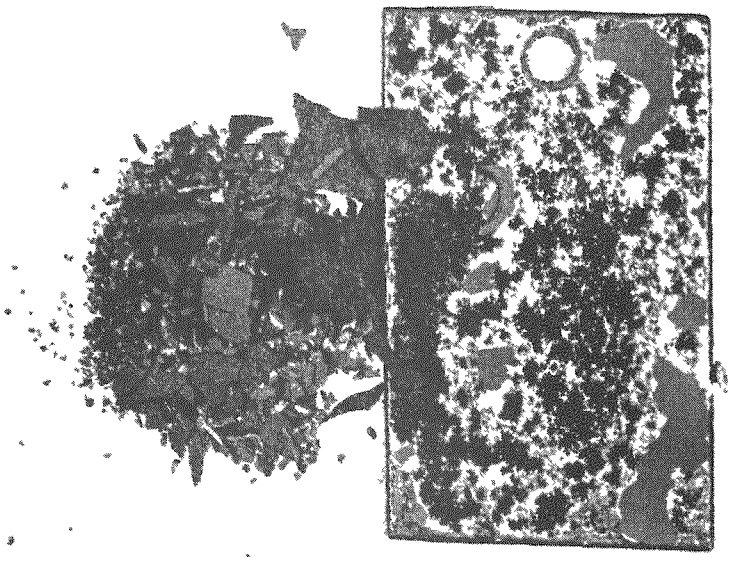

a. Niobium-12.5 a/o Vanadium

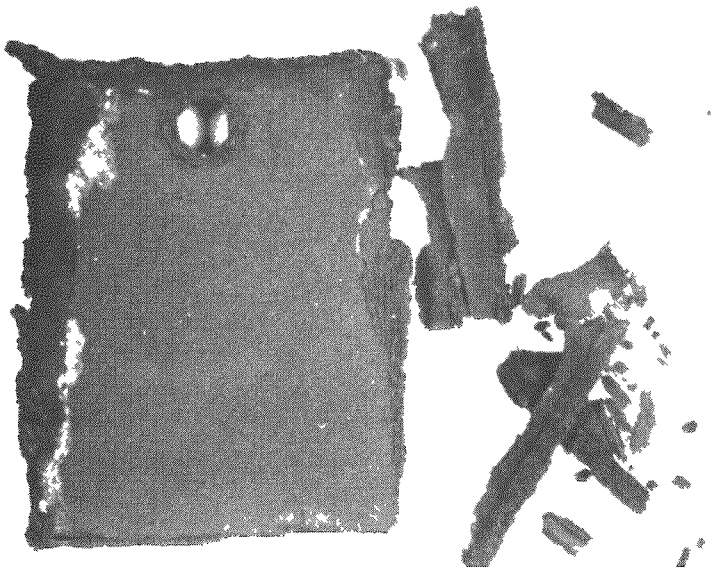

b. Niobium-17.5 a/o Vanadium

FIGURE 15. PHOTOGRAPHS OF NIOBIUM-VANADIUM ALLOYS OXIDIZED 6 HR IN AIR AT 1000 C

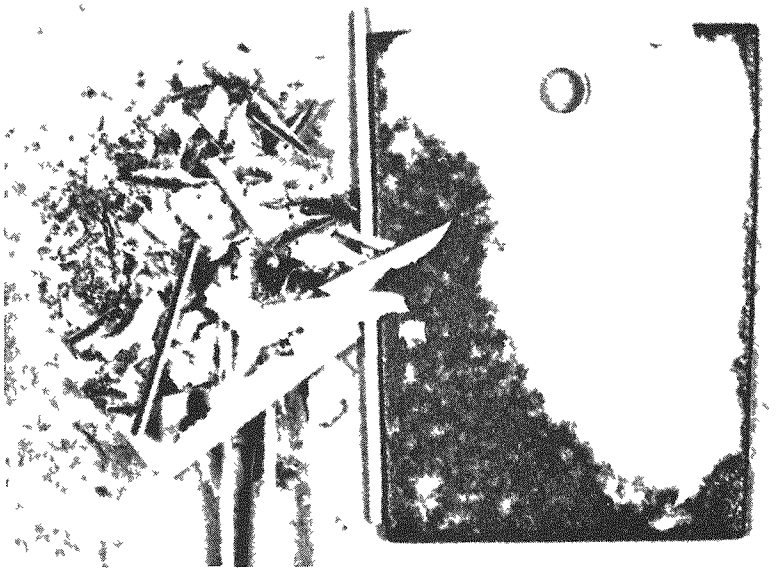

a. Niobium-2.5 a/o Molybdenum

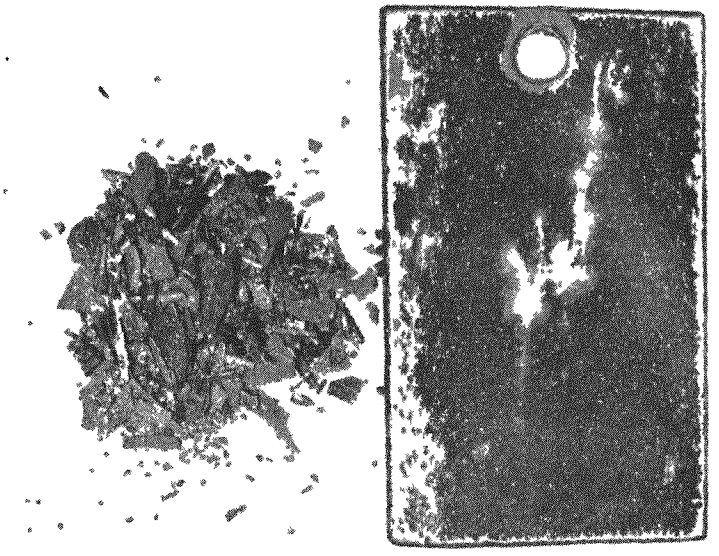

b. Niobium-7.5 a/o Molybdenum

FIGURE 16. PHOTOGRAPHS OF NIOBIUM-MOLYBDENUM ALLOYS OXIDIZED 6 HR IN AIR AT 1000 C

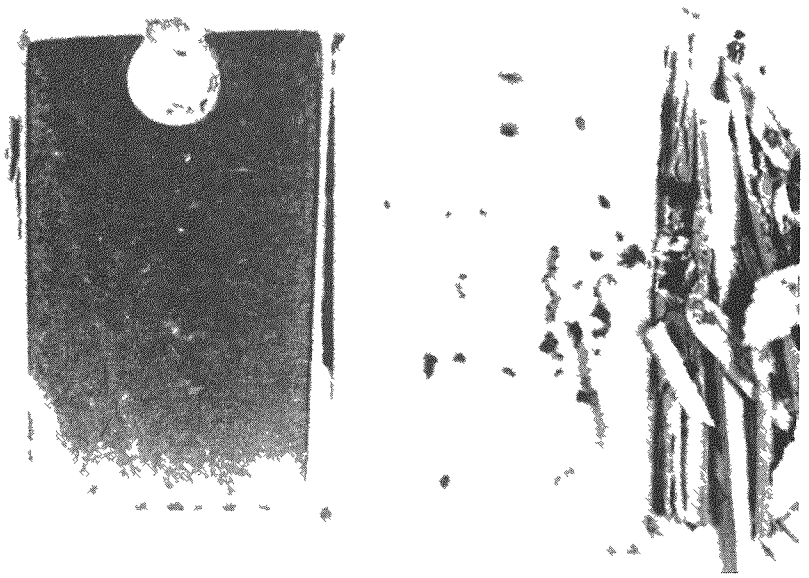

a. Oxidized 3 Hr at 1000 C

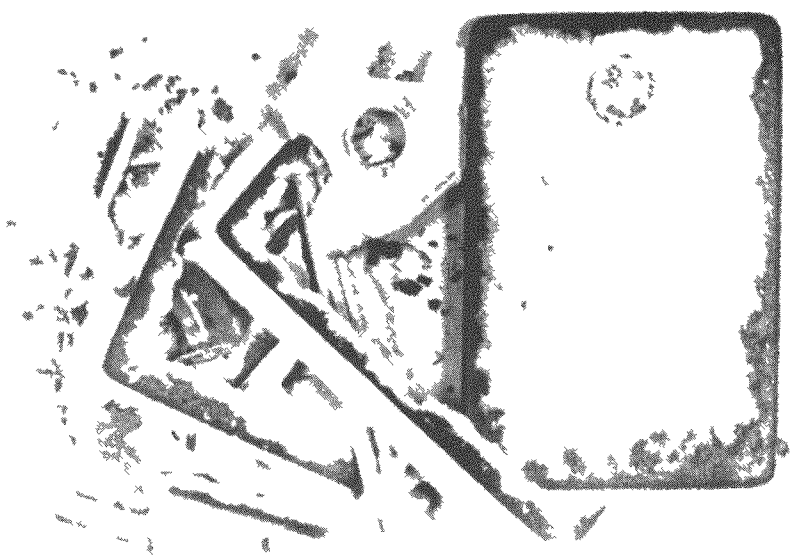

b. Oxidized 2.5 Hr at 1200 C

FIGURE 17. PHOTOGRAPHS OF NIOBIUM-5 a/o TUNGSTEN OXIDIZED IN AIR

No significant effect was observed up to 5 a/o iron, but the addition of 5 a/o rhenium caused an increase in the oxidation rates.

Scale Examination. The scales on all of the binary alloys were examined visually and metallographically. Selected scales were also analyzed chemically and by X-ray diffraction. Most of the alloys, especially those which did not exhibit improved oxidation resistance, formed scales similar to those formed on pure niobium, i.e., a thin, dark, adherent underlayer, and a porous, white, outer seal. Beneficial additions, including chromium, molybdenum, titanium, and vanadium, appeared to stabilize the subscale, allowing it to grow to a greater thickness, and to reduce the amount of porous outer oxide. The nonprotective oxides which formed at 1000 C on higher alloys of chromium, molybdenum, and vanadium were dark, and appeared to have been partially liquid during oxidation.

Metallographic examination revealed single-phased gray scales on all alloys, similar to those on pure niobium. Internal oxidation occurred in the niobium-titanium and niobium-zirconium alloy cores, as can be seen in Figure 18.

Chemical analyses of selected scales formed in undried air at 800 C are given in Table 8. Unfortunately, the best alloys formed too little scale to permit sampling for analysis. Scales on the niobium-tantalum, -tungsten, and -zirconium alloys decreased in oxygen content to 21.8 to 23.4 w/o oxygen alloys at the 25 a/o alloying level compared with 27.3 w/o oxygen analyzed on the pure niobium scale and 30.1 w/o oxygen in stoichiometric Nb_2O_5. The oxides of these metals (Ta_2O_5, WO_3, and ZrO_2) contain less than 26 w/o oxygen, indicating that the scales may be a mixture or double oxide of Nb_2O_5 with the addition-metal oxides. However, low alloys with chromium and titanium also formed scales with lower oxygen content than pure niobium, although their oxides (Cr_2O_3 and TiO_2) contain more than 40 w/o oxygen.

Metal analyses of the scales suggest that tantalum and zirconium are enriched in the scale, while niobium and titanium enter the scale in the same ratio as in the alloy, and chromium, molybdenum, and vanadium are depleted in the scale as compared with the alloy. No conclusions are possible in the cases of aluminum-, cobalt-, iron-, manganese-, nickel-, or silicon-alloy scales since the alloying levels were all less than 0.5 w/o.

X-ray diffraction identifications of scales formed at 1000 C are given in Table 9. The titanium and zirconium scales contained complex oxides, identified from the patterns published by Roth and Coughenour[11]. The lower molybdenum-, tungsten-, and vanadium-alloy scales contained modified Nb_2O_5, while the 24 a/o chromium and 25 a/o vanadium scales were composed of an unidentifiable oxide. The presence of metallic tungsten in the niobium-10 a/o tungsten scale results from the low thermodynamic stability of WO_3 compared with Nb_2O_5.

Contamination Studies. The contamination resistance of all alloys was evaluated by KHN traverses in the same manner as was done for pure niobium. The data for the niobium-titanium, -chromium, and -zirconium alloys are representative of those obtained and are shown in Figures 19 and 20. The diffusion rates associated with the contamination curves were assumed to represent the oxygen-diffusion rates, since oxygen

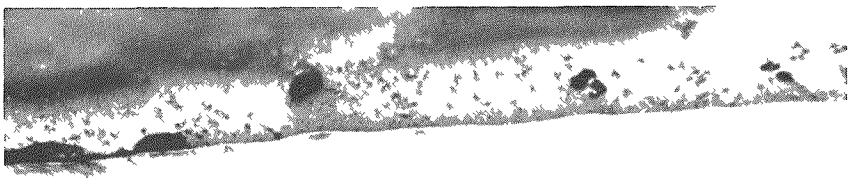

Nb_2O_5-TiO_2 scale

Hard zone

Titanium subscale

Base alloy

250X N44398

a. Niobium-30 a/o Titanium Alloy

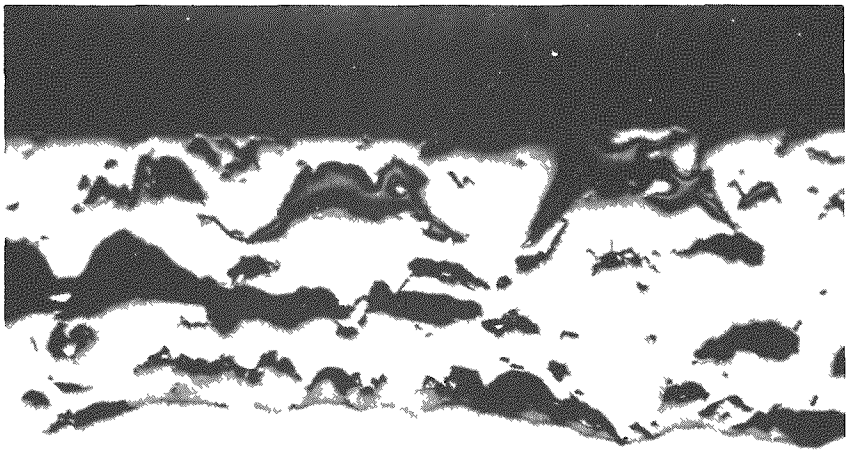

Nb_2O_5-ZrO_2 scale

Zirconium subscale

Base alloy

100X N44405

b. Niobium-35 a/o Zirconium Alloy

FIGURE 18. PHOTOMICROGRAPHS SHOWING SCALES AND SUBSCALES FORMED DURING 6-HR AIR OXIDATION AT 1000 C

TABLE 8. ANALYSES OF SELECTED NIOBIUM ALLOY SCALES FORMED BY REACTION WITH UNDRIED AIR AT 800 C (INTERMITTENT-WEIGHING TESTS)

Alloy Composition (Balance Niobium)					Chemical Analysis of Scale			
	Nominal Addition		Estimated[a] Actual Addition,	Exposure Time,	Alloy[b] Addition,	Oxygen[c],	Niobium[b],	
Alloy Addition	a/o	w/o	w/o	hr	w/o	w/o	w/o	Remarks
None	100	100	100	5	0	27.3	Balance	Nb_2O_5 contains 30.1 w/o oxygen
Ti	5	2.6	2.4	5	1.40	28.0	Balance	
	10	5.4	4.7	10	4.02	23.7	Balance	
	25	14.7	13.6	20	10.0	--	--	
V	5	2.8	2.4	10	1.34	--	--	Sample too small for accurate calculations
	10	5.8	5.0	10	--	--	--	Sample gained weight; insufficient oxide for chemical analysis
	25	15.5	13.2	5	8.1	18.1	52.7	
Mo	5	5.2	5.2	20	1.50	--	--	Sample lost following oxidation
	25	25.6	22.5	5	4.03	24.2	Balance	MoO_3 probably volatilized
Cr	5	2.9	1.7	5	0.22	28.4	67.8	
	25	15.7	9.1	5	2.56	--	--	Sample too small for accurate calculations
Ta	5	9.3	9.3	5	9.4	30.0	Balance	
	25	39.3	39.3	5	40.0	23.4	Balance	
W	5	9.4	9.4	5	6.0	27.6	Balance	
	25	39.8	39.8	1	21.2	23.3	Balance	
Zr	5	4.9	4.9	5	4.5	25.5	Balance	
	25	24.6	24.6	5	24.0	21.8	Balance	
Al	5	1.51	<0.2	5	0.05	Balance	69.3	
Fe	1	0.60	0.23	5	0.31	Balance	68.2	
Si	1	0.30	0.23	5	0.60	Balance	67.9	
Mn	1	0.59	0.04	5	0.09	Balance	68.1	
Co	1	0.64	0.30	5	0.01	Balance	67.5	
Ni	1	0.63	0.30	5	0.04	Balance	69.0	

(a) Estimated from weight-loss data during melting and spectrographic analysis.
(b) By wet chemical analysis.
(c) Vacuum-fusion analysis.

TABLE 9. OXIDES FORMED ON NIOBIUM ALLOYS IN AIR AT 1000 C

Alloy Composition (Balance Niobium), a/o	Air Atmosphere	Oxide Phases		Remarks
		Inner Scale	Outer Scale	
5 Ti	Undried	--	$M' + H' - Nb_2O_5$[a]	Higher symmetry than Nb_2O_5
10 Ti	Dry	$M + H - Nb_2O_5$ and $+ 3Nb_2O_5 \cdot TiO_2$	$M + H - Nb_2O_5$ and $3Nb_2O_5 \cdot TiO_2$	
20 Ti	Dry	$M + H - Nb_2O_5$, $3Nb_2O_5 \cdot TiO_2$, and $Nb_2O_5 \cdot TiO_2$	$M + H - Nb_2O_5$, $3Nb_2O_5 \cdot TiO_2$, and $Nb_2O_5 \cdot TiO_2$	
25 Ti	Undried	$M - Nb_2O_5$	$M - Nb_2O_5$	
30 Ti	Dry	$M + H - Nb_2O_5$ and $3Nb_2O_5 \cdot TiO_2$	$M + H - Nb_2O_5$ and $3Nb_2O_5 \cdot TiO_2$	
45 Zr	Dry	$M - Nb_2O_5$, ZrO_2, and $Nb_2O_5 \cdot 6ZrO_2$	$M - Nb_2O_5$, ZrO_2, and $Nb_2O_5 \cdot 6ZrO_2$	Monoclinic oriented ZrO_2 in both scales
5 V	Undried	$M' + H' - Nb_2O_5$	$M' + H' - Nb_2O_5$	
10 V	Undried	$M' + H' - Nb_2O_5$	Unknown phase	
12.5 V	Dry	$M + H - Nb_2O_5$	$M + H' - Nb_2O_5$	Inner scale oriented
25 V	Dry	--	Unknown phase	
1 Mo	Undried	$M' - Nb_2O_5$	$H - Nb_2O_5$	
5 Mo	Undried	$M - Nb_2O_5$	$M - Nb_2O_5$	
7.5 Mo	Dry	$M' + H' - Nb_2O_5$	$H' - Nb_2O_5$	Inner scale oriented
10 Mo	Dry	$M + H - Nb_2O_5$	$M' + H - Nb_2O_5$	Marked shift in lattice parameters
3 Cr	Undried	--	$M - Nb_2O_5$	
6 Cr	Undried	--	$M' + H' - Nb_2O_5$	
14.5 Cr	Undried	--	$M' + H' - Nb_2O_5$	
24 Cr	Dry	--	Unknown phase	Same pattern as 25 a/o V
10 W	Dry	--	$M' + H - Nb_2O_5$ and W	Same pattern as 10 a/o Mo plus metallic tungsten

(a) H' and M' indicate slight shift in lines compared to H and $M - Nb_2O_5$.

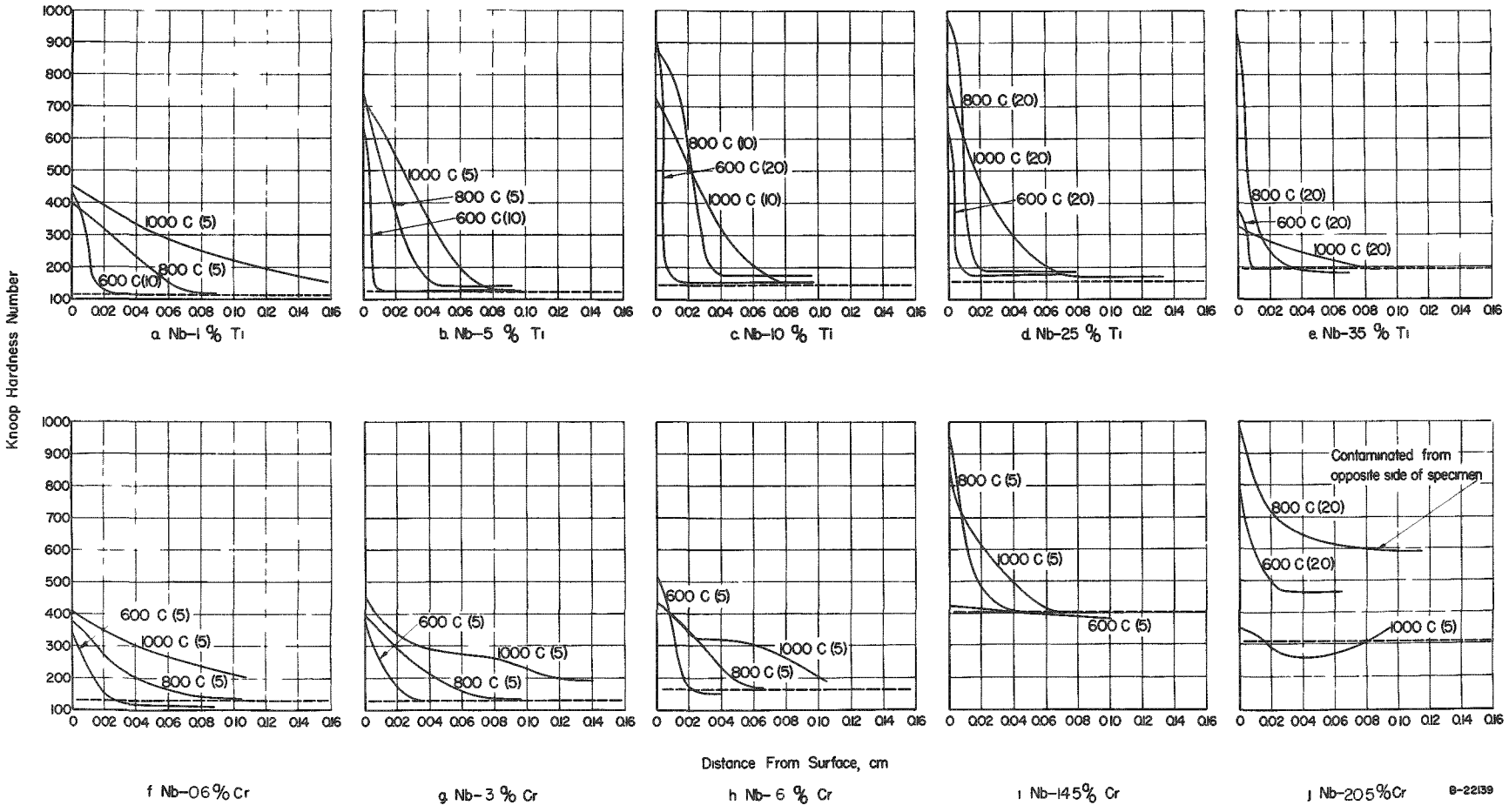

FIGURE 19. DEPTH OF OXYGEN CONTAMINATION IN NIOBIUM-TITANIUM AND -CHROMIUM ALLOYS

Exposure temperature and time in hours is indicated for each curve.

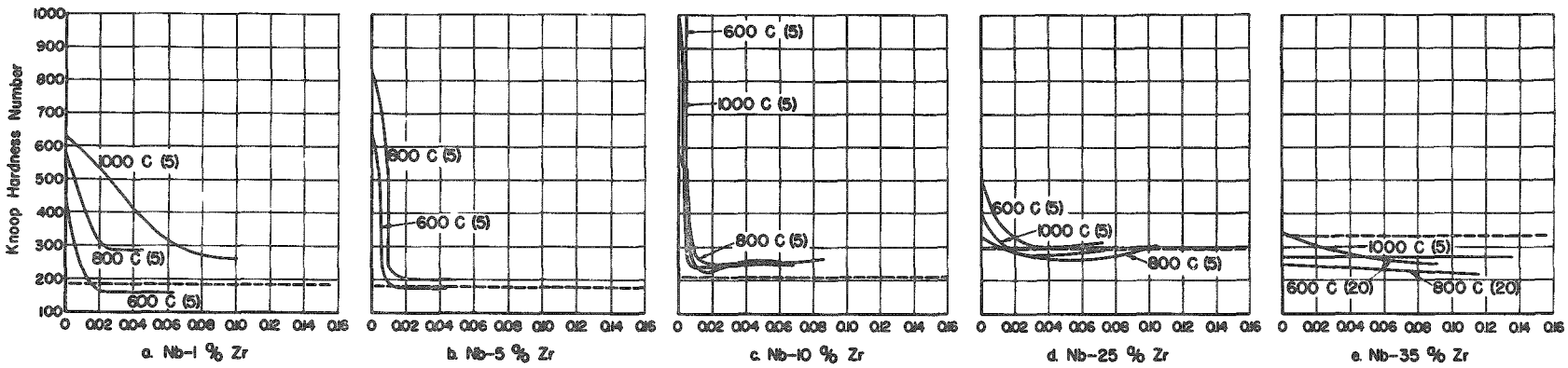

FIGURE 20. DEPTH OF OXYGEN CONTAMINATION IN NIOBIUM-ZIRCONIUM ALLOYS

was concluded to be the major contaminant in unalloyed niobium. The diffusion rates in each alloy and the associated activation energies, as determined graphically from diffusivity-inverse temperature plots, are given in Table 10. Titanium in amounts from 10 to 35 a/o and zirconium in the 20 to 35 a/o range were most effective in reducing oxygen-diffusion rates. The apparent mechanism involved is reaction of the oxygen to precipitate either titanium or zirconium oxide, forming the internal scale noted previously. The 20.5 a/o chromium and 25 a/o vanadium alloys also had lower oxygen diffusivities than unalloyed niobium.

Niobium Ternary Alloys

The effects of ternary alloying were evaluated first by a screening survey on the oxidation behavior at 600 to 1000 C of a large number of cast alloys. The most attractive systems were subsequently further studied by continuous-weighing tests on wrought ternary alloy strips at 1000 and 1200 C. The procedures followed in these tests were identical to those followed in the evaluation of binary alloys.

Intermittent Weight-Gain Tests. Alloys surveyed in the cast condition consisted of ternary combinations of chromium, molybdenum, titanium, and vanadium with niobium, and ternary additions of aluminum, iron, nickel, silicon, vanadium, tungsten, and zirconium to niobium-chromium, -molybdenum, -titanium, and -vanadium bases. The alloys investigated and the results obtained are given in Table 11 as average linear oxidation rates, although linear and parabolic behaviors cannot be distinguished in this type of test.

Chromium, molybdenum, and vanadium additions significantly improve the oxidation resistance of alloys containing moderate amounts of titanium. However, this improvement decreases with increasing titanium content, and only slight improvement is indicated at 25 to 30 a/o titanium. A typical example is the effect of vanadium on the oxidation rates of niobium-titanium alloys, seen in Figure 21.

The intereffects of chromium, molybdenum, and vanadium appear similar to those found for niobium-titanium-base alloys, in that ternary alloying becomes less effective as the minima observed in the binary systems are approached.

Ternary additions of silicon, tantalum, tungsten, and zirconium increased the oxidation rates of niobium-chromium, -molybdenum, and -vanadium alloys, as seen in Table 10. Small amounts of silicon are detrimental to oxidation resistance both as binary and ternary additions, although the mechanism of this effect is not known. Aluminum and nickel had little effect as ternary additions at the low levels investigated.

Ternary additions of 1 to 5 a/o aluminum, cobalt, iron, nickel, silicon, tungsten, or 12.5 a/o tantalum to binary bases containing 12.5 to 24 a/o titanium had little effect on the oxidation behavior. However, addition of 12.5 a/o zirconium to niobium-12.5 a/o titanium caused an increase in the oxidation rate.

Continuous Weight-Gain Tests. Eleven compositions were further evaluated by continuous-weighing oxidation tests at 1000 and 1200 C. Nine of these alloys were

TABLE 10. ACTIVATION ENERGIES FOR OXYGEN DIFFUSION FROM AIR IN NIOBIUM-RICH BINARY ALLOYS

Alloy System	Activation Energy, Q, cal per mole
Pure niobium	24,900
Niobium-titanium	30,800
Niobium-chromium	21,300
Niobium-vanadium	31,600
Niobium-tantalum	35,100
Niobium-tungsten	24,400
Niobium-manganese	23,000
Niobium-iron	26,600
Niobium-cobalt	21,700
Niobium-nickel	24,000
Niobium-aluminum	28,000

TABLE 11. WEIGHT-GAIN AND WEIGHT-LOSS RATES FOR NIOBIUM TERNARY ALLOYS OXIDIZED IN AIR (INTERMITTENT-WEIGHING TESTS)

Nominal Alloy Composition (Balance Niobium)[a], a/o	Cast Hardness, VHN	Weight-Gain Rate, 10^{-6} g/(cm^2)(sec)			Weight-Loss Rate, 10^{-6} g/(cm^2)(sec)		
		600 C	800 C	1000 C	600 C	800 C	1000 C
100 Nb	115	1.58	9.35	6.72	5.11	20.2	8.88
Niobium-Vanadium-Base Alloys							
10 V	172	0.028	0.194	0.972	+[b]	+	1.94
2.5 V-2.5 Mo	149	0.058	0.41	1.14	0.010	0.36	1.70
2.5 V-5 Mo	164	0.042	0.68	1.15	0.054	1.39	1.80
5 V-2.5 Mo	166	0.053	0.44	1.19	0.003	0.475	1.81
5 V-5 Mo	197	0.033	0.78	0.88	0.39	1.56	2.51
2.5 V-17.5 Ti	168	0.031	0.38	0.95	+	0.77	1.17
5 V-5 Ti	170	0.028	0.58	1.53	+	1.15	2.62
5 V-10 Ti	179	0.045	0.98	1.10	+	3.12	1.65
5 V-15 Ti	193	0.033	0.41	0.92	+	1.00	1.16
5 V-20 Ti	194	0.028	0.26	0.78	+	0.033	0.90
7.5 V-2.5 Ti	185	0.031	0.45	1.20	+	0.052	2.96
2.0 V-0.4 Cr	145	0.120	2.41	4.28	0.049	3.63	7.27
2.1 V-1.7 Cr	166	0.047	2.13	2.65	+	2.41	4.56
3.8 V-0.7 Cr	207	0.061	0.79	2.27	0.023	0.84	3.96
3.8 V-0.4 Cr	201	0.033	0.99	2.41	+	1.10	4.30
4.8 V-14.2 Cr	303	0.013	0.15	1.61	0.99	+	2.50
5 V-20 Zr	287	0.189	2.16	5.58	0.59	5.08	9.65
5 V-5 W	227	0.100	2.71	10.1	0.27	9.02	26.6
5 V-5 Ta	188	0.025	2.04	4.49	+	1.21	8.41
10 V-5 Ni	299	0.042	0.30	1.13	0.103	+	1.38
Niobium-Molybdenum-Base Alloys							
5 Mo	166	0.083	0.584	1.28	--	--	--
5 Mo-5 Ti	166	0.031	2.70	1.97	0.033	9.74	4.24
5 Mo-10 Ti	314	0.028	2.04	1.07	+	6.06	1.91
5 Mo-15 Ti	212	0.031	0.98	0.85	+	3.22	1.13
5 Mo-20 Ti	185	0.056	0.47	0.75	+	0.99	0.86
10 Mo-10 Ti	225	0.045	1.96	0.93	+	6.41	1.60
2.1 Mo-2.5 Cr	155	0.050	0.66	1.14	0.078	2.15	1.98
4.2 Mo-1.5 Cr	164	0.044	0.49	1.29	0.060	0.70	3.07
4.2 Mo-2.3 Cr	196	0.036	0.48	1.80	0.059	3.48	5.84
4.7 Mo-10.6 Cr	279	0.029	1.15	0.47	0.014	4.63	0.50
5 Mo-5 W	224	0.035	3.72	6.12	1.04	10.23	18.44
5 Mo-12.5 Ta	186	0.028	2.11	1.22	0.057	5.02	3.15
5 Mo-5 Ni	256	0.124	0.90	1.99	0.81	1.79	3.77
5 Mo-1 Al	172	0.053	0.53	1.01	0.033	1.16	2.59
5 Mo-1 Si	235	0.026	2.71	4.28	1.13	6.41	11.20
Niobium-Chromium-Base Alloys							
15.2 Cr	345	0.14	1.42	1.69	1.03	1.28	9.0
1.0 Cr-9.1 Ti	151	0.025	1.26	1.40	+	3.61	3.05
2.4 Cr-18.2 Ti	165	0.081	0.29	0.70	0.11	0.29	0.95
4.3 Cr-12.3 Ti	183	0.067	0.45	1.08	+	0.66	1.74
4.1 Cr-5.2 Ti	180	0.022	1.49	1.47	+	4.74	2.38
8.8 Cr-12.1 Zr	299	0.89	1.65	10.28	3.85	6.47	20.8
8.9 Cr-5.3 W	279	0.033	2.33	2.83	0.15	8.47	5.27
8.0 Cr-12.6 Ta	192	0.24	1.83	9.45	0.73	4.85	19.74
7.8 Cr-0.04 Ni	258	0.42	9.94	6.39	1.28	22.2	13.1
19.7 Cr-0.5 Al	287	0.17	0.40	3.00	1.21	0.77	5.93
18.4 Cr-0.8 Si	325	0.20	2.57	6.55	0.96	9.54	11.56
Niobium-Titanium-Base Alloys							
25 Ti	156	0.028	0.167	0.528	0.0	0.25	1.39
12.5 Ti-12.5 Zr	197	0.011	0.83	2.94	0.46	3.30	4.13
20 Ti-5 W	198	0.031	0.50	0.77	+	2.04	1.11
12.5 Ti-12.5 Ta	143	0.028	1.61	2.20	+	4.56	3.85
23 Ti-2 Ni	215	0.061	0.31	2.10	0.48	0.66	3.36
25 Ti-5 Ni	253	0.028	0.19	0.82	+	+	1.22
23 Ti-2 Fe	168	0.029	0.23	0.99	+	0.027	1.34
23 Ti-2 Co	213	0.023	0.20	1.03	+	+	1.41
24 Ti-1 Si	198	0.050	0.29	1.08	+	0.143	1.41
24 Ti-1 Al	166	0.044	0.27	1.10	+	0.155	1.55

(a) Compositions for chromium-containing alloys are corrected on the basis of weight losses during melting.
(b) Plus sign indicates specimen gained weight.

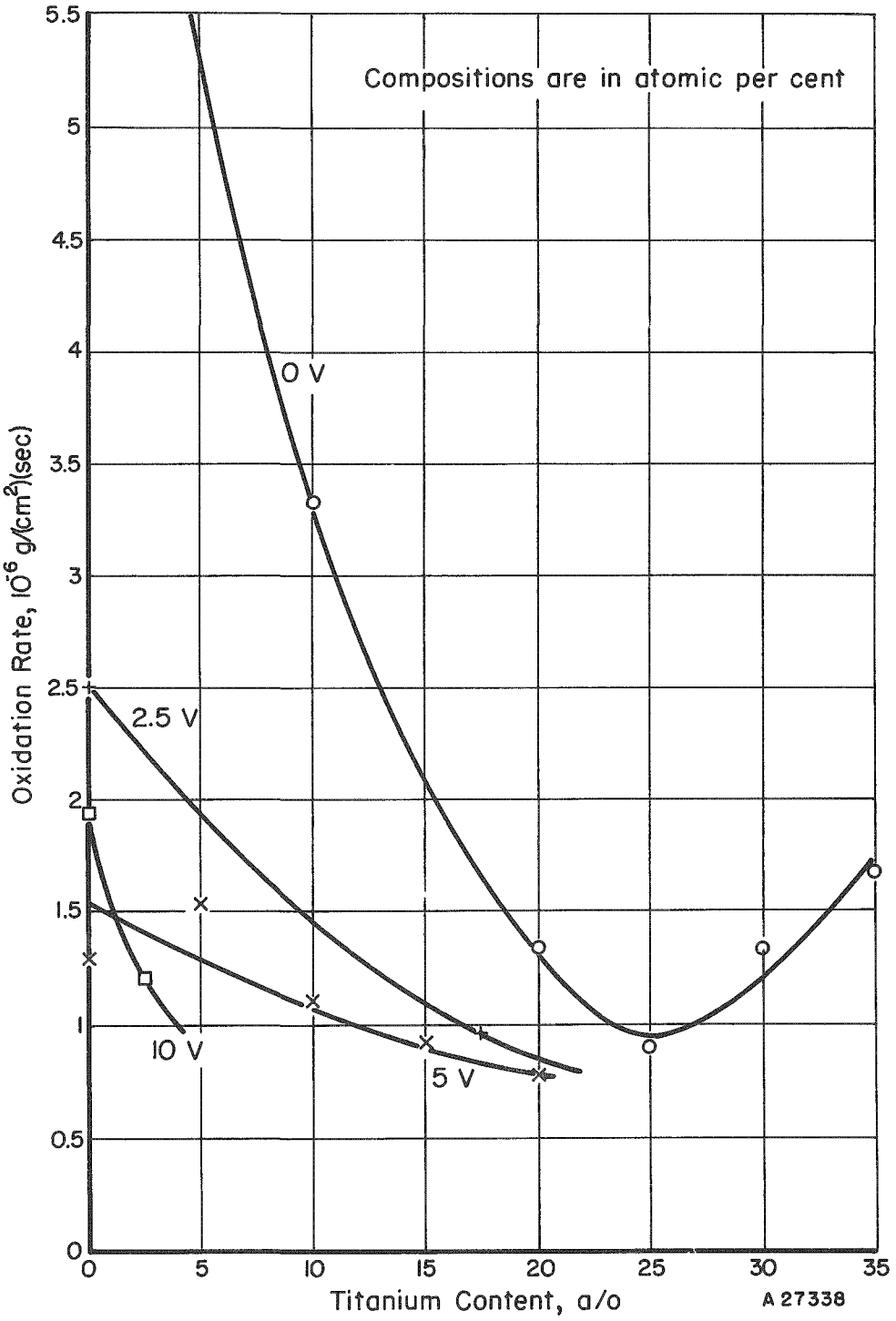

FIGURE 21. EFFECTS OF VANADIUM ON OXIDATION RATES OF NIOBIUM-TITANIUM ALLOYS AT 1000 C IN AIR

niobium-titanium-base with ternary additions of chromium, molybdenum, and vanadium, while two were niobium-molybdenum-chromium and niobium-molybdenum-vanadium. The niobium-titanium-base alloys were hot fabricable but the niobium-molybdenum-base alloys were unfabricable and were tested in the cast condition. Hardness and fabrication data on these ternary alloys is given in Appendix A.

Rate data for the reaction of ternary alloys are given in Table 12. These data generally confirm the results obtained from the screening survey, but also show that some improvement over the best binary alloys is possible. Reaction curves for these ternary alloys are given in Appendix C.

Niobium-titanium-vanadium alloys oxidized at moderately low rates, but the time period for parabolic oxidation was less than for either the niobium-titanium or -vanadium binary alloys. The subsequent linear rates were low, however. The best alloy of the three tested was niobium-16 a/o titanium-8.5 a/o vanadium, which had approximately the same oxidation rate as niobium-25 a/o titanium, the best binary alloy. The oxidized samples are shown in Figure 22.

Each of the niobium-titanium-molybdenum ternary alloys formed adherent scales and showed parabolic behavior over the 6-hr test period at 1000 C. The weight gains at both 1000 and 1200 C were comparable with those of the best binary alloys. However, the observation of white smoke during testing of the 17.5 a/o titanium-6 a/o molybdenum and 23 a/o titanium-8 a/o molybdenum alloys at 1000 C indicates that MoO_3 was volatilizing from the scale. Thus, these compositions are not attractive in spite of their low weight gains.

Niobium-titanium-chromium alloys exhibit good oxidation resistance at both 1000 and 1200 C. Although parabolic behavior does not extend for more than 1 hr, the linear rates are low. The niobium-20 a/o titanium-2 a/o chromium and niobium-28 a/o titanium-6 a/o chromium alloys show 8 and 15 per cent improvements, respectively, over the best binary alloy, based on 5-hr weight gains.

Niobium-molybdenum-base alloys also show improved oxidation resistance. Niobium-7.5 a/o molybdenum-10.5 a/o chromium oxidized 20 per cent slower than niobium-25 a/o titanium. Molybdenum oxide apparently does not volatilize from the scales on these alloys, as no smoking was observed.

TABLE 12. OXIDATION BEHAVIOR OF NIOBIUM TERNARY ALLOYS IN DRY AIR (CONTINUOUS-WEIGHING TESTS)

Corrected Alloy Composition (Balance Niobium)[a], a/o	Oxidation Behavior at 1000 C: Parabolic Reaction Rate, 10^{-8} $g^2/(cm^4)(sec)$	Oxidation Behavior at 1000 C: Time for Transition to Linear, min	Oxidation Behavior at 1000 C: Linear Reaction Rate, 10^{-6} $g/(cm^2)(sec)$	Oxidation Behavior at 1000 C: Weight Gain After 5 Hr, 10^{-3} g per cm^2	Oxidation Behavior at 1200 C: Parabolic Reaction Rate, 10^{-8} $g^2/(cm^4)(sec)$	Oxidation Behavior at 1200 C: Time for Transition to Linear, min	Oxidation Behavior at 1200 C: Linear Reaction Rate, 10^{-6} $g/(cm^2)(sec)$	Oxidation Behavior at 1200 C: Weight Gain After 2 Hr, 10^{-3} g per cm^2
Niobium-Titanium-Vanadium Alloys								
10.5Ti-5V	1.52	70	0.80	20.3	14.9	20	4.6	44.0
16Ti-8.5V	0.87	80	0.65	15.7	7.2	40	2.6	27.2
22.5Ti-11V	1.37	25	2.8	46.5	7.5	10	5.1	43.2
Niobium-Titanium-Molybdenum Alloys								
12Ti-4Mo	1.90	>360	--	18.3	4.7	10	(4.3)	40.0
17.5Ti-6Mo	1.38	>360	--	16.2	6.5	5	(3.7)	39.4
23Ti-8Mo	1.29	>360	--	15.3	6.6	15	4.3	30.5
Niobium-Titanium-Chromium Alloys								
12Ti-1.5Cr	1.39	15	1.39	30.6	--	0	5.6	53.6
20Ti-2Cr	0.22	60	0.83	13.6	(2.7)	5	4.5	39.7
28Ti-6Cr	0.32	45	0.65	12.6	1.9	10	4.3	31.7
Niobium-Molybdenum-Base Alloys								
5.5Mo-8V	1.1	>360	--	14.0	10.2	240	1.53	26.6
7.5Mo-10.5Cr	0.79	>360	--	11.9	1.33	10	2.3	19.1

(a) Niobium-titanium-base compositions were corrected on the basis of spectrographic analyses; niobium-molybdenum-base compositions are estimated on the basis of melting weight losses.

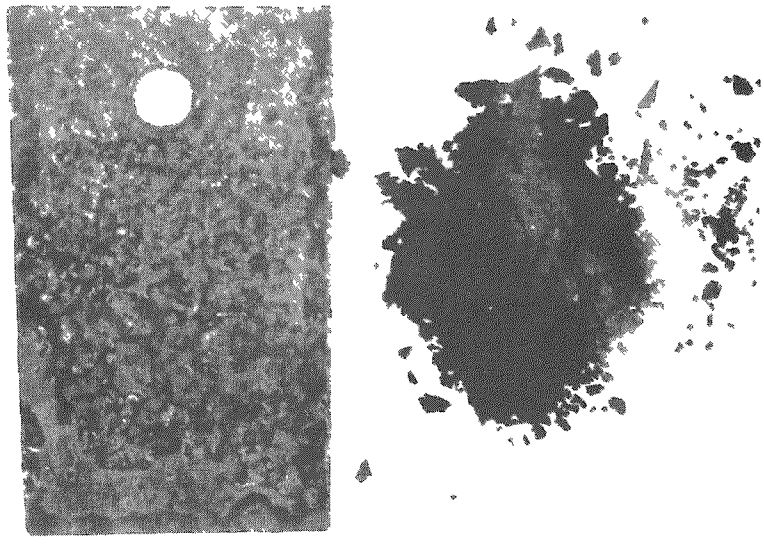

a. Oxidized 6 Hr at 1000 C

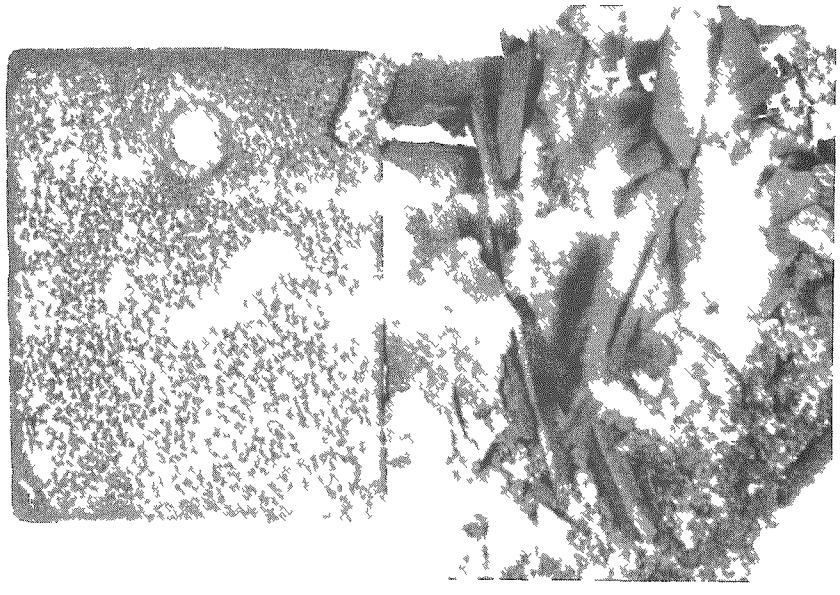

b. Oxidized 6 Hr at 1200 C

FIGURE 22. PHOTOGRAPHS OF NIOBIUM-16 a/o TITANIUM-8.5 a/o VANADIUM OXIDIZED IN AIR

DISCUSSION

Theoretical Aspects

The oxidation behavior of metals can usually be classified into one or more of four types, according to the time-dependent nature of the oxidation reaction.[12] These types are the logarithmic, cubic, parabolic, and linear relationships, and are written as

$$W = k_a \log (At + 1) \text{ (logarithmic)}, \tag{3}$$

$$W^3 = k_c t \text{ (cubic)}, \tag{4}$$

$$W^2 = k_p t \text{ (parabolic)}, \tag{5}$$

$$W = k_\ell t \text{ (linear)}, \tag{6}$$

where

W is the specific weight gain, g per cm^2

k is the rate constant

A is a constant

t is time, sec.

The logarithmic relationship describes the growth of very thin films, up to thicknesses of 100 A or so, such as the films which form on aluminum at room temperature. The cubic relationship holds for slightly thicker films, such as those formed on copper between 100 and 250 C. Since these relationships are applicable to relatively thin films formed at lower temperatures, they are not applicable to the present study and will not be discussed further.

The parabolic relationship has been found to describe the oxidation behavior of many metals and alloys. The theoretical aspects of parabolic behavior have been well developed by Wagner, Hauffe, and others. The parabolic relationship describes the growth of moderately thick* films which are fully adherent and protective. The rate of reaction is controlled by ionic diffusion through the film, and at any given time is inversely proportional to the film thickness. This relationship is written as

$$\frac{dW}{dt} = \frac{1}{2}\frac{k_p}{W}, \tag{7}$$

which, on integration, leads to Equation (5).

The oxides which form during parabolic oxidation can be classified according to their semiconducting properties, as determined partially from the temperature and pressure dependencies of their electrical conductivities. The various types are:

*Thick in the sense that strong electrical fields do not act through the film as in the case of thin films which grow logarithmically.

(1) Metal-excess semiconductor

(2) Anion-deficit semiconductor

(3) Metal-deficit semiconductor

(4) Anion-excess semiconductor.

The metal-excess and anion-deficit semiconductors have interstitial metal ions and oxygen-ion vacancies in the oxide lattice, respectively, while the metal-deficit and anion-excess semiconductors are characterized by metal-ion vacancies and interstitial oxygen ions, respectively. From the results of Pranatis and Seigle[3], Nb_2O_5 can be classified as either a metal-excess or anion-deficit semiconductor. Hence, diffusion through Nb_2O_5 occurs by movement of either interstitial metal ions or by oxygen-ion vacancies.

The parabolic reaction rates vary with temperature according to the usual Arrhenius-type relationship,

$$K_p = K_p' e^{-\Delta H/RT}. \tag{8}$$

Pressure effects on the parabolic rates vary according to the semiconducting properties of the scale. The oxidation rates of metals forming metal-deficit oxides (containing metal-ion vacancies) such as copper and nickel decrease with decreasing oxygen pressure according to a fractional power of the pressure. Metals forming metal-excess oxides (interstitial metal ions) are less affected by oxygen pressure because they have a small number of defects at the oxide-gas interface. For metals forming oxides in which oxygen-ion diffusion predominates, pressure effects have been noted but not correlated with the oxide structure.

Contamination of the base metal occurs by diffusion of oxygen into the metal from the innermost oxide layer. The amount of contamination is temperature dependent, but does not vary with pressure as long as bare metal is unexposed.

Linear oxidation occurs when the reaction product is volatile, molten, or porous. The theoretical aspects of linear oxidation are much less well developed than for parabolic oxidation. Several qualitative explanations for the observation of linear behavior have been advanced:

(1) Destruction of the oxide film exposes bare metal to the attacking gas, and the reaction is controlled by the rate of combination,

$$Me^+ + O^- \rightarrow MeO,$$

which occurs directly at the metal-gas interface, or by the rate of dissociation of the attacking gas.

(2) Only the outer layers of the film are destroyed (or rendered non-protective) and a thin film remains adherent to the metal. The reaction is controlled by the diffusion resistance of this layer, which remains at constant thickness, leading to a linear reaction.

A useful criterion for determining whether protective or nonprotective (solid) scales will be formed involves the scale/metal volume ratio, commonly known as the Pilling-Bedworth ratio. Ratios less than unity indicate that the oxide occupies less volume than the original metal and the oxide is expected to be porous. Ratios greater than unity indicate that the oxide occupies a larger volume and should be adherent and protective. This concept has been modified recently[13,14], since oxides which grow by metal-ion diffusion form a new oxide at the oxide-gas interface and are unaffected by the volume ratio. In cases where oxygen-ion diffusion predominates, the new oxide forms at the metal-oxide interface and is affected by the volume ratio. Scales with very high volume ratios (>2.5) which grow by oxygen-ion diffusion may become porous through cracking due to excessive compressive stresses generated by the high volume ratio.

The reaction occurring when a duplex scale is formed, consisting of a porous layer overlaying a compact layer, may be treated as a combination of two simultaneous reactions, or as two successive reactions. Webb, Norton, and Wagner[15] have described the oxidation of tungsten as consisting of parabolic growth of an adherent blue subscale and simultaneous linear transformation of the blue scale to a yellow porous scale. The reaction becomes completely linear when the linear rate of transformation of the adherent scale to the porous scale equals the instantaneous rate of formation of the adherent scale. Cathcart, Campbell, and Smith[16], however, showed that the reaction of niobium with oxygen at 500 C consists of an initial parabolic reaction, but after a certain temperature-dependent period, the outer portion of the scale blisters. After this point, the reaction is linear, being controlled by diffusion through a constant-thickness remnant of the initial film. The theories of Webb, et al., and Cathcart, et al., thus differ as to whether breakdown of the protective film occurs simultaneously with its growth or after a certain thickness has been reached.

The temperature dependency of linear reaction rates follows the Arrhenius relationship,

$$K_\ell = K_\ell' e^{-\frac{\Delta H}{RT}}. \qquad (9)$$

The pressure dependency of linear reactions is complicated, since pressure affects both diffusion rates and the thickness of the adherent subscale. Pressure dependency of linear reactions has also been correlated with absorption of the gas at the scale-gas interface.

Contamination during linear reactions is essentially identical with that occurring during parabolic reactions, provided that the oxide phase at the metal-oxide interface is unchanged.

The theoretical aspects of alloying effects on oxidation behavior have been reviewed recently by Kubaschewski and Hopkins[12]. Although the behavior of only a few simple systems can at present be calculated with any degree of certainty, two principles are known to be effective. These principles include:

(1) The valence effects of the alloying addition

(2) The ability of the alloying addition to preferentially form a new, protective scale.

On the basis of the present work, a third principle affecting alloy behavior has been deduced. This concerns size effects of the alloying addition.

The effects of valence on the oxidation behavior depend on the type of semiconducting oxide formed by the base metal. As pointed out earlier, metal-excess and anion-deficit semiconductors have interstitial metal ions and oxygen-ion vacancies, respectively. The addition of metal ions of higher valence than the base metal decreases the number of interstitial metal ions or oxygen-ion vacancies in order to maintain electrical neutrality in the oxide. Since these defects are the means by which diffusion occurs through the scale, reduction in their number decreases ionic diffusion rates and thus the oxidation rate of the alloy. The addition of metal ions of lower valence acts oppositely, increasing the number of defects and increasing the alloy oxidation rate.

Conversely, if the oxide is of the metal-deficit or anion-excess types, higher-valence additions act to increase oxidation rates and lower-valence additions decrease the oxidation rates.

The effects of valence have been studied mostly on base metals which form completely adherent scales, i.e., those which oxidize parabolically. The effects are expected to be identical in the adherent subscale which forms during linear oxidation. Other effects of the additions, however, such as variations in the equilibrium thickness of the subscale, make the valence effects difficult to distinguish when linear oxidation prevails.

In the range beyond the solubility limit for the addition-metal ions in the base-metal scale, new oxides must form. These may consist of mixed oxides or pure oxides of the alloying addition. The locale of formation of the new oxides, i.e., at the metal-oxide or oxide-gas interface, is determined by the concentration of the alloy addition at the metal surface and the thermodynamic stability of the addition oxide as compared with the base-metal oxide. Additions with higher oxide stabilities than the base metal will preferentially form their own oxides (in the idealized case) at the metal-oxide interface at relatively low alloying levels, provided also that ionic diffusion rates in the new oxides are lower than in the base-metal oxides. The amount of alloying necessary to allow the addition oxide to form at the metal-oxide interface can be calculated in simple cases. However, in most cases, the situation is complicated because complex oxides are formed. The generalization regarding the relative thermodynamic stabilities of the new oxide is still valid. Other criteria of the effectiveness of alloying in the higher alloying range include the mechanical and physical stabilities of the new oxides. The new oxides should be mechanically stable toward cracking and must be solid if they are to be protective.

Internal oxidation may also result during oxidation of an alloy if the addition forms oxides which are considerably more stable thermodynamically than those of the base metal. In alloys of this type, oxygen diffusing into the metal core from the scale preferentially reacts with the constituent whose oxide is most stable, precipitating the oxide of this constituent in a matrix of the oxygen-saturated base metal. Contamination rates are reduced in alloys of this type as compared with the unalloyed base.

The relationship between size of the alloying atoms and oxidation behavior has not been studied in detail. At lower alloying levels, however, the alloy atoms would be

expected to enter the scale substitutionally provided that their ionic sizes are not too different from that of the base-metal ions. It has previously been shown that the lattice parameter of FeO (metal-deficit semiconductor) is increased by addition of smaller Mg^{+} ions, since these ions occupy the metal-ion vacancies.[12] Size effects in metal-excess and anion-deficit oxides would differ as a solution of new metal ions would be by replacement of base-metal ions. As will be shown later, a definite correlation was found between the relative ionic sizes of alloying additions to niobium and their effect on the oxidation resistance of niobium. Briefly, this work indicates that larger ions increase the linear oxidation rate, while smaller ions decrease the oxidation rate and promote more protective scales.

The temperature dependency of alloy-oxidation rates is similar to that for pure metals and can be expressed by an Arrhenius-type relationship. The pressure dependency of alloy-oxidation rates has received little attention. It is probably similar to that for pure metals, i.e., is determined by the semiconducting properties of the oxide and by pressure effects on the equilibrium scale thickness if the oxidation behavior is linear.

Correlation of Experimental Data

The observation of a duplex scale on unalloyed niobium, the inner layer of which is preferentially oriented, affords a basis for speculation on the mechanisms of niobium oxidation. Since both the inner adherent portion and the outer porous portion of the scale consist primarily of Nb_2O_5 (only traces of NbO were noted in the inner scale), the lower oxides are apparently not present in sufficient quantity to affect the oxidation reaction.

The initial reaction is proposed to be formation of an adherent layer of Nb_2O_5, which grows by diffusion of oxygen through the scale to the metal-oxide interface, where reaction of niobium and oxygen ions continues to form Nb_2O_5.

The adherent Nb_2O_5 layer continues to grow until compressive stresses in its outer layer cause this layer to buckle. The compressive stresses arise from the very high oxide/metal volume ratio (2.59) of niobium. The outer layer continues to buckle, forming the porous, nonprotective white oxide, until the adherent layer is reduced to a stable thickness. At low temperatures, i.e., up to about 600 C, the adherent scale probably grows to greater than its stable thickness before buckling, but at higher temperatures the scale begins to crack upon reaching the stable thickness. These proposed reactions are illustrated diagrammatically in Figure 23.

The stable scale thickness can be calculated by rewriting Equation (7) as:

$$W = \frac{1}{2}\frac{k_p}{k_\ell}, \qquad (10)$$

where W is the stable scale thickness, k_p is the parabolic reaction rate, and k_ℓ is the linear reaction rate. Although the initial parabolic rates of unalloyed niobium could not be obtained from the unalloyed-niobium reaction data obtained in this work, the magnitude of these rates may be deduced from interpolation between alloy parabolic rates

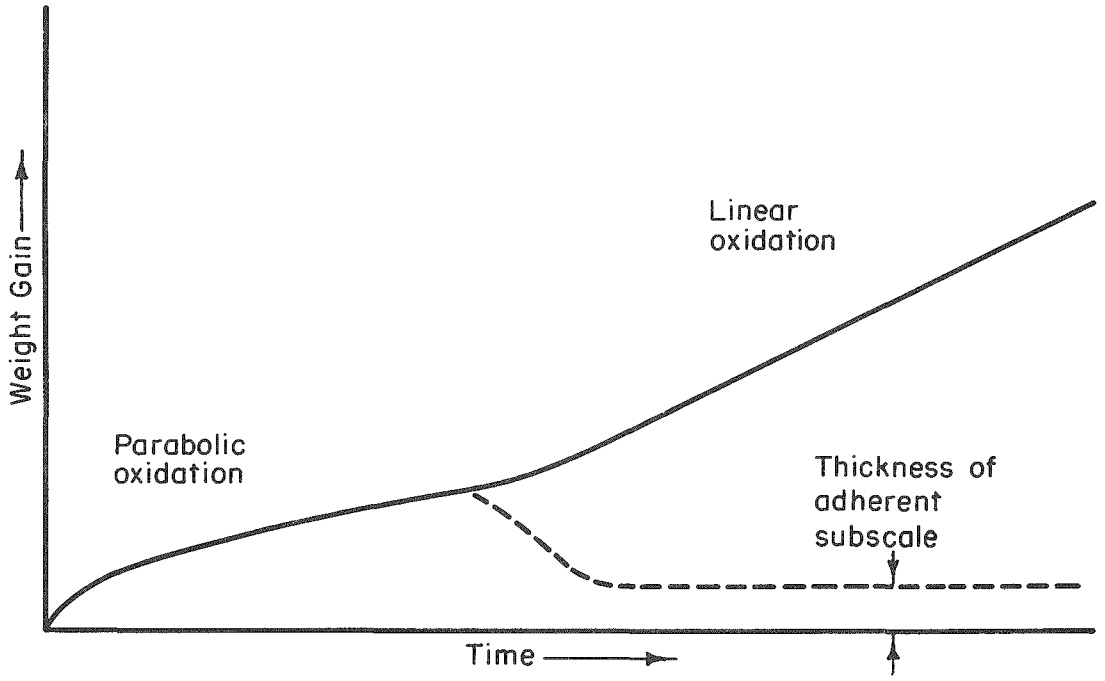

a. Behavior at Low Temperatures

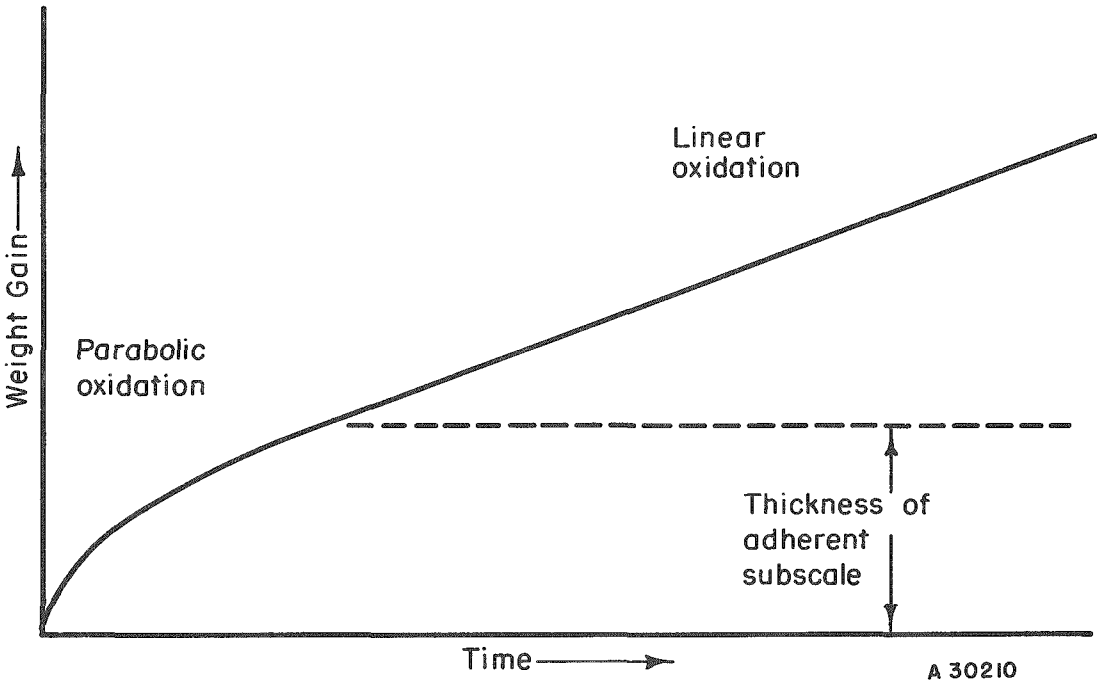

b. Behavior at High Temperatures

FIGURE 23. DIAGRAMMATIC ILLUSTRATION OF OXIDATION BEHAVIOR OF NIOBIUM AT LOW AND HIGH TEMPERATURES

extrapolated to zero alloying content and the low-temperature parabolic rates of Gulbransen and Andrew[4]. These relationships are shown in Figures 24 and 25. Estimated values for the stable inner-scale thickness are calculated in Table 13 and are seen to range from 1.3 μ at 600 C to 80 μ at 1200 C. The increase in stable-scale thickness with temperature might be expected to result from the increasing plasticity of Nb_2O_5 with temperature.

TABLE 13. REACTION RATES AND ESTIMATED STABLE-SCALE THICKNESSES OF NIOBIUM IN AIR

Temperature, C	Measured Linear Reaction Rate, $g/(cm^2)(sec)$	Estimated Parabolic Reaction Rate, $g^2/(cm^4)(sec)$	Calculated Thickness of Inner Scale		Calculated Transition Time, Parabolic to Linear, sec
			g per cm^2	μ	
600	5.4×10^{-7}	2×10^{-10}	1.9×10^{-4}	1.3	1.7×10^{2}
800	3×10^{-6}	6.5×10^{-9}	1.1×10^{-3}	7.4	1.8×10^{2}
1000	9.5×10^{-6}	9.3×10^{-8}	5×10^{-3}	33	2.6×10^{2}
1200	1.6×10^{-5}	4×10^{-7}	1.2×10^{-2}	80	3.8×10^{2}

The proposed mechanism does not account for the breaks in the rate-versus-temperature plot (Figure 1), but does account for the presence of the inner layer of scale and provides a model whereby the rate-controlling reaction in linear oxidation (diffusion through the adherent subscale) is similar to that which has proven so helpful in understanding fully parabolic reactions.

The effects of alloying on niobium oxidation can be related to certain properties of the alloy additions and their oxides. As described previously, three types of effects are found:

(1) Valence effects

(2) Size effects

(3) New-scale effects.

The valence, ionic size, and oxide characteristics of each alloy addition investigated are listed in Table 14. Table 15 summarizes the anticipated and observed oxidation effects of those additions (which were investigated in detail) according to the mechanisms which are believed to be involved.

In the low alloying range where the addition ions are soluble in Nb_2O_5, the data lend strong support to the fact that the size effect predominates over the other mechanisms. Thus, for alloy concentrations up to about 15 a/o, chromium, molybdenum, tungsten, and vanadium, which have ionic radii ranging from 9 to 15 per cent

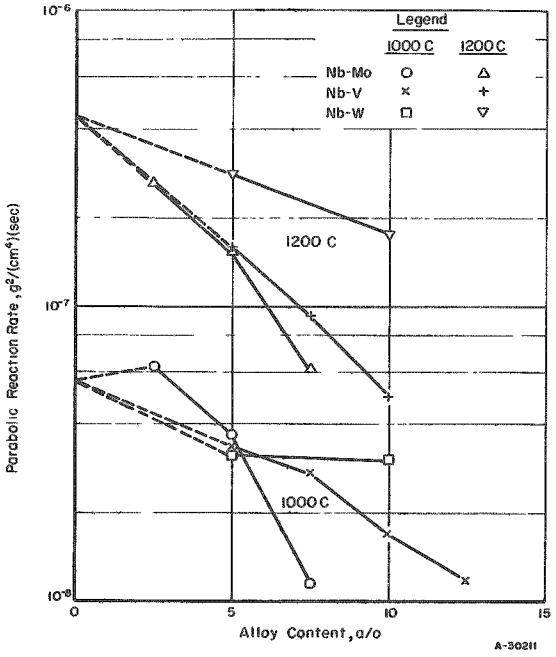

FIGURE 24. EXTRAPOLATION OF ALLOY REACTION RATES TO ZERO ALLOY CONTENT

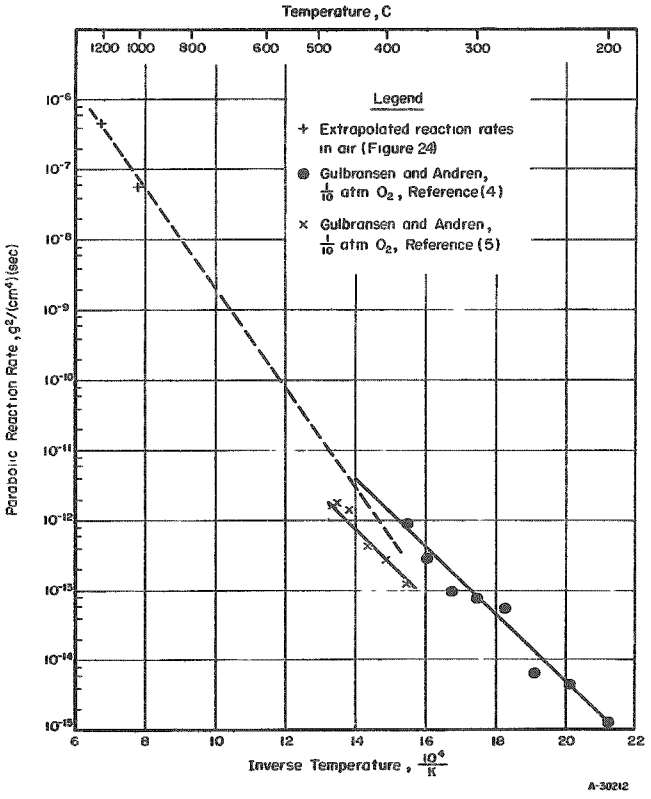

FIGURE 25. RELATIONSHIP BETWEEN EXTRAPOLATED HIGH-TEMPERATURE REACTION RATES AND PUBLISHED LOW-TEMPERATURE REACTION RATES FOR UNALLOYED NIOBIUM

TABLE 14. VALENCE, IONIC SIZE, AND OXIDE CHARACTERISTICS OF ALLOYING ELEMENTS ADDED TO NIOBIUM[12,17,18,19]

Element	Valence	Goldschmidt Ionic Radius, A	Oxide Properties: $-\Delta F$ at 1300 K, kcal per g atom of oxygen	Oxide Properties: Melting Point, C	Oxide Properties: Boiling Point, C	Oxide Properties: Conductivity at 20 C, $ohm^{-1}\ cm^{-1}$	Oxide Properties: Oxide-Metal Volume Ratio
Mn	2	0.80	69.3	1790	--	1×10^{-8}	1.79
Zr	4	0.79	101.4	2715	--	$<10^{-8}$	1.56
Co	2	0.72	33.3	1810	--	1×10^{-2}	1.86
Ni	2	0.69	28.6	1960	--	8×10^{-4}	1.65
Nb	5	0.69	63.9	1460	--	1.2×10^{1}	2.69
Ta	5	0.68	70.8	>1900	--	1×10^{-5}	2.54
Ti	4	0.68	84.8	1860	--	4×10^{0}	1.73
Fe	3	0.64	39.0	--	--	2.1×10^{1}	2.14
Cr	3	0.63	63.6	2440	--	1.2×10^{-4}	2.07
Mo	6	0.62	35.5	795	1460	1.3×10^{-7}	3.24
W	6	0.62	41.3	1470	1750	5×10^{-2}	3.35
V	5	0.59	49.6	660	--	3×10^{0}	3.19
Re	7	0.56	21.6	266	363	$<10^{-8}$	1.67
Al	3	0.50	100.3	2020	--	$<10^{-8}$	1.49
Si	4	0.41	77.2	1713	--	$<10^{-8}$	2.21
Be	2	0.35	112.8	1283	--	$<10^{-8}$	1.68
B	3	0.23	76.5	450	--	$<10^{-8}$	2.02

TABLE 15. EFFECTS OF BINARY ALLOYING ON OXIDATION OF NIOBIUM

Alloy Addition	Expected Effects of Addition Properties on Oxidation Behavior: Low Alloy Range, Size Effect	Low Alloy Range, Valence Effect	High Alloy Range, Properties of Addition Oxide Evident: Physical Stability	Thermodynamic Stability	Mechanical Stability	Diffusion Resistance	Observed Oxidation Effects
V	Improve mechanical stability of scale	No effect	Poor	--	--	--	Vanadium stabilizes Nb_2O_5 toward cracking up to 12.5 a/o at 1000 C, and partially stabilizes Nb_2O_5 up to 10 a/o at 1200 C; at higher levels a partially molten complex scale forms and causes rapid linear oxidation
Mo	Improve mechanical stability of scale	Decrease diffusion rates in scale	Poor	--	--	--	Molybdenum stabilizes Nb_2O_5 toward cracking up to 7.5 a/o at 1000 C, and partially stabilizes Nb_2O_5 up to 10 a/o at 1200 C; size effects are more prominent than valence effects; at higher alloying levels a partially molten complex scale forms and causes rapid linear oxidation
W	Improve mechanical stability of scale	Decrease diffusion rates in scale	Good	Lower than niobium	Poor	Low	Tungsten has little effect at 1000 C; at 1200 C tungsten improves the mechanical stability of Nb_2O_5 up to 12.5 a/o
Cr	Improve mechanical stability of scale	Increase diffusion rates in scale	Good	Same as niobium	Good	Good	Chromium improves the oxidation resistance of niobium to about 15 a/o; above this level a partially liquid scale forms, decreasing the oxidation resistance
Ti	No effect	Increase diffusion rates in scale	Good	Higher than niobium	Good	Poor	Titanium has little effect at low alloying levels; at high alloying levels complex Nb_2O_5-TiO_2 scales form and oxidation resistance is improved; titanium also causes internal oxidation
Zr	Decrease mechanical stability of scale	Increase diffusion rates in scale	Good	Higher than niobium	Good	Good	Zirconium at low alloying levels increases the linear oxidation rate because of its unfavorable size factor; at levels of 25 a/o and higher, zirconium forms a complex scale which improves the oxidation resistance; zirconium also causes internal oxidation
Fe	Improve mechanical stability of scale	Increase diffusion rates in scale	Good	Lower than niobium	Good	Poor	Iron additions of 1 and 5 a/o have no significant effects on oxidation behavior
Re	Improve mechanical stability of scale	Decrease diffusion rates in scale	Poor	--	--	--	The addition of 5 a/o rhenium causes increased linear oxidation rates because of formation of a volatile oxide

lower than that of niobium, were most effective in improving niobium's oxidation resistance. These elements promoted mechanical stabilization of the scale and parabolic oxidation behavior. Each of these effects is attributed to the smaller ionic size of these additions, which improves the scale stability by reducing the unfavorably high scale/metal volume ratio of niobium.

Zirconium provides a good example of the deleterious effect of an adverse ionic size relationship. The Zr^{4+} ion is 16 per cent larger than Nb^{5+}, and at the 10 a/o level caused a significant increase in the 1000 C oxidation rate. The larger zirconium ions tend to increase the already unfavorable volume ratio and reduce the stable inner-scale thickness, increasing the linear oxidation rates.

The reason for the failure of iron to effect any improvement in the mechanical stability of the scale is not known, but may be due to iron being in a lower valence state than assumed, which would have a larger ionic radius. Despite its low ionic size, rhenium showed no size effect. This, however, was due to the low boiling point of Re_2O_7. Thus, smoke was observed during testing of the niobium-5 a/o rhenium alloy at 1000 and 1200 C, indicating that a volatile oxide was being formed.

The relationship between ionic size and oxidation behavior is clearly shown in Figure 26. Here, the 1000 C 5-hr weight gains and the 1200 C 2-hr weight gains for the 10 a/o alloys are averaged, since zirconium and tungsten exhibited their maximum effects at different temperatures.

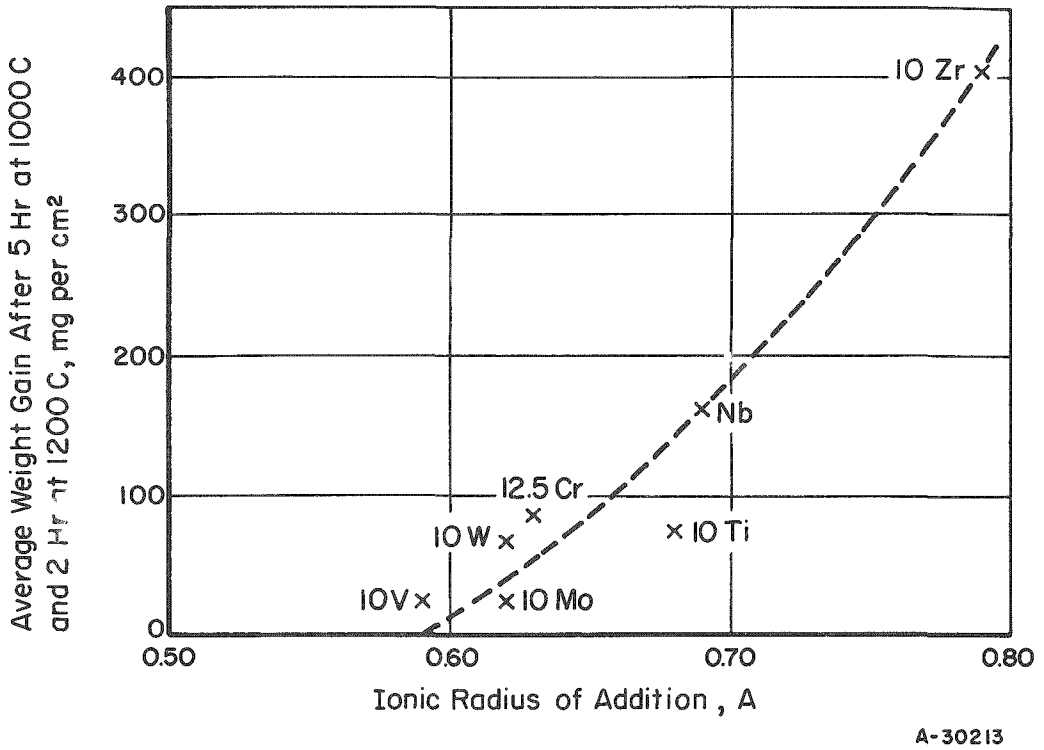

FIGURE 26. RELATION BETWEEN IONIC RADIUS OF ALLOY ADDITION AND AVERAGE OF 5-HR 1000 C WEIGHT GAIN AND 2-HR 1200 C WEIGHT GAIN FOR 10 OR 12.5 a/o ALLOYS

Valence effects were also expected and observed in the low alloying range. Thus, molybdenum, with a valence of +6, shows a greater specific effectiveness than vanadium, with a valence of +5. Similarly, zirconium, with a valence of +4, is quite detrimental at 1000 C and low alloying levels. The valence effect, however, appears of less importance here than the size effects.

Above the 10 to 15 a/o alloy-addition level, the oxidation behavior of niobium can be related to the properties of the addition-metal oxides. Thus, for higher alloys the oxidation behavior is determined by the properties of new scales which form. For example, it is seen in Table 13 that of the eight additions investigated extensively (chromium, iron, molybdenum, rhenium, titanium, tungsten, vanadium, and zirconium), only titanium and zirconium have higher thermodynamic oxide stabilities than niobium. The oxides of these elements are also physically and mechanically stable, and have lower electrical conductivities than Nb_2O_5, suggesting lower ionic diffusion rates. Hence, titanium and zirconium would be expected to form either their own oxides or stable mixed oxides at moderate alloying levels.

Wagner[20] has shown that the ability of one oxide to grow underneath another on a binary alloy depends on the relative dissociation pressures of the oxides in question. For simple systems of two metals forming only one oxide each, and assuming that no complex oxides are formed and metal diffusion rates in the core are known, the concentration at which one oxide will displace the other can be calculated. In the present case, this cannot be done because each component forms several oxides. Nevertheless, the principle that new oxides having greater stabilities may displace Nb_2O_5 at the metal/oxide interface is still valid.

Actually, titanium and zirconium form mixed oxides with Nb_2O_5.[11] These oxides are more stable than Nb_2O_5 and promote parabolic oxidation behavior and reduced rates at levels of 25 a/o and higher where they can form in sufficient quantity to be effective.

Molybdenum, rhenium, and vanadium form oxides which melt or volatilize when their solubilities in Nb_2O_5 are exceeded. The critical concentrations for loss of oxidation resistance due to formation of these oxides are about 10 a/o molybdenum, <5 a/o rhenium, and 15 a/o vanadium. Above these concentrations, these elements form either their own oxide or complex oxides with Nb_2O_5 which induce rapid linear oxidation. As with titanium and zirconium, the oxidation behavior changes gradually with composition after the Nb_2O_5 solubility limit is exceeded, becoming more characteristic of the addition metal. Chromium was also observed to form a partially molten scale at 24 a/o, possibly as the result of a eutectic reaction in the Nb_2O_5-Cr_2O_3 system.

In ternary combinations, it is of interest to note that chromium, molybdenum, and vanadium were not as effective in promoting parabolic oxidation when added to niobium-titanium as when added to pure niobium. The solubilities of these metal ions in the complex Nb_2O_5-TiO_2 scale are apparently reduced as compared with their solubilities in Nb_2O_5. Further evidence of reduced solubilities is the smoking of niobium-titanium-base alloys containing 4 a/o or more molybdenum.

The niobium-molybdenum-chromium and niobium-molybdenum-vanadium alloys were the most oxidation-resistant of all the alloy compositions investigated in this work.

Other recent work[21-24] has shown that multiple additions of elements capable of forming spinel-type oxides are also effective in improving the oxidation behavior of niobium. Chromium-cobalt, titanium-aluminum, and iron-aluminum are examples of these types of additions. The alloying level must be sufficiently high to allow formation of the new scales for these types of additions to be effective.

CONCLUSIONS

(1) Niobium reacts linearly with 1 atm of oxygen at 400 to 1400 C.

(2) Contamination of the base metal during oxygen or air oxidation results from oxygen diffusion from the scale.

(3) The niobium-air and niobium-oxygen reactions are essentially identical.

(4) Alloying affects oxidation behavior according to:

  (a) Relative ionic size

  (b) Relative valence

  (c) Properties of the alloy-element oxide.

(5) Valence and size effects are operative to alloying levels of approximately 15 a/o.

(6) Size effects are greater than valence effects.

(7) Important properties of the alloy addition oxide, which determine oxidation behavior above the 15 a/o alloying level, include thermodynamic, physical, and mechanical stabilities, and electrical resistivity.

(8) The most effective additions for improving the oxidation behavior are those capable of forming new, stable, diffusion-resistant oxides.

REFERENCES

(1) Brauer, G., Z. anorg. u. allgem. Chem., 248, 1-31 (1941).

(2) Zachariasen, W. H., "Physics Division Report for Month Ending April 15, 1945", University of Chicago, CF-2926 (April 15, 1945).

(3) Pranatis, A. L., and Seigle, L. L., Sylvania Electric Products, Progress Report No. SEP-235 (February, 1957); Progress Report No. SEP-240 (April, 1957). Classified.

(4) Gulbransen, E. A., and Andrew, K. F., "Kinetics of the Reactions of Columbium and Tantalum With O_2, N_2, and H_2", J. Metals, 188, 586 (March, 1950).

(5) Gulbransen, E. A., and Andrew, K. F., "Oxidation of Niobium Between 375 and 700 C", J. Electrochem. Soc., 105, 4 (January, 1958).

(6) Inouye, H., "Scaling of Columbium in Air", Proceedings of 1956 Regional Conference on Reactive Metals, AIME-IMD Special Report No. 5 (January, 1957).

(7) Belle, J., and Mallett, M. W., "Kinetics of High-Temperature Oxidation of Zirconium", J. Electrochem. Soc., 101, 399 (1954).

(8) Seybolt, A. W., "Solid Solubility of Oxygen in Columbium", Trans. AIME, 200, 774 (1954).

(9) Ang, C. Y., and Wert, C., "Some Properties of Columbium Containing Nitrogen", Trans. AIME, 197, 1032 (1953).

(10) Ang, C. Y., "Activation Energies and Diffusion Coefficients of Oxygen and Nitrogen in Niobium and Tantalum", Acta Met., 1, 123 (March, 1953).

(11) Roth, R. S., and Coughenour, L. W., "State of Equilibrium in the Systems Titania-Niobia and Zirconia-Niobia", R.P. 2621, J. Research, Natl. Bur. Standards, 55, 4 (1955).

(12) Kubaschewski, O., and Hopkins, B. E., Oxidation of Metals and Alloys, Butterworths, London (1953).

(13) Young, L., "Anomalies in the Growth of Anodic Oxide Films on Rough Surfaces", Acta Met., 5, 711 (1957).

(14) Vermilyea, D. A., "On the Mechanism of Oxidation of Metals", Acta Met., 5, 492 (1957).

(15) Webb, W. W., Norton, J. T., and Wagner, C., "Oxidation of Tungsten", J. Electrochem. Soc., 103, 107 (1956).

(16) Cathcart, J. V., Campbell, J. J., and Smith, G. P., "The Microtopography of Oxide Films on Niobium", J. Electrochem. Soc., 105, 442 (1958).

(17) Smithells, C. J., Metals Reference Book, Butterworths, London (1955).

(18) Coughlin, J. P., "Contributions to the Data on Theoretical Metallurgy", Bur. Mines Bull. 542 (1954).

(19) Meyer, W., Ztschr. Elektrochem., 50, 274 (1944).

(20) Wagner, C., "The Formation of Composite Scales Consisting of Oxides of Different Metals", J. Electrochem. Soc., 103, 627 (November, 1956).

(21) Michaels, A. B., "The Oxidation of Columbium-Base and Tantalum-Base Alloys", Talk presented at AIME Regional Conference on Reactive Metals, Buffalo, New York (May, 1958).

(22) Hix, H. B., "Compositions of Matter", U. S. Patent No. 2,822,268, assigned to E. I. du Pont de Nemours and Co., Inc. (February 4, 1958).

(23) Rhodin, T. N., Jr., "Metal Production", U. S. Patent No. 2,838,396, assigned to E. I. du Pont de Nemours and Co., Inc. (June 10, 1958).

(24) Rhodin, T. N., Jr., "Niobium-Base High Temperature Alloys", U. S. Patent No. 2,838,395, assigned to E. I. du Pont de Nemours and Co., Inc. (June 10, 1958).

WDK:DJM:CTS:RIJ/all

APPENDIX A

HARDNESS AND FABRICATION DATA FOR 50-G NIOBIUM BINARY AND TERNARY ALLOY INGOTS

TABLE A-1. HARDNESSES AND FABRICATION CHARACTERISTICS OF 50-G NIOBIUM BINARY ALLOY INGOTS

Alloy Addition, a/o		As-Cast Hardness,	Fabrication Temperature[b],	Total Reduction,	Annealed Hardness,	Quality of
Nominal	Corrected[a]	VHN	C	per cent	VHN[c]	Strip
100 Nb[d]		120	R.T.	80	120	Excellent
10 Ti	9.5 Ti	123	R.T.	87	127	Excellent
20 Ti	19 Ti	145	R.T.	87	154	Excellent
25 Ti	24.5 Ti	145	R.T.	87	162	Excellent
30 Ti	30.5 Ti	151	R.T.	86	160	Excellent
35 Ti	34 Ti	155	R.T.	86	169	Excellent
5 V	4.5 V	152	R.T.	87	143	Good
7.5 V	6.5 V	168	R.T.	85	169	Good
10 V	9 V	196	R.T.	89	191	Good
12.5 V	10.5 V	209	R.T.	88	210	Fair
15 V	--	239	1200	88	215	Good
17.5 V	14 V	264	1200	88	281	Good
25 V	24 V	285	1000	88	314	Good
2.5 Mo	2.5 Mo	128	R.T.	88	126	Good
5 Mo	5 Mo	154	R.T.	88	146	Good
7.5 Mo	7.5 Mo	175	R.T.	88	205	Fair
10 Mo	10 Mo[e]	199	1000	88	219	Good
12.5 Mo	12.5 Mo[e]	247	1000	--	--	Poor
15 Mo	15 Mo[e]	268	1000	--	--	Poor
25 Mo	25 Mo[e]	304	1000	88	--	Good
10 Cr	6 Cr[e]	272	--	--	--	Not fabricable
15 Cr	3.5 Cr	154	--	--	--	Not fabricable
20 Cr	12.5 Cr[e]	302	--	--	--	Not fabricable
25 Cr	4.5 Cr	305	1200	84	--	Poor
30 Cr	--	428	1200	84	--	Poor
35 Cr	24 Cr[e]	474	1200	84	283	Good
10 Zr	10.5 Zr	187	1000	87	199	Good
25 Zr	26 Zr	212	1000	87	266	Good
35 Zr	36 Zr	283	1000	87	306	Good
45 Zr	46 Zr	289	1000	87	302	Good
1 W	1 W	147	R.T.	(80)	--	Good
5 W	4.5 W	175	R.T.	(80)	--	Good
10 W	9.5 W	230	1200	84	266	Good
12.5 W	12 W[e]	256	1000	81	299	Fair
15 W	14.[illegible][e]	299	1000	--	--	Poor
25 W	24 W[e]	348	1200	84	--	Poor
5 Fe	5 Fe	167	R.T.	86	127	Excellent
10 Fe	--	262	1000	79	330	Fair
20 Fe	--	455	1000	--	--	Poor
5 Re	5 Re[e]	242	1000	79	274	Fair
10 Re	10 Re[e]	336	1000	--	--	Poor

(a) Compositions corrected on basis of spectrographic analyses to nearest 0.5 a/o, except where otherwise noted.
(b) Ingots rolled at room temperature were bare; hot-rolled ingots were encapsulated in evacuated stainless steel packs.
(c) Annealed 1 hr at 1500 C under 0.1-μ pressure after fabricating.
(d) Data for pure niobium are averages of several ingots.
(e) Compositions corrected on basis of weight-loss data.

TABLE A-2. HARDNESSES AND FABRICATION CHARACTERISTICS OF 50-G NIOBIUM TERNARY ALLOYS

Alloy Addition, a/o		As-Cast Hardness, VHN	Fabrication Temperature, C	Total Reduction, per cent	Annealed Hardness, VHN	Quality of Strip
Nominal	Corrected					
12.5 Ti-4 Mo	12 Ti-4 Mo	171	1000	79	177	Good
19 Ti-6 Mo	17.5 Ti-6 Mo	192	1000	81	227	Good
25 Ti-7.5 Mo	23 Ti-8 Mo	206	1000	81	260	Good
12.5 Ti-7.5 Cr	12 Ti-1.5 Cr	136	1000	81	240	Excellent
19 Ti-11 Cr	20 Ti-2 Cr	192	1000	79	235	Excellent
25 Ti-15 Cr	28 Ti-6 Cr	230	1000	79	348	Good
12.5 Ti-6 V	10.5 Ti-5 V	175	1000	81	268	Excellent
19 Ti-9 V	16 Ti-8.5 V	199	1000	79	262	Good
25 Ti-12.5 V	22.5 Ti-11 V	243	1000	81	287	Good
11 Cr-5.5 Mo	1.5 Cr-4.5 Mo	212	1000	--	--	Poor
6 Mo-9 V	5 Mo-7.5 V	254	1000	79	--	Poor

APPENDIX B

REACTION CURVES FOR BINARY NIOBIUM ALLOYS WITH DRY AIR AT 1000 AND 1200 C (CONTINUOUS-WEIGHING TESTS)

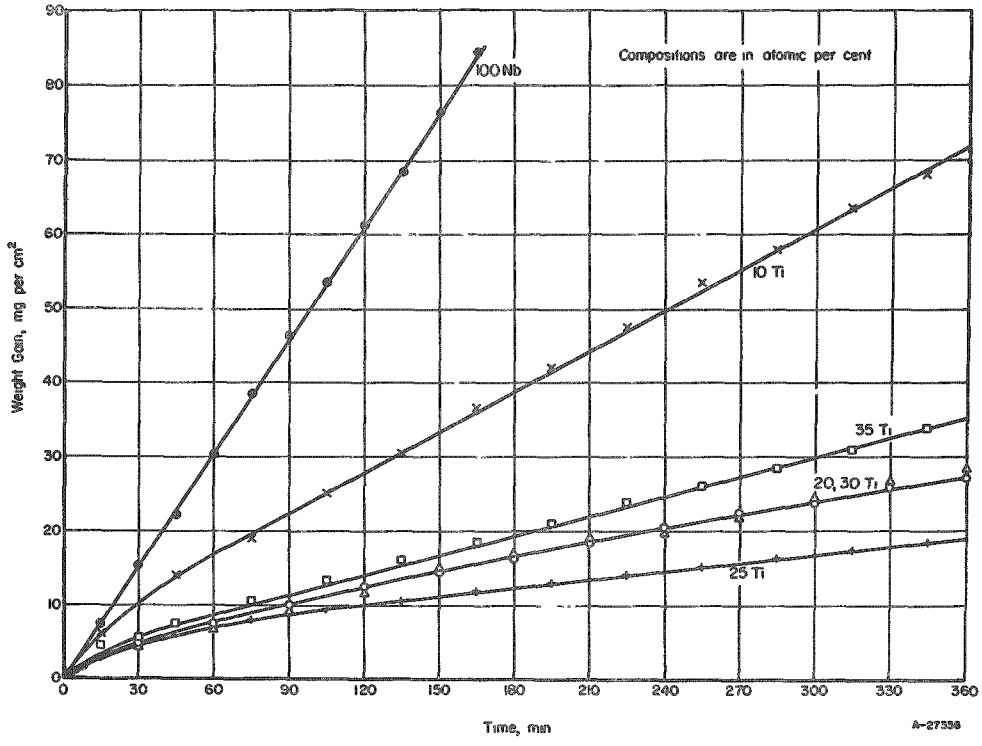

FIGURE B-1. REACTION OF NIOBIUM AND NIOBIUM-TITANIUM ALLOYS WITH AIR AT 1000 C

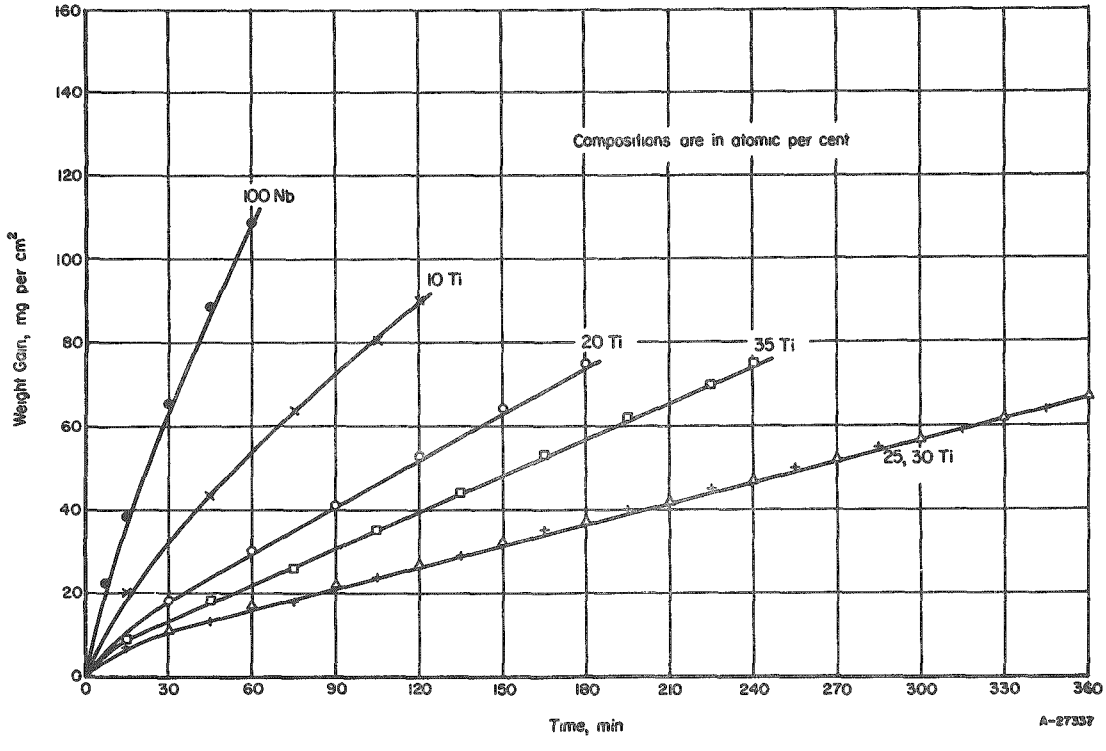

FIGURE B-2. REACTION OF NIOBIUM AND NIOBIUM-TITANIUM ALLOYS WITH AIR AT 1200 C

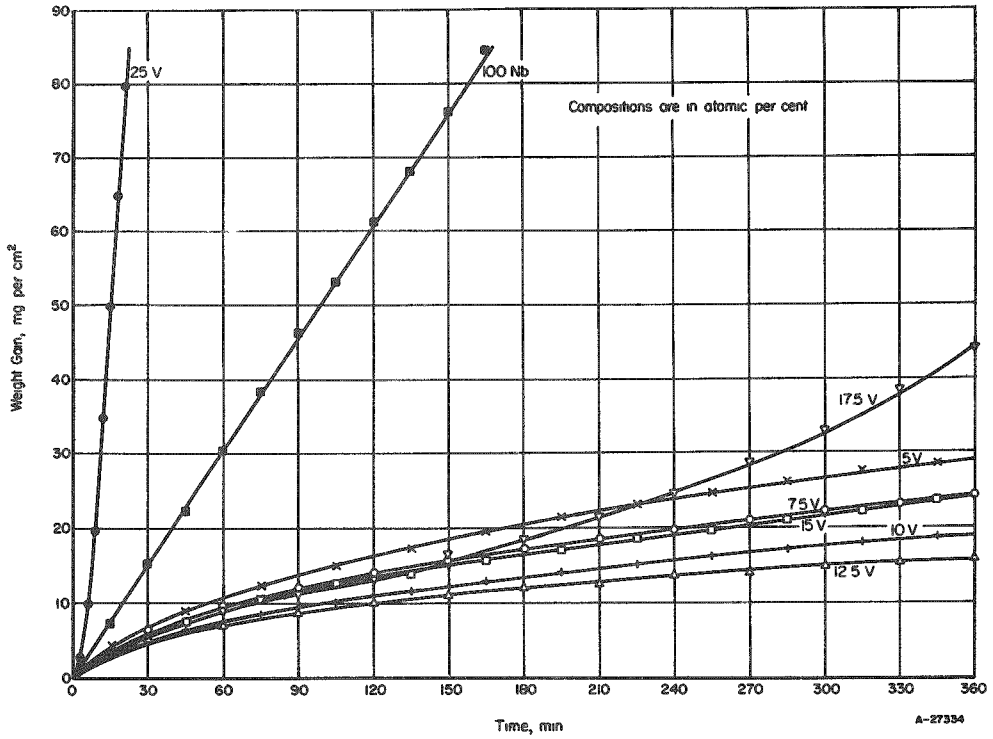

FIGURE B-3. REACTION OF NIOBIUM AND NIOBIUM-VANADIUM ALLOYS WITH AIR AT 1000 C

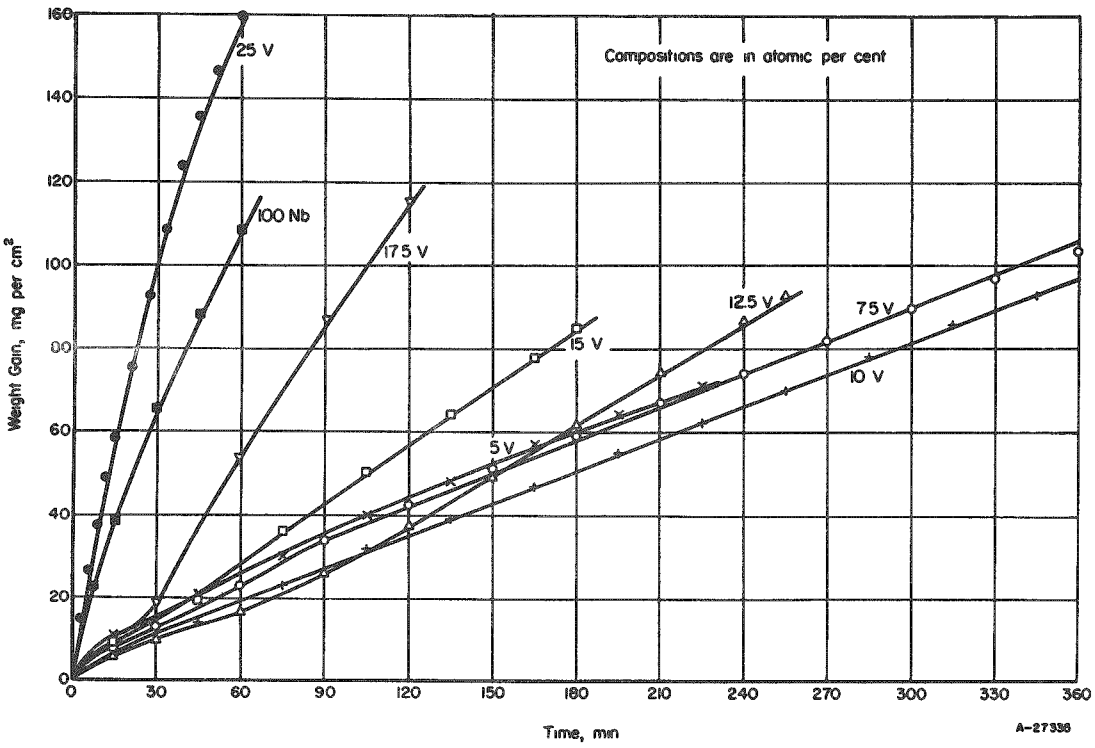

FIGURE B-4. REACTION OF NIOBIUM AND NIOBIUM-VANADIUM ALLOYS WITH AIR AT 1200 C

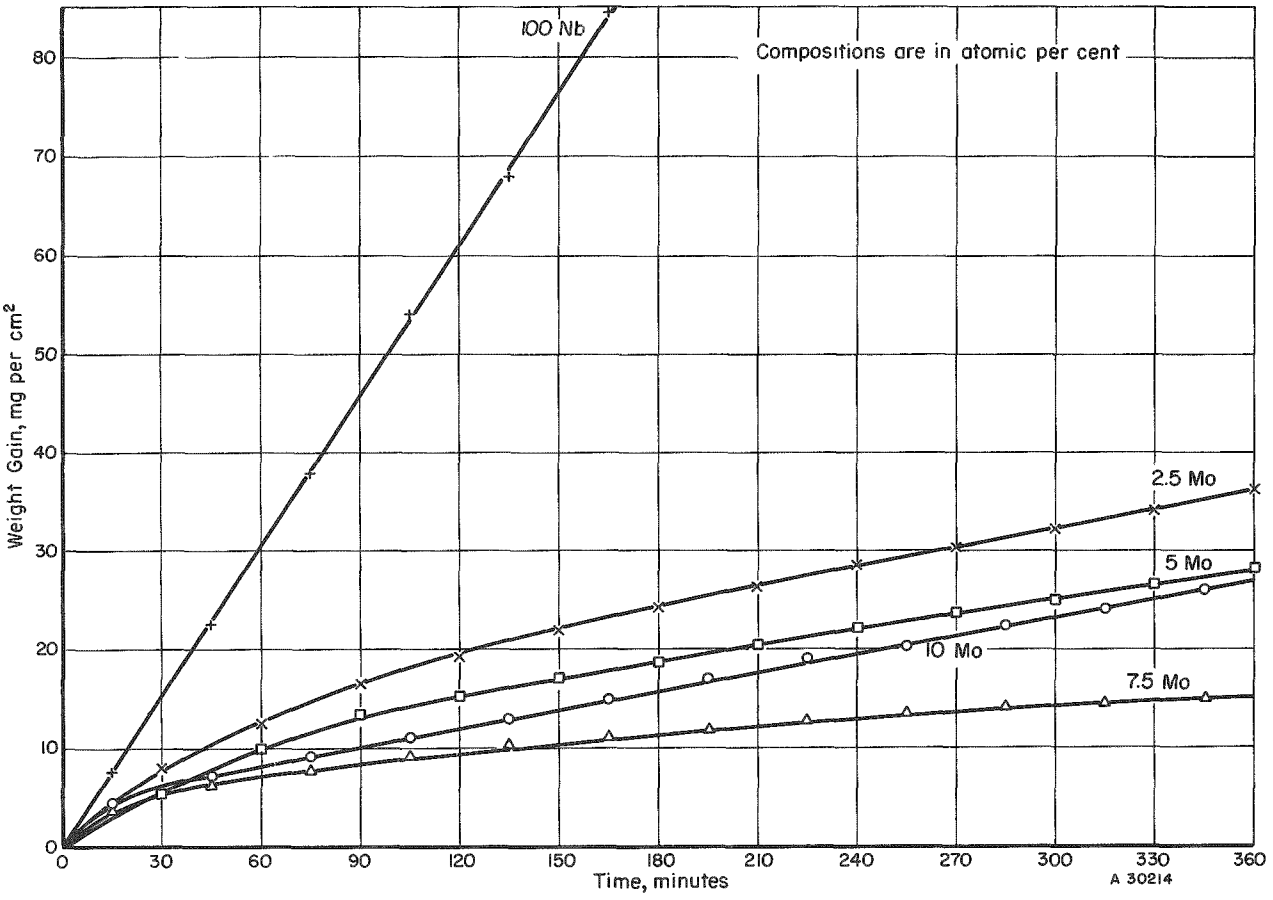

FIGURE B-5. REACTION OF NIOBIUM AND NIOBIUM-MOLYBDENUM ALLOYS WITH AIR AT 1000 C

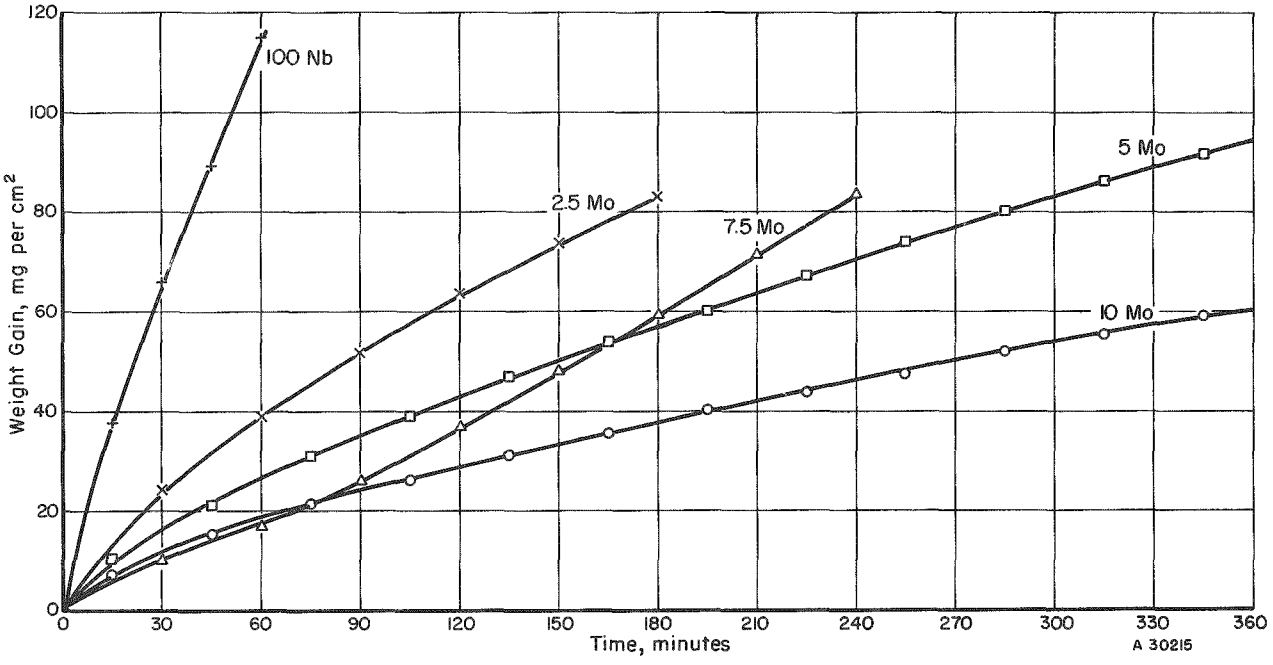

FIGURE B-6. REACTION OF NIOBIUM AND NIOBIUM-MOLYBDENUM ALLOYS WITH AIR AT 1200 C

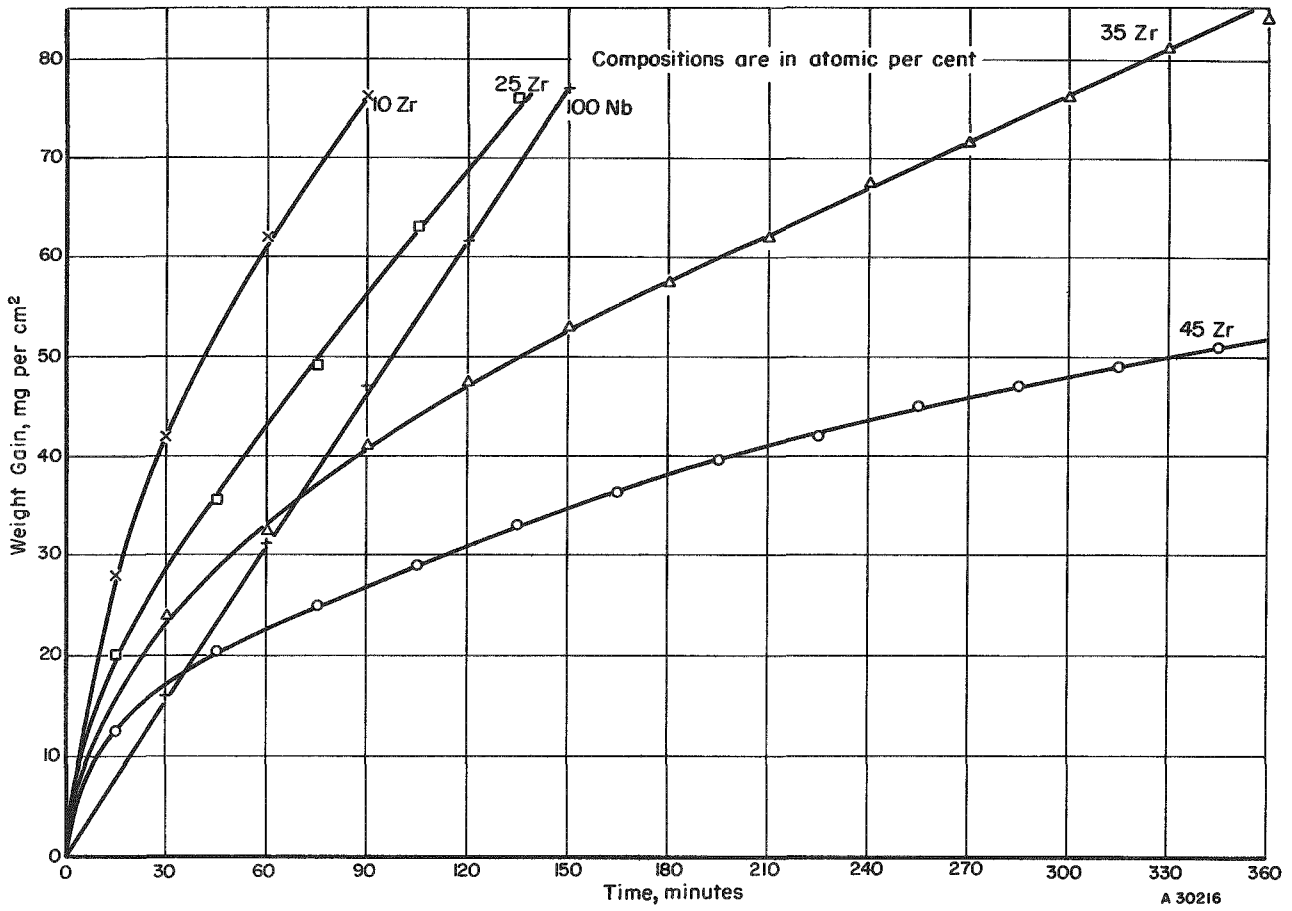

FIGURE B-7. REACTION OF NIOBIUM AND NIOBIUM-ZIRCONIUM ALLOYS WITH AIR AT 1000 C

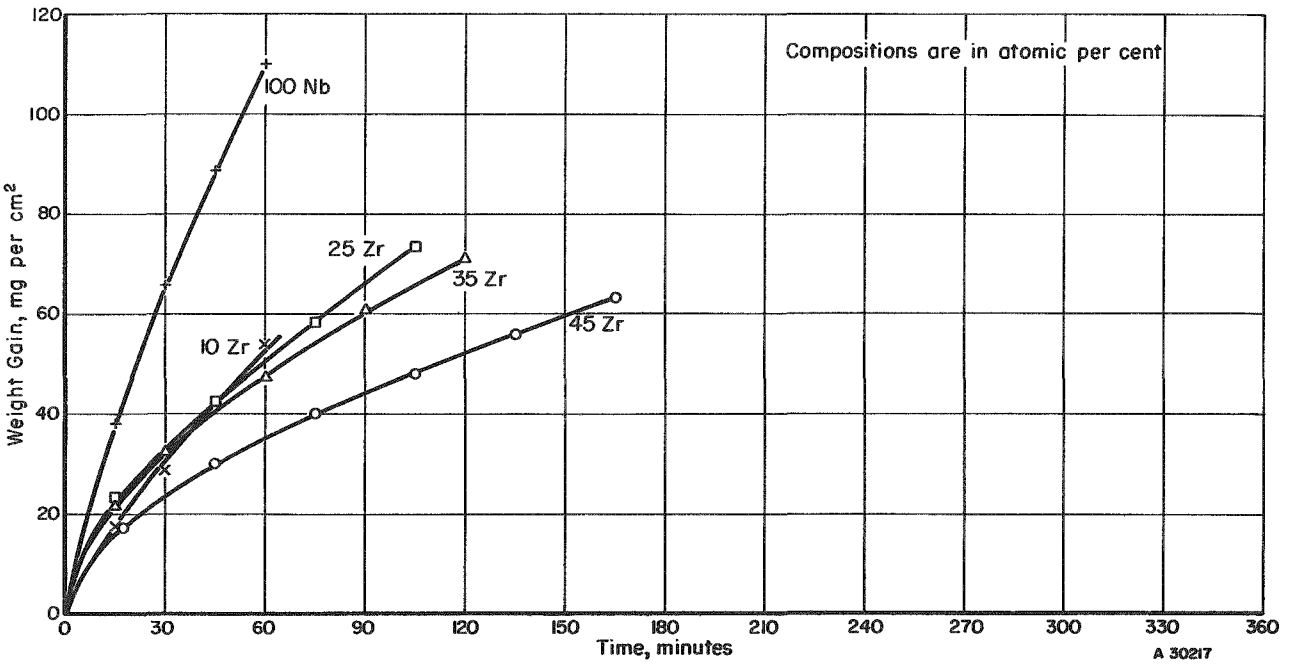

FIGURE B-8. REACTION OF NIOBIUM AND NIOBIUM-ZIRCONIUM ALLOYS WITH AIR AT 1200 C

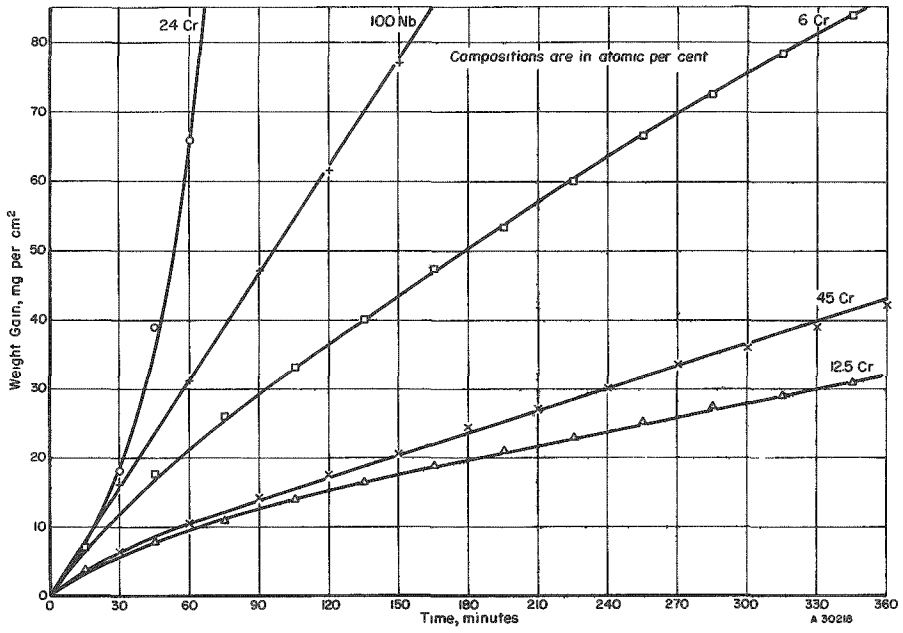

FIGURE B-9. REACTION OF NIOBIUM AND NIOBIUM-CHROMIUM ALLOYS WITH AIR AT 1000 C

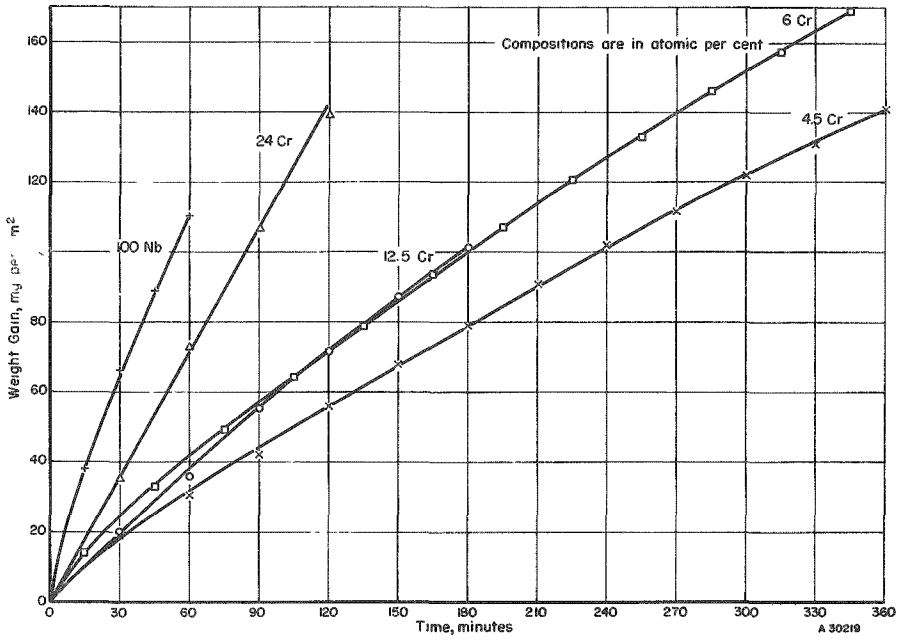

FIGURE B-10. REACTION OF NIOBIUM AND NIOBIUM-CHROMIUM ALLOYS WITH AIR AT 1200 C

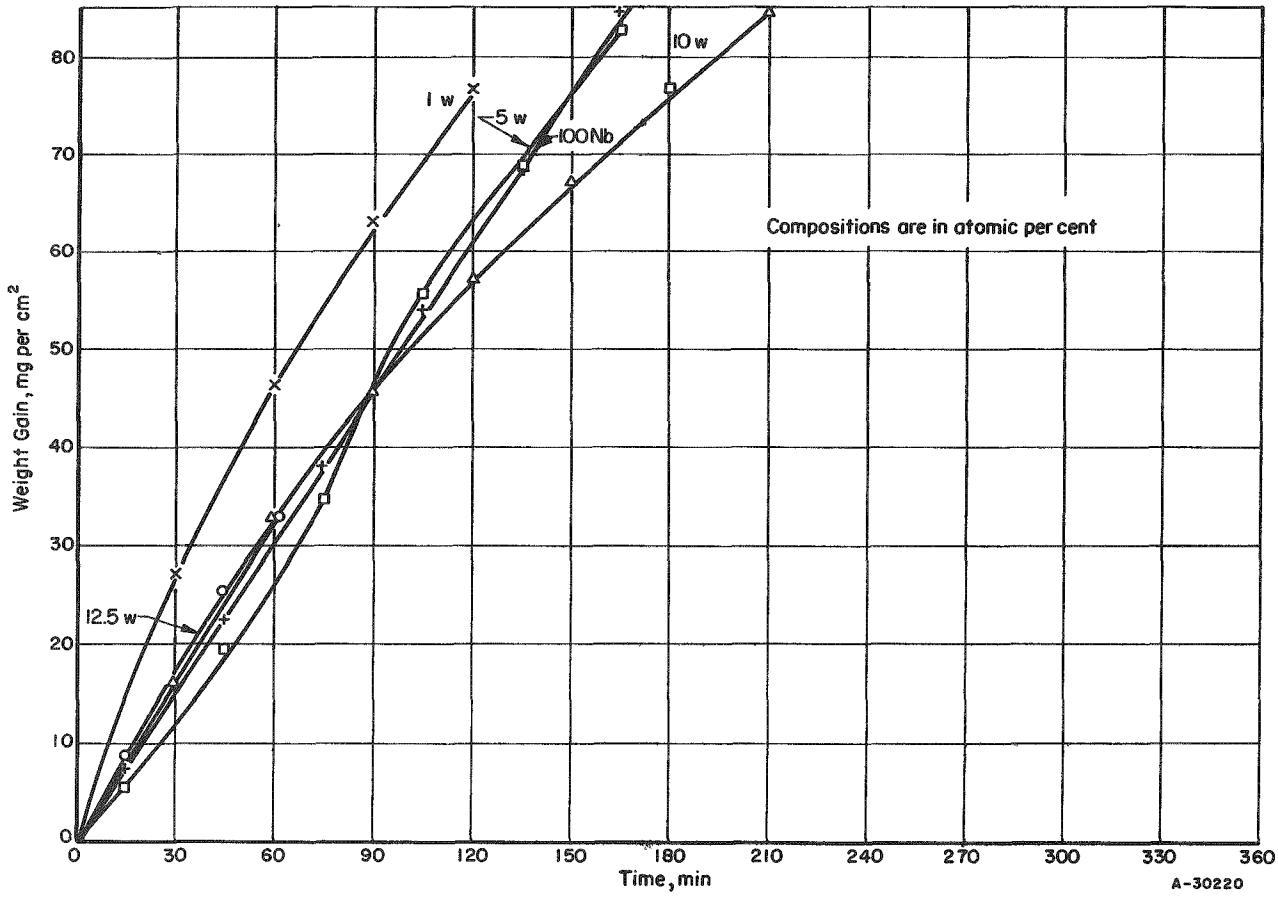

FIGURE B-11. REACTION OF NIOBIUM AND NIOBIUM-TUNGSTEN ALLOYS WITH AIR AT 1000 C

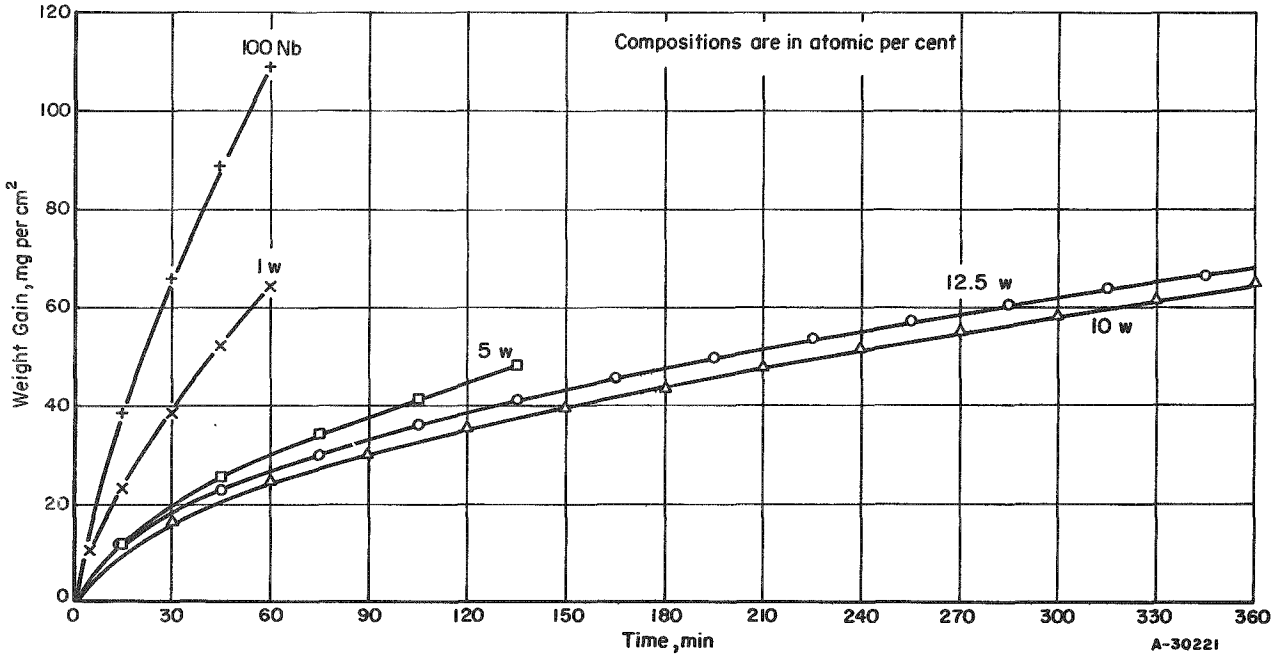

FIGURE B-12. REACTION OF NIOBIUM AND NIOBIUM-TUNGSTEN ALLOYS WITH AIR AT 1200 C

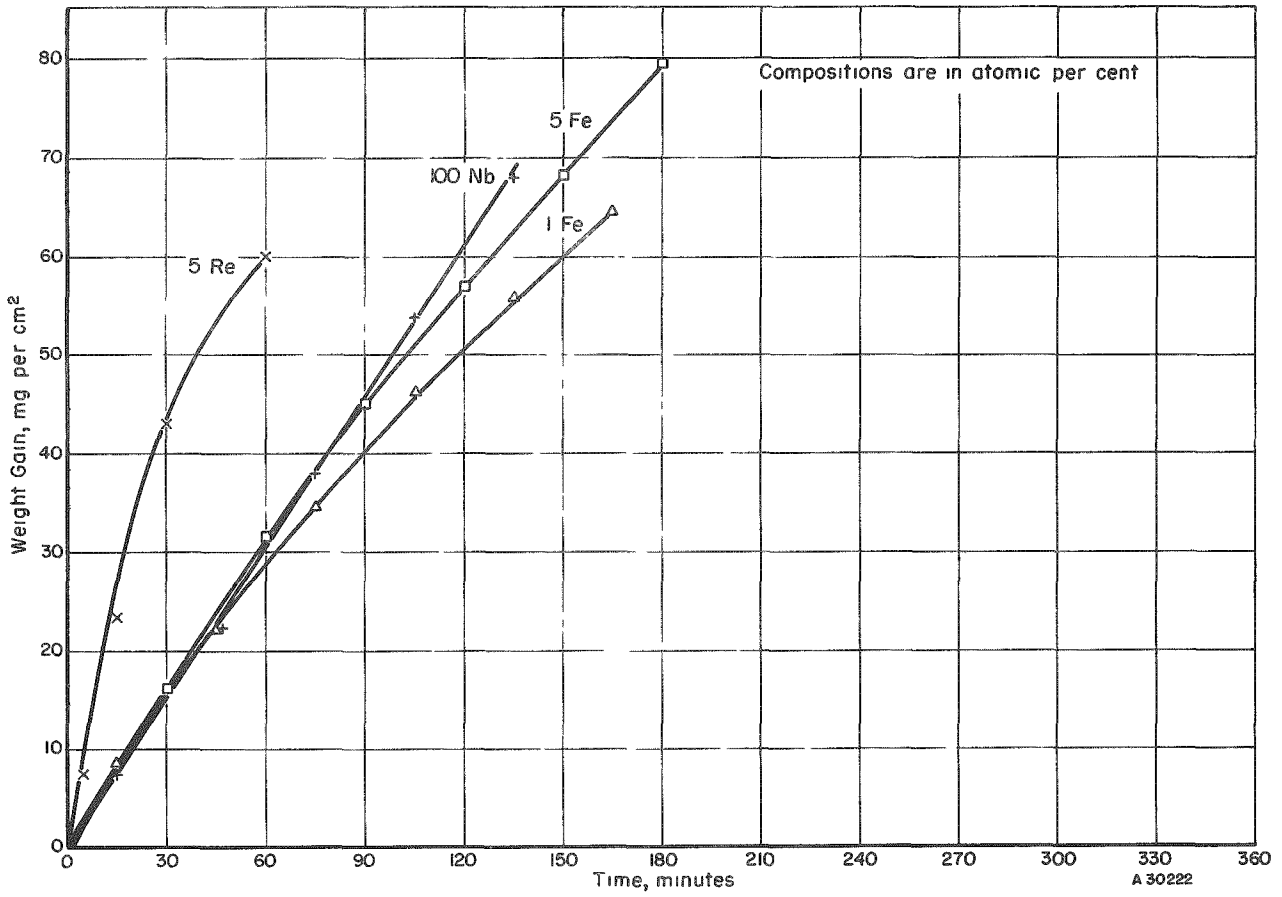

FIGURE B-13. REACTION OF NIOBIUM, NIOBIUM-IRON, AND NIOBIUM-RHENIUM ALLOYS WITH AIR AT 1000 C

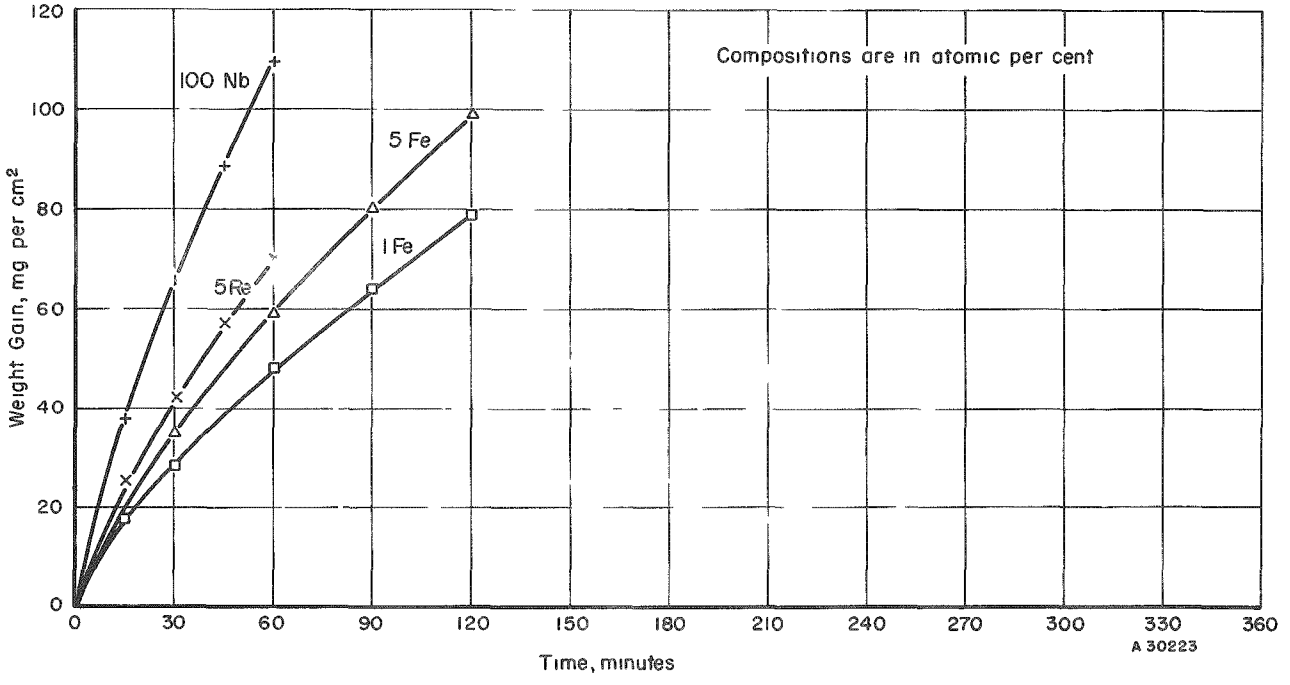

FIGURE B-14. REACTION OF NIOBIUM, NIOBIUM-IRON, AND NIOBIUM-RHENIUM ALLOYS WITH AIR AT 1200 C

APPENDIX C

REACTION CURVES FOR TERNARY NIOBIUM ALLOYS WITH DRY AIR AT 1000 AND 1200 C (CONTINUOUS-WEIGHING TESTS)

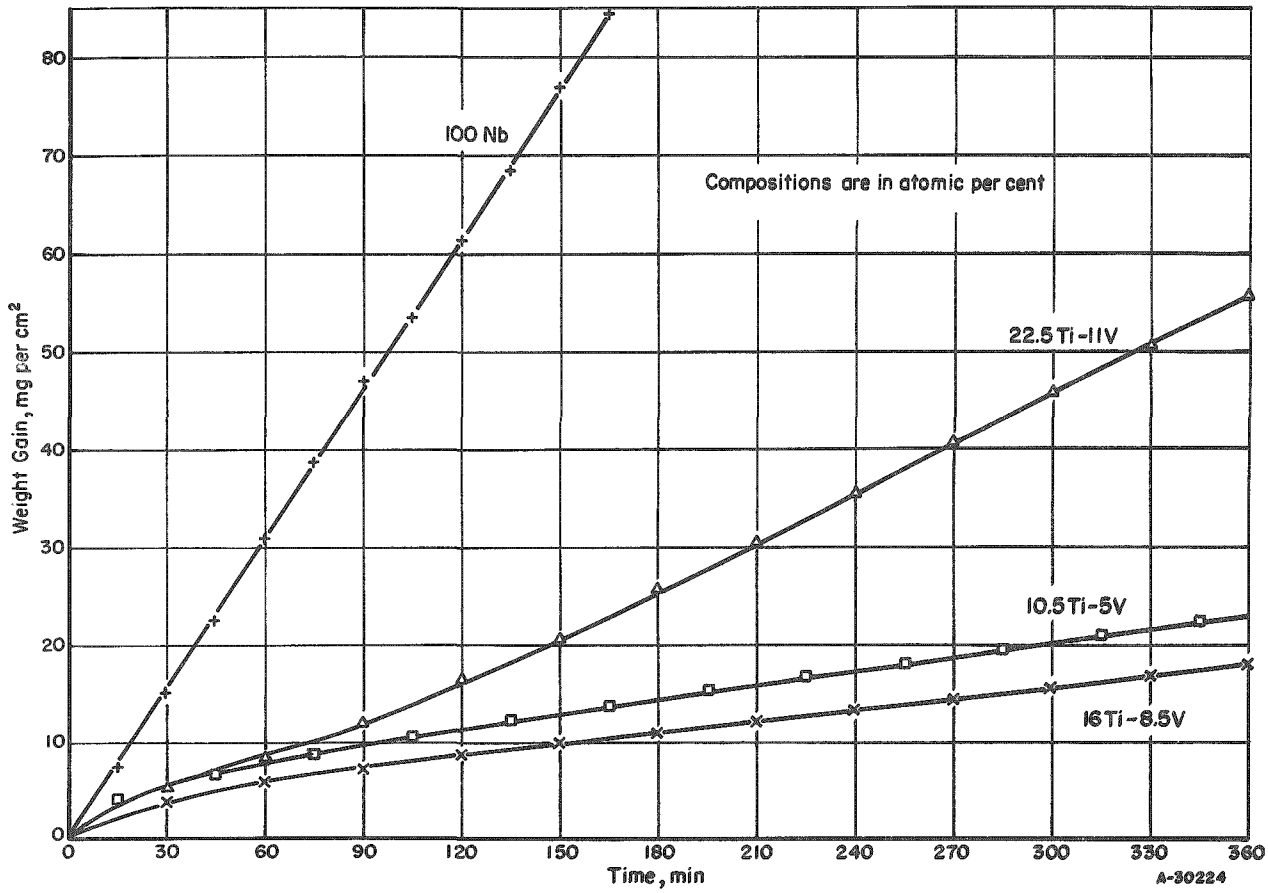

FIGURE C-1. REACTION OF NIOBIUM AND NIOBIUM-TITANIUM-VANADIUM ALLOYS WITH AIR AT 1000 C

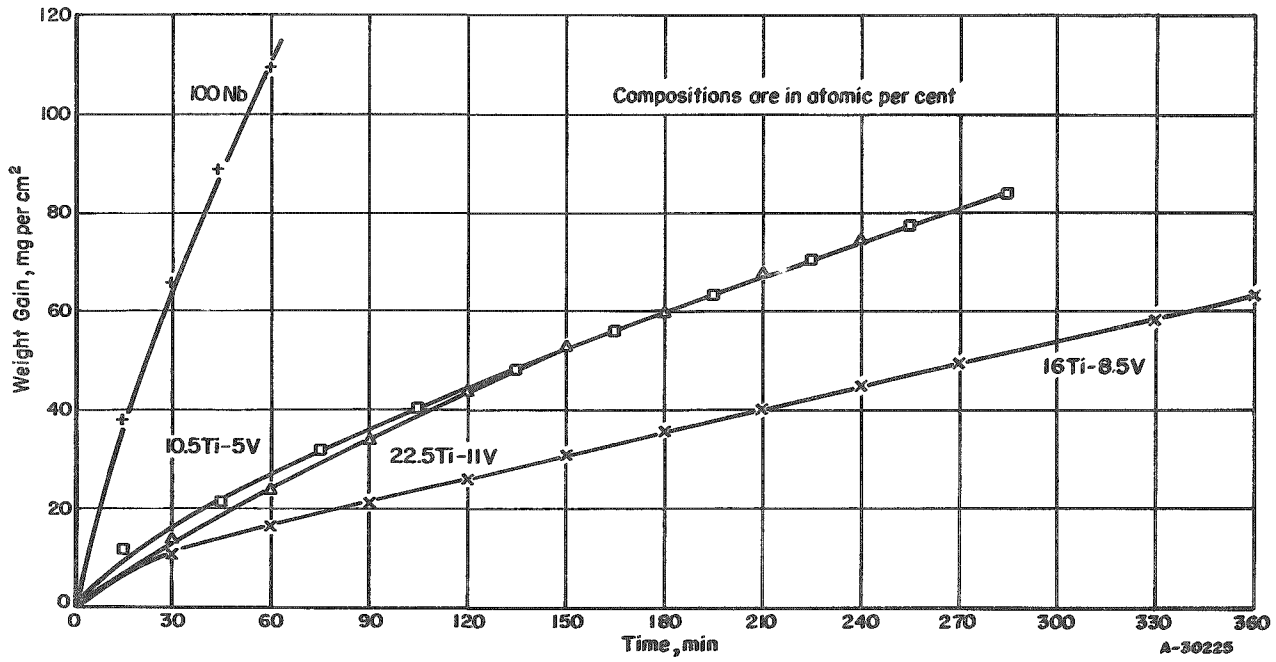

FIGURE C-2. REACTION OF NIOBIUM AND NIOBIUM-TITANIUM-VANADIUM ALLOYS WITH AIR AT 1200 C

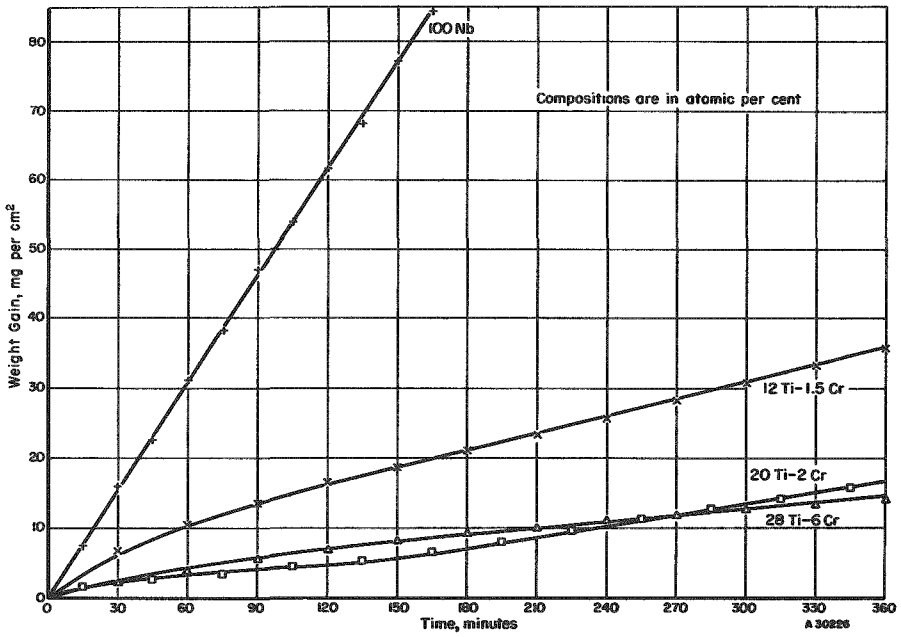

FIGURE C-3. REACTION OF NIOBIUM AND NIOBIUM-TITANIUM-CHROMIUM ALLOYS WITH AIR AT 1000 C

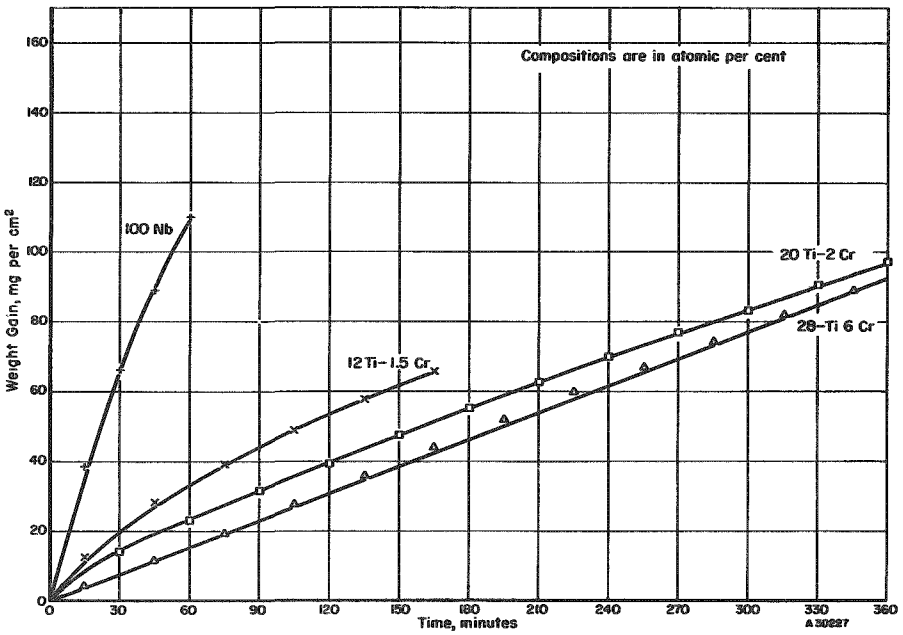

FIGURE C-4. REACTION OF NIOBIUM AND NIOBIUM-TITANIUM-CHROMIUM ALLOYS WITH AIR AT 1200 C

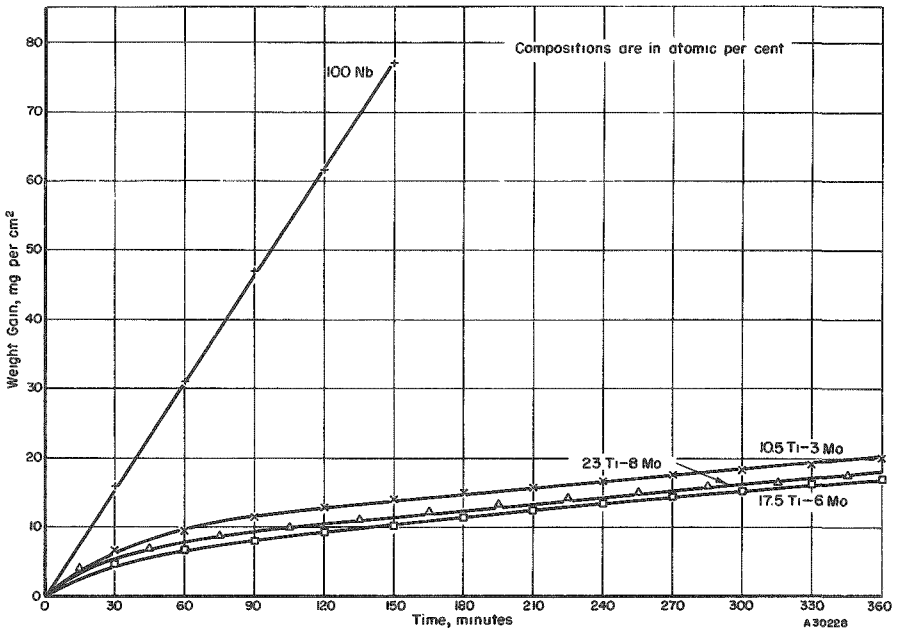

FIGURE C-5. REACTION OF NIOBIUM AND NIOBIUM-TITANIUM-MOLYBDENUM ALLOYS WITH AIR AT 1000 C

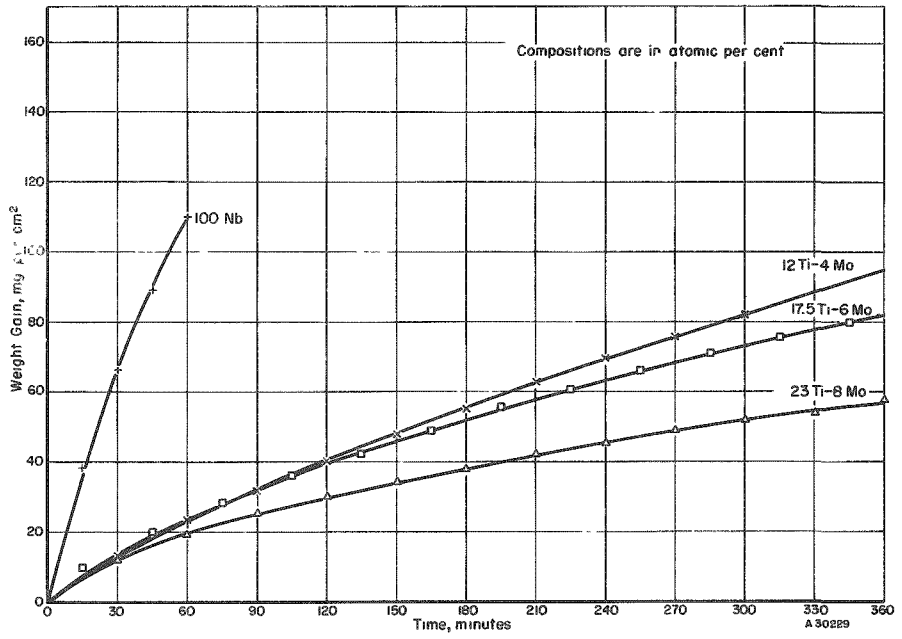

FIGURE C-6. REACTION OF NIOBIUM AND NIOBIUM-TITANIUM-MOLYBDENUM ALLOYS WITH AIR AT 1200 C

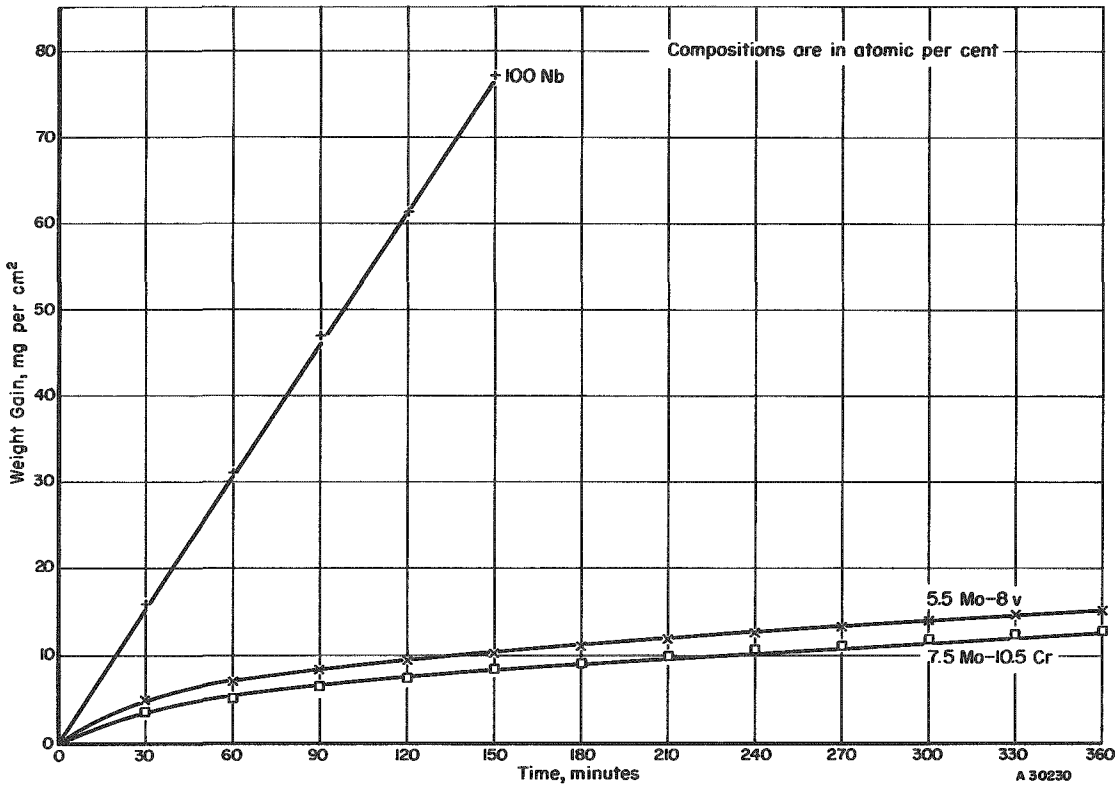

FIGURE C-7. REACTION OF NIOBIUM, NIOBIUM-MOLYBDENUM-VANADIUM, AND NIOBIUM-MOLYBDENUM-CHROMIUM ALLOYS WITH AIR AT 1000 C

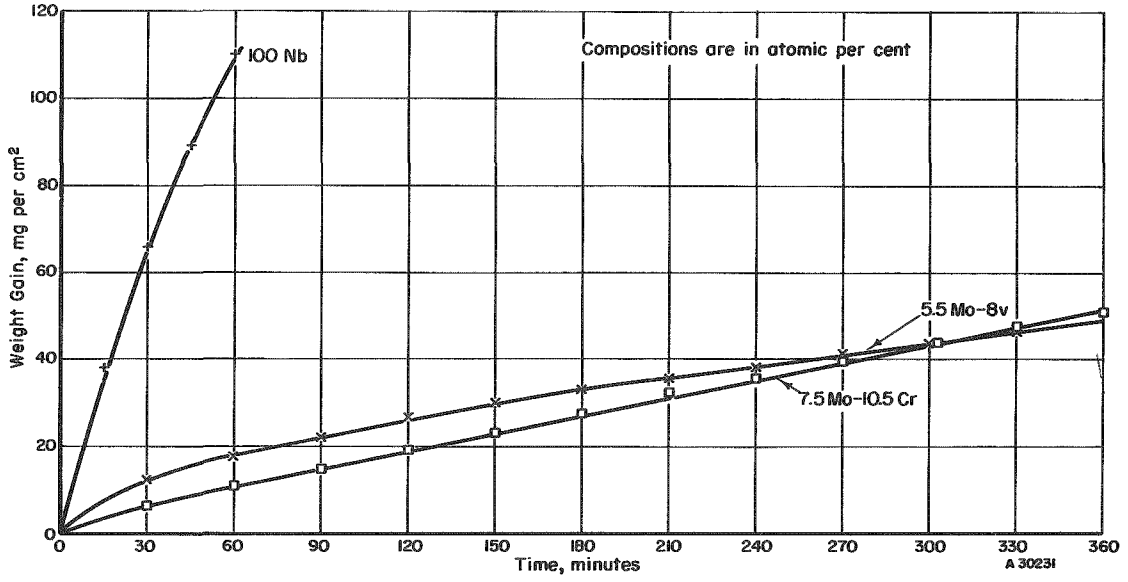

FIGURE C-8. REACTION OF NIOBIUM, NIOBIUM-MOLYBDENUM-VANADIUM, AND NIOBIUM-MOLYBDENUM-CHROMIUM ALLOYS WITH AIR AT 1200 C